universität wien

DIPLOMARBEIT

Titel der Diplomarbeit

Studies on the interactions of plectin with laminin receptors in Schwann cells

angestrebter akademischer Grad

Magister der Naturwissenschaften (Mag. rer.nat.)

Verfasser:	Karl-Leopold Wögenstein
Studienrichtung /Studienzweig (lt. Studienblatt):	Molekulare Biologie
Betreuer:	Univ.-Prof. Dr. Gerhard Wiche

Wien, im Dezember 2010

Danksagung

Ohne Anspruch auf Vollständigkeit danke ich im Folgenden:

Prof. Dr. Gerhard Wiche für die Möglichkeit an einem spannenden Gebiet zu forschen und dafür, dass er meine Forschungen in die richtigen Bahnen gelenkt hat.
Dr. Gernot Walko, der für mich kein besserer Betreuer hätte sein können. Ich bin froh Gernot mit gutem Gewissen als Mentor und Freund zu bezeichnen.
Karin Gross für Hilfestellungen bei der Expression und dem Aufreinigen von Proteinen.
Irmgard Fischer für das Vermitteln ihrer Künste in faszinierenden Methoden und Techniken.
Mag. Waltraud Kutschera für ihre unverzichtbaren Bemühungen Geräte, Reagenzien und die allgemeinen Umgangsformen in Schuss zu halten.
Elisabeth Jursa für Hilfestellungen in Zellkulturfragen.
Gerlinde Aschauer für ihre Unterstützung mit der von mir ungeliebten Bürokratie.
Dr. Günther Rezniczek für Beratung in wissenschaftlichen und informatischen Belangen.
Dr. Peter Fuchs für Feedback, Hilfestellungen und einem großen Beitrag zur gemütlichen Atmosphäre im Labor 2.
Der gesamten **Wiche-Gruppe**, im speziellen natürlich den Mitgliedern des Labors 2, für die schöne Zeit.
Prof. Dr. Fritz Propst und seiner Gruppe für Hilfestellungen und Feedback.
Meinen universitären und außerunversitären **Freunden**, im Besonderen Mag in spe. Christoph Miksch für das Korrekturlesen dieser Diplomarbeit.

Meiner Familie für ihre bedingungslose Unterstützung in allen Belangen.

Und zuletzt danke ich meiner Partnerin **Annika**, dafür dass ich jeden Tag neben ihr aufwachen und einschlafen darf und sie mich in der Realität verankert und verhindert, dass ich ein verschrobener Wissenschafts-Sonderling werde.

Table of contents

Abbreviations

ABD	actin-binding domain
AMPK	AMP-activated protein kinase
AP	alkaline phosphatase
ARP complex	actin related protein complex
ATP	adenosin tri phosphate
BCIP	5-bromo-4-chloro-3-indolylphosphate
BPAG1	bullous pemphigoid antigen 1
BSA	bovine serum albumin
CH, CH1, CH2	calponin homology (domain 1,2)
CNS	central nervous system
Co-IP	co-immunoprecipitation
DGC	dystrophin-glycoprotein complex
DMF	dimethyl-formamide
DRP2	dystrophin-related protein 2
DTT	dithiotreitole
EB-PA	epidermolysis bullosa-pyloric atresia
EB-MD	epidermolysis bullosa simplex-muscular dystrophy
ECM	extracellular matrix
EDTA	ethylene-diamine tetra-acetic acid
EGTA	ethylene glycole-bis (ß-aminoethylether)-N,N,N',N'-tetra-acetic acid
GAR	Gas2 homology region
GFAP	glial fibrillar acidic protein
GSR repeats	glycine-serine-arginine repeats
IF	intermediate filament
IFBD	intermediate filament binding domain
IPTG	isopropoyl-ß,D-thiogalactopyranoside
JXP	juxtaparanodes
MACF1	microtubule actin cross-linking factor 1
MAP	microtubule associated protein
MT	microtubule
MTOC	microtubule organizing centre

PBS	phosphate-buffered saline
PMSF	phenyl-methyl-sulfonyl-fluorid
PNS	peripheral nervous system
PRD	plakin-repeat domain
RACK1	receptor of activated C-kinase 1
RT	room temperature
SC	Schwann cell
SDS	sodium dodecyl sulfate
SDS-PAGE	SDS-polyacrylamide gel electrophoresis
SH3	Src homology 3
TB	terrific broth

Introduction

A eukaryotic cell is a busy microcosmos. Proteins must be transported to specific locations. Organelles have to be positioned at their correct intracellular location and the polarity of the cell has to be maintained. The plasma membrane needs to be mechanically supported and the overall shape of the cell has to be regulated. But when it is time for the cell to divide, the well cared-for organization is lost and has to be rearranged rapidly. The previously duplicated chromosomes need to be separated from each other and must be segregated to the future daughter cells, and once time has come for them to break their physical linkages, their plasma membranes have to be divided. To carry out all these tasks, the cell is crucially dependent on a complex system of networked filaments called the cytoskeleton.

The cytoskeleton

The cytoskeleton is composed of three different protein families, each of them forming filamentous structures. These cytoskeletal filament systems are assembled from protein subunits and hence are dynamic structures with their dynamics being defined by the rates of polymerization and depolymerization. This feature also enables them to react rapidly and energy-efficiently to any change occuring to the cell or its surrounding. Each one of the three systems fulfills different functions within the cell but at the same time is dependent on cooperation with the other filament systems.

The three major cytoskeletal components are the actin microfilaments, the intermediate filaments and the microtubules (Alberts, 2008).

Actin filaments

Actin filaments are composed of actin monomers - globular polypeptides that assemble head to tail to form a polarized noncovalently bound polymer. Two actin filaments built in this fashion, intertwine to create a double-helical structure (Figure 1). Actin filaments are able to form linear bundles, so called actin stress fibers – (O'Neill, 2009) , two dimensional meshworks, called lamellipodia (Bugyi and Carlier, 2010), or three dimensional gels, as can be found in the cell cortex. Each actin subunit has the ability to

tightly bind ATP molecules and hydrolyze them. This enzymatic activity is very low in the free (G-actin) form and strongly increases when in the filamentous form (F-actin). Together with the fact that one end of the actin filament (the plus end) binds new subunits more readily, this leads to a phenomenon known as treadmilling (Wegner, 1976), whereby this chemical kinetic view of polymerization dynamics is gaining complexity with the observation that structural states of the polymer itself also influence the polymerization dynamics. This theory is called structural plasticity (Kueh and Mitchison, 2009).

Actin is distributed throughout the cell, but is highly concentrated at the periphery. The initiation of the actin polymerization, called nucleation, takes place near the plasma membrane. Actin's major roles in the cell are: regulating the cell's shape; cell migration, endocytosis, vesicle trafficking, and to generate contraction forces such as in the sarcomers of skeletal muscle or in the contractile ring during cytokinesis (Goley and Welch, 2006). Several accessory proteins, binding to actin, have been described. These proteins are able to influence actin polymerisation dynamics, regulate bundling of actin filaments and enable the microfilament system to form structures like lamellipodia (for review see Lee and Dominguez, 2010). The actin related protein complex (ARP complex) is known to control nucleation of actin filaments in branched actin networks (Ma et al., 1998). Proteins like thymosin and profilin influence actin polymerisation by binding to free actin subunits (Yarmola and Bubb, 2004). Other proteins, like gelsolins are able to sever actin filaments, thus causing restructuring of the filament system (McGough et al., 2003). Filamin cross-links actin filaments into a three dimensional network which has the physical properties of a gel (Tseng et al., 2004). In contrast α-actinin packs actin filaments into tight contractile bundles containing bipolar arrays of myosin II, called stress fibers (Otto, 1994; Naumanen et al., 2008) . Moreover, other proteins link actin to membranous junctional complexes. Motorproteins of the myosin superfamily bind to actin filaments and undergo conformational changes upon binding and hydrolsis of ATP molecules. In this fashion they move along the actin filament and are integral parts of contractile actin bundles (Inoue et al., 1979). These, and many more accessory proteins work together to orchestrate the highly regulated events involved in cell contraction and migration. Often, cytoskeletal rearrangements are induced by extracellular signals. These signals converge on the Rho protein family of monomeric GTPases, which themselves

trigger signaling cascades leading to major actin rearrangements (Ridley et al., 1999), such as the formation of stress fibers and the consequent cell contractility.

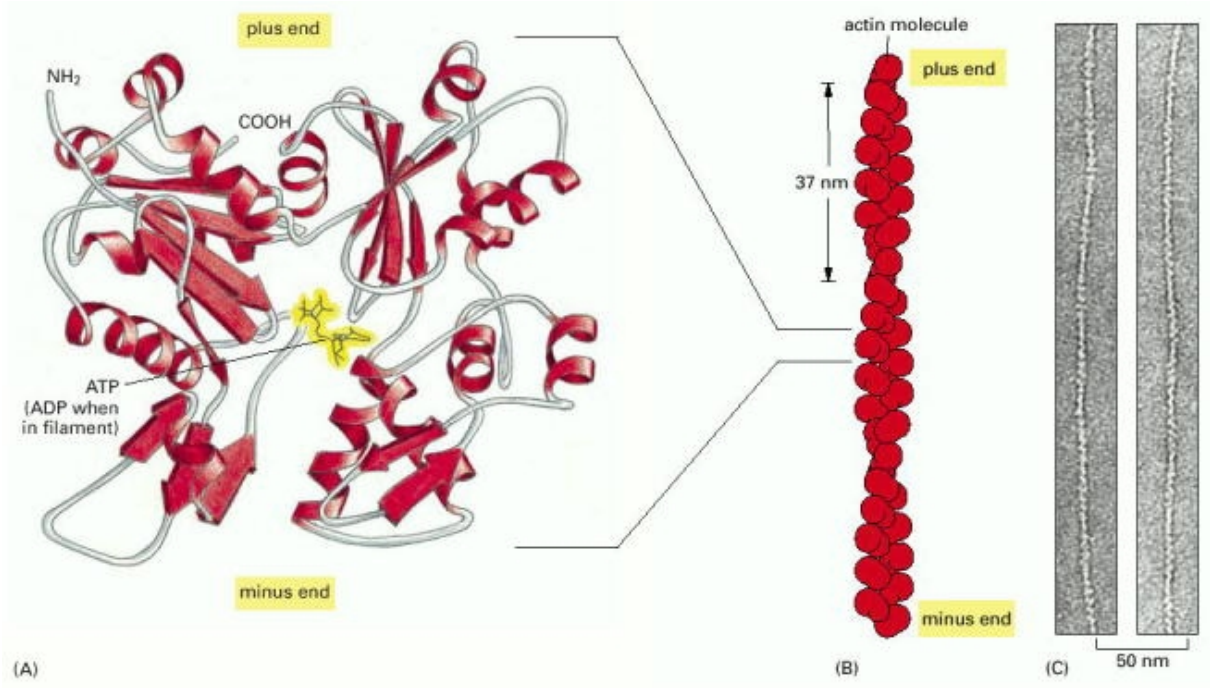

Figure 1. Depiction of an actin monomer and actin filament. (A) The actin monomer has a nucleotide (ATP or ADP) bound in a cleft in the center of the molecule. (B) Arrangements of monomers in an actin filament. Two protofilaments wind around each other to form a helical structure, with a twist repeating every 37 nm. Subunits in the helix have the same orientation. (C) Electron micrographs of negatively stained actin filaments. (modified from Alberts, 2008)

Microtubules

Microtubules (MTs) are dynamic filamentous polymers. MTs have various functions inside the cell. They direct intracellular transport, determine the position of organelles and are involved in chromosome segregation, morphogenesis and directed migration. MTs are formed from globular heterodimers which are built from two different tubulin monomers, α- and ß-tubulin. 13 protofilaments consisting of tubulin heterodimers arranged in linear fashion assemble laterally and form a stiff hollow tube with an outer diameter of approximately 25 nm. The microtubules have a distinct structural polarity with α-tubulin on one end and ß-tubulin on the other (Figure 2). Like actin monomers, the tubulin monomers are able to bind and hydrolyze nucleotide triphosphates. Actin monomers bind ATP molecules, whereas tubulin binds and hydrolyzes GTP. Thus the treadmilling phenomenon can also be observed in microtubules. Another dynamic

property of microtubules is called dynamic instability. When the concentration of free tubulin subunits falls under a critical concentration, the GTP hydrolysis can proceed more rapidly than the addition of GTP-tubulin dimers at the growing plus end of the microtubule. Then the protective GTP cap is lost and rapid shrinking of the filament occurs, which is called catastrophe. Eventually the MT is rescued when the concentration of free tubulin rises and the GTP cap is restored (Desai and Mitchison, 1997). The (slower growing) minus end of microtubules is anchored at microtubule-organizing centres (MTOC). Often cells possess only one MTOC which is then called the centrosome. The MT plus ends are free for the addition of tubulin subunits and grow to the periphery of the cell. To fulfill their numerous functions, microtubules are dependent on specific microtubule associated proteins (MAPs) that regulate microtubule dynamics and their interaction with other proteins (Mandelkow and Mandelkow, 1995). MAPs like tau or MAP2 can bind to microtubules and thereby stabilize them. These MAPs have, in addition to their binding domain, another domain projecting away from the microtubule that can bind to a second microtubule, thus crosslinking the two fibers (Weisshaar and Matus, 1993). The length of the projecting arm determines the packing density of the MT bundles. There are also proteins binding to microtubules that cause destabilization, like members of the kinesin superfamily (Waters and Salmon, 1996). Moreover, capping proteins like EB1 can help to position microtubules to their correct intracellular locations (Muhua et al., 1998).

Motor proteins represent a fascinating group of cytoskeletal proteins. They use energy released by ATP hydrolysis for repeated cycles of conformational change to move alongside cytoskeletal filaments (for review see Wade, 2009). Microtubule binding motorproteins comprise two superfamilies, the kinesins and the dyneins. Most kinesins walk towards the plus end of the microtubule. They are involved in mitotic and meiotic spindle formation and chromosome separation during cell division. Dyneins are unrelated to kinesins and most of them move towards the minus end of microtubules. They are important for vesicle trafficking, localization of the Golgi apparatus and drive the beating of cilia and flagella (Mallik and Gross, 2004).

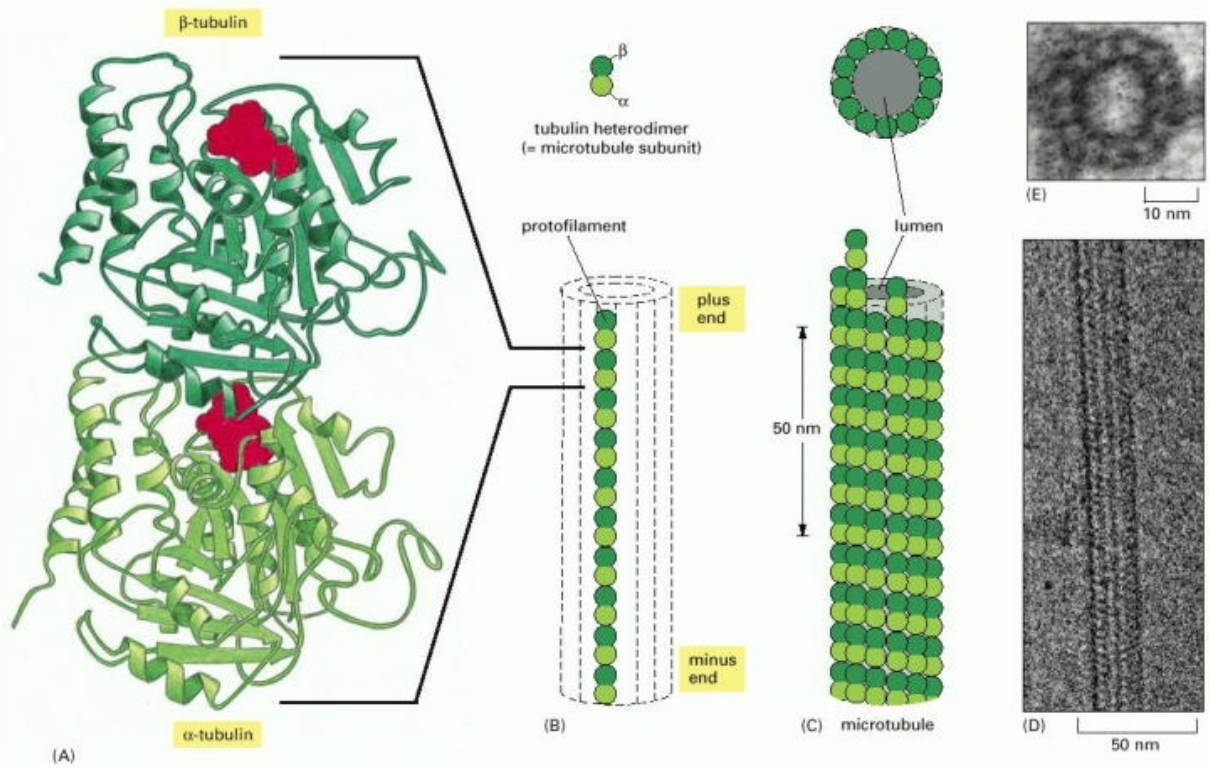

Figure 2. The structure of a microtubule and its subunit. (A) The subunit of a microtubule filament is a tightly bound α- and ß-tubulin heterodimer. The bound GTP nucleotides are shown in red. The GTP in α-tubulin is a tightly bound, integral part of the molecule that, unlike the GTP in ß-tubulin, is not involved in polymerization dynamics. (B) A single protofilament is built from tubulin heterodimers (= MT subunits) that are arranged head to tail. (C) The microtubule is a stiff hollow tube formed from 13 protofilaments that are aligned in parallel. (D) Electron micrograph of a microtubule. (E) Electron micrograph of a microtubule cross section, showing 13 protofilaments. (modified from Alberts, 2008)

Intermediate filaments

Intermediate filaments (IFs) are ropelike structures, approximately 10 nm in diameter. IFs are built from a heterogeneous group of proteins. The individual IF proteins are grouped into six types according to their amino acid sequences, net acidic charge and secondary structure predictions. Acidic and basic IF proteins are grouped as Type I and II. According to their mode of assembly, these two types, which include all keratins, can be grouped as assembly group 1. Assembly group 2 consists of type III and IV IF proteins and constitute the largest group of IF proteins. Desmin, paranemin, synemin, peripherin, GFAP and vimentin are grouped into type III, whereas α-internexin, the neurofilament proteins, nestin and syncollin are grouped into type IV. The nuclear lamins are grouped into type V and constitute the assembly group 3. Type VI IF proteins are only found in lens cells and have not been classified into an assembly group to date. Although they

fulfill various functions in different cell types, and despite their heterogeneity, all IF proteins share high amounts of structural similarities. They are all built from a highly conserved α-helical rod domain which is flanked by variable N-terminal head and C-terminal tail domains (Eriksson et al., 2009) (Figure 3).

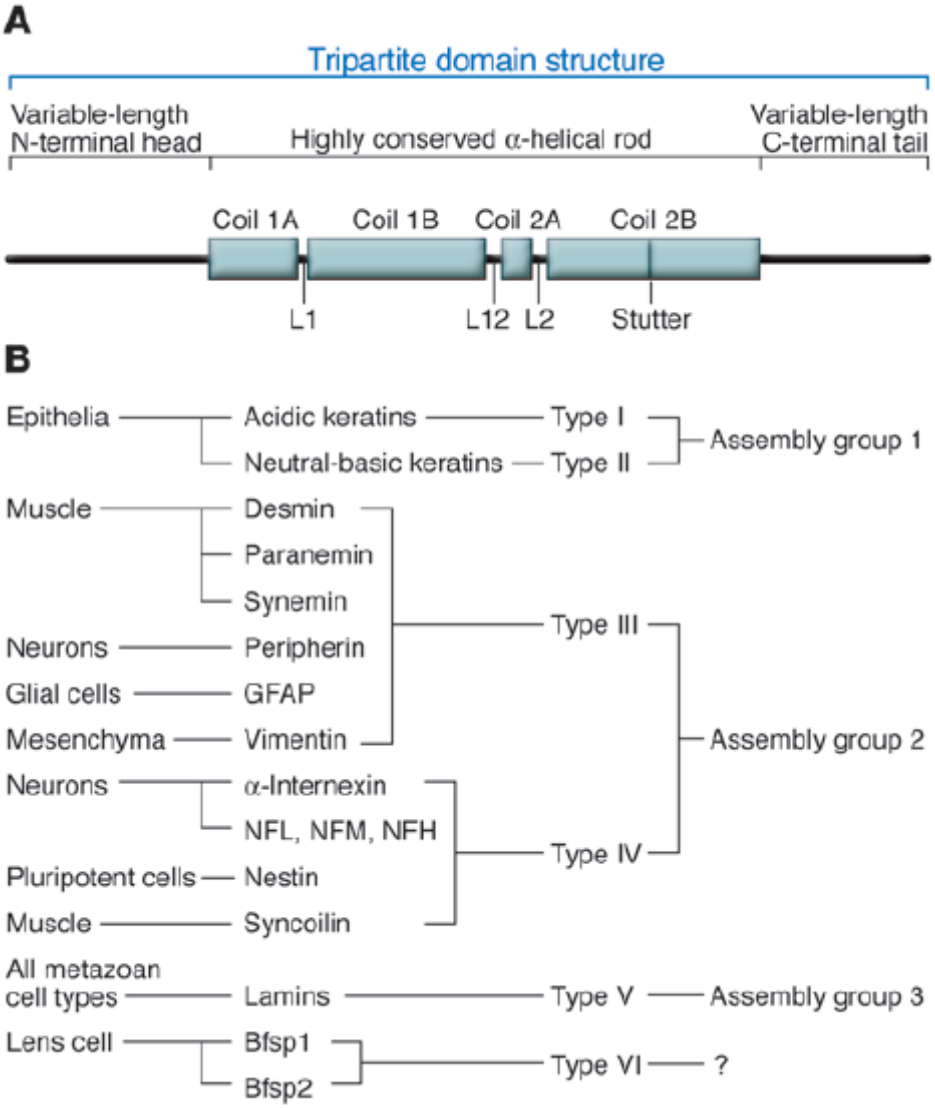

Figure 3. Intermediate filament classification. (A) The basic tripartite domain structure common to all IF proteins. A highly conserved α-helical rod domain is flanked by variable N- and C-terminal structures. (B) Based on the rod domain amino acid sequences, net acidic charge and secondary structure predictions, cytoskeletal IF proteins were grouped in four sequence homology classes (types I-IV). Nuclear IFs make another group (V). Group VI IFs are very specialized intermediate filaments only found in the lens of the eye. (modified from Eriksson et al., 2009)

Cellular organization of intermediate filaments

The IF network system consists of two individual networks. One, being located inside the nucleus, is attached to the nuclear pores, the inner nuclear membrane and chromatin. The other system, being cytoplasmic, connects intercellular junctional complexes with the outer nuclear envelope. Additionally, the cytoplasmic IF system is interlinked with the microtubule and the actin filament system. Interactions with the junctional adhesive complexes like desmosomes or hemidesmosomes and the other filament systems are mediated by a group of proteins called "plakins" (discussed below). The IF system also interacts with organelles like the Golgi apparatus, mitochondria, endosomes and lysosomes (Toivola et al., 2005; Kim and Coulombe, 2007). The nuclear and the cytoplasmic IF systems are interlinked by proteins of the outer nuclear membrane. Thus a mechanical continuum reaching from the extracellular matrix (ECM) to the nucleus exists inside a cell.

Intermediate filament assembly

To assemble into ropelike structures, two IF monomers align in parallel and in register to form a coiled coil dimer (Herrmann et al., 2007). One IF dimer, representing the basic building block of IFs, then lines up side by side with another, thus creating a staggered tetramer of antiparallel coiled-coil dimers. The tetramer is the soluble subunit form of IFS. When eight tetramers are packed together in a helical array, a robust ropelike filament is formed. (Herrmann et al., 2007). As a consequence of the antiparallel association of the dimers, intermediate filaments have no intrinsic polarity.

Intermediate filament assembly is independent of nucleotide hydrolysis, but remodeling and structural performance of IFs in vivo is dependent on kinases, phosphatases and chaperones (Green et al., 2005).

Intermediate filaments and disease

Over 40 genetically determined diseases are known today that are caused by mutations in IF-encoding genes (Fuchs and Cleveland, 1998; Irvine and McLean, 1999; Omary et al., 2004; Kim and Coulombe, 2007). Best characterized, is a disease, caused by mutations in keratin 5 or keratin 14 called epidermolysis bullosa simplex (EBS). EBS is a severe skin disease in which the basal keratinocytes layer of the epidermis is easily detached from the dermis when the skin is exposed to physical stress. (Bonifas et al., 1991; Coulombe et al., 1991; Lane et al., 1992). At least 13 mutations in laminin A that cause human diseases

have been described. Affected patients show symptoms including muscular dystrophies and premature aging (Bonne et al., 1999; Liu and Zhou, 2008). Mutations in desmin and GFAP were also described (Li et al., 2002; Goldfarb et al., 2004), and have been shown to cause muscular dystrophies, cardiomyopathies and a neuronal disease called Alexander disease respectively.

The plakin/cytoskeletal linker protein family

Plakins are large multidomain proteins that crosslink cytoskeletal filaments or link them to junctional complexes (Sonnenberg and Liem, 2007). They were first discovered in epithelial cells, where they connect IFs to desmosomes and hemidesmosomes (for review see Ruhrberg and Watt, 1997). The first plakin protein identified was named desmoplakin, due to the plaque like appearance of these junctional complexes (Mueller and Franke, 1983). Owing to the capacity of plakin proteins to link two or more cytoskeletal networks and the fact that most plakins do not localize in a plaque like pattern, these proteins have also been called cytolinkers (Wiche, 1998).

To date, seven members of the cytoskeletal linker protein family have been characterized in mammals (Figure 4): desmoplakin, envoplakin, periplakin, bullous pemphigoid antigen 1 (BPAG1), microtubule actin cross-linking factor 1 (MACF1) - also referred to as ACF7 - epiplakin and plectin (reviewed in Jefferson et al., 2004). Plakins are built from combinations of specific domains. A plakin domain, built by several spectrin repeats interrupted by an SH3 domain, is common to all cytoskeletal linkers with the exception of epiplakin. Additionally, according to specific functions of the individual proteins they possess domains that bind to actin (ABD), microtubules (GAR and GSR-containing domain) and intermediate filaments (PRD and linker region) (Leung et al., 2002). It is noteworthy that in plectin the intermediate filament binding occurs not at the PRDs themselves but in a linker region between the PRDs. Furthermore microtubules do not bind to the GAR and GSR-containing domains in plectin. The PRD is composed of varying numbers of repeating unit subdomains, termed A and B and C, depending on their degree of sequence similarity to each other (Leung et al., 2002). Epithelial cytoskeletal linker proteins possess a coiled-coil spectrin repeat-containing rod that enables them to form dimers (Janda et al., 2001).

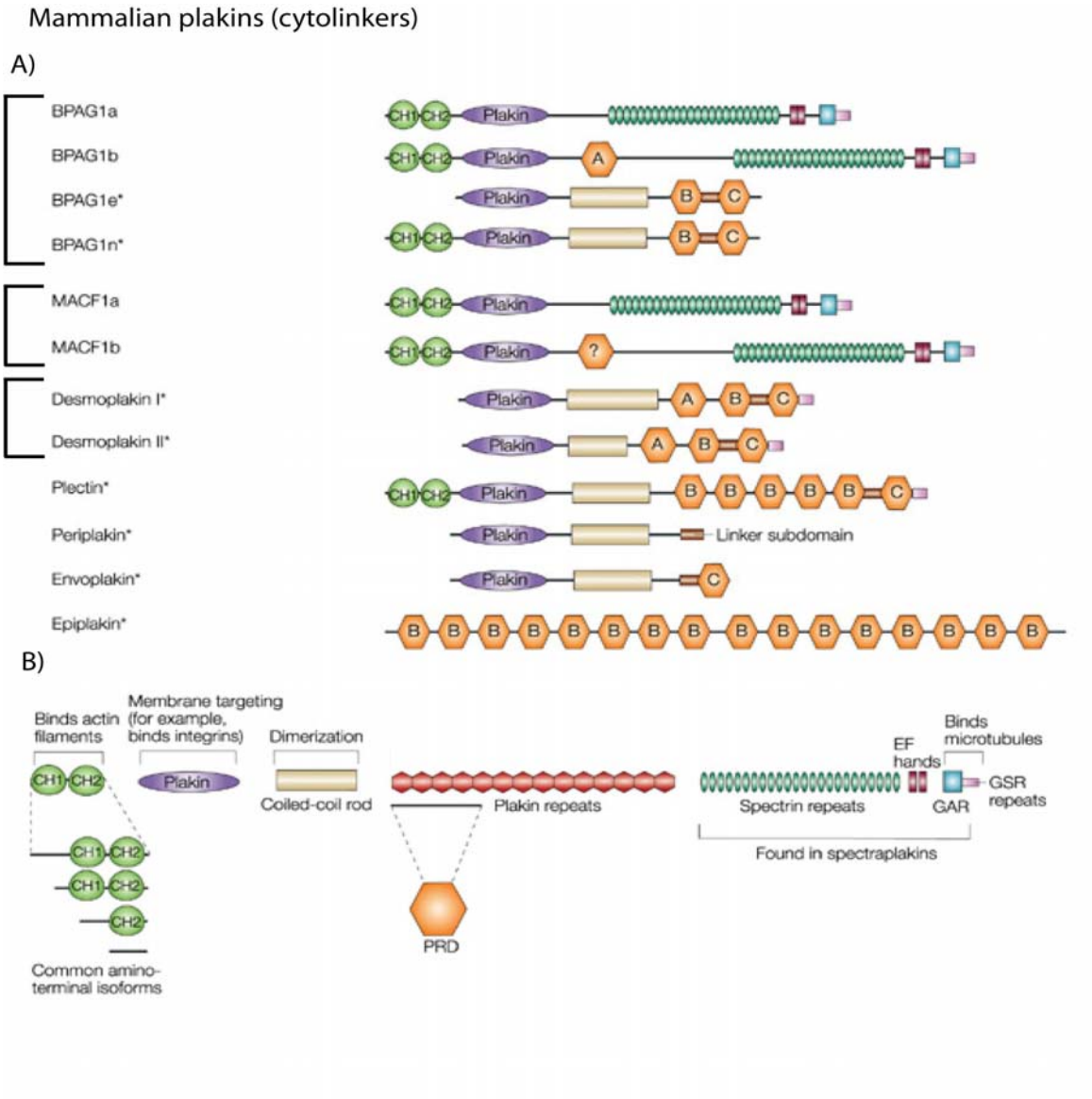

Figure 4. Schematic illustration of the plakin (cytolinker) family members and some of their splice variants. (A) The epithelial plakins (names highlighted with asterisks) display a characteristic tripartite structure (with the noteable exception of epiplakin) with a globular plakin domain at the amino terminus (purple), a central coiled-coil rod domain (yellow) and a variable number of plakin-repeat domains (PRDs) at the carboxyl terminus (orange); PRDs are grouped into three classes termed A, B and C, and these domains are connected by linkers that can also harbor plakin repeat (PR)-like motifs (brown). In the spectraplakins, the central coiled-coil rod domain that is found in the epithelial plakins is replaced by numerous spectrin repeats (green). The number of spectrin repeats and PRs vary between different plakins. (B) Schematic figure showing all important domains common to plakins in detail. The known function of each domain is indicated above the domains.
GAR, GAS2 related; GSR repeats, glycine-serine-arginine repeats; calponin-homology domain, CH. (modified from Jefferson et al., 2004)

Cytoskeletal linker proteins are mostly expressed in tissues that have to withstand severe mechanical stress, such as epithelia and skeletal muscle cells (Leung et al., 2002). There they crosslink cytoskeletal filaments and also connect them to membrane complexes. Hence it is no surprise that most pathological situations resulting from dysfunction of cytoskeletal linker proteins lead to disorders involving tissue fragility (for review see Sonnenberg and Liem, 2007).

Plectin

Pectin is a large cytoskeletal protein of approximately 500 kDa that is abundantly expressed in a wide variety of mammalian tissues and cell types (Wiche, 1989). Its unique combination of protein domains allows plectin to bind to all three major cytoskeletal filament systems; actin filaments, IFs and microtubules. Additionally plectin can bind to various plasma membrane-associated cytoskeleton junctional complexes (Pytela and Wiche, 1980; Koszka et al., 1985; Foisner et al., 1988; Andrä et al., 1998; Wiche, 1998), thus making it the most versatile cytoskeletal linker protein known to date.

Plectin consists of globular N- and C-terminal domains which are separated from each other by a 200 nm long α-helical rod domain (Figure 5). This tripartite structure is shared with other plakin family members except for envoplakin, periplakin and epiplakin. The C terminus is encoded by a single huge exon (exon 32). It comprises six plakin repeat domains (PRD), which all contain a core region made of a 19 amino acid motif that is tandemly repeated (Wiche et al., 1991). Linker regions between the repeats are believed to form loop-like structures that are susceptible for interactions with other proteins. Plectin's IF binding site resides in the linker region between PRD 5 and 6 (Nikolic et al., 1996). Among proteins that were identified as capable to bind to this site are vimentin (Foisner et al., 1988), cyto-keratins (Rezniczek et al., 1998), desmin (Reipert et al., 1999), neurofilaments, and GFAP (Foisner et al., 1988). Additionally integrin β_4 was shown to also interact with the C terminus (Rezniczek et al., 1998). Further interaction partners at this site are RACK1 (Osmanagic-Myers and Wiche, 2004) and AMPK (Gregor et al., 2006).

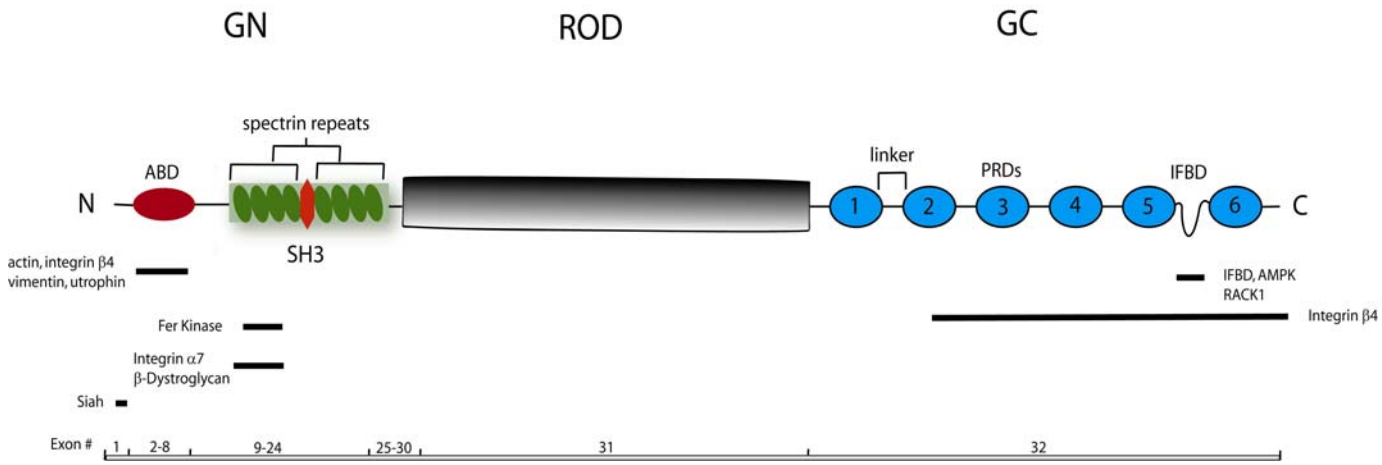

Figure 5. Schematic illustration of plectin's binding domains. Like most plakins, plectin has a tripartite structure which comprises a central rod domain (ROD), flanked by globular C- (GC) and N-terminal (GN) domains. The N-terminal structure contains the actin-binding domain (ABD) and a plakin domain, which is formed of eight spectrin repeats interrupted by a SH3-like domain. The C terminus is built from six homologous repeat domains (PRD) interrupted by linker regions. The N and the C termini both contain multiple binding sites for other proteins. The intermediate filament binding domain (IFBD) is located in the linker region between PRD 5 and 6. Interacting proteins are listed and defined binding regions are indicated by black bars. Coding exons are shown at the bottom.

The rigid α-helical rod is able to form coiled-coil dimers with a second plectin molecule. Being 200 nm large, the rod is perfectly suited to act as a molecular spacer between different cytoskeletal networks (Foisner and Wiche, 1987).

The N-terminal domain of plectin contains a highly conserved actin-binding domain (ABD), which consists of a pair of calponin-homology (CH) subdomains. This domain does not only interact with actin, but also with vimentin, integrin β_4, utrophin, nesprin 3α and dystrophin (Seifert et al., 1992; Rezniczek et al., 1998; Sevcik et al., 2004; Wilhelmsen et al., 2005; Rezniczek et al., 2007). Another feature of the globular N-terminal domain is a plakin domain. It consists of several spectrin repeats, interrupted by an SH3 domain.

In addition to its stabilizing and connecting features, plectin was shown to serve as a scaffolding protein for signaling molecules. Again plectin showed to be extremely

versatile. Plectin's size and the multidomain structure seem ideally suited for this purpose (Andrä et al., 1998; Osmanagic-Myers and Wiche, 2004; Osmanagic-Myers et al., 2006).

Plectin shows an unusual complex transcript diversity. 14 alternatively spliced first exons, 11 of them directly splicing into exon 2 were identified (Fuchs et al., 1999). The 11 plectin isoforms thus generated differ in their respective tissue expression patterns, protein stability, intracellular localization and specific functions (Rezniczek et al., 2003; Rezniczek et al., 2007; Hijikata et al., 2008; Winter et al., 2008; Kostan et al., 2009). In some cases two additional exons (2α and 3α) are optionally spliced into the ABD-encoding sequence, thereby creating fine-tuned acting-binding domains with different binding affinities for actin (Fuchs et al., 1999). In addition, plectin isoforms lacking exon 31, which encodes the rod domain, are expressed in various tissues (Elliott et al., 1997). The functions of these rodless-plectin isoforms are not known to date.

Plectin in disease

Plectin was originally believed to protect cells against mechanical stress. When it was shown that mutations in the plectin gene caused EBS–MD (an autosomal recessive disease characterized by skin blistering combined with muscular dystrophy) (Chavanas et al., 1996; Gache et al., 1996; McLean et al., 1996; Pulkkinen et al., 1996; Smith et al., 1996), EBS with pyloric atresia (an autosomal recessive disease variant that manifests with severe neonatal skin blistering and gastric abnormalities) (for review see Pfendner and Uitto, 2005) or epidermolysis bullosa simplex (EBS)–Ogna (an autosomal dominant skin blistering disease) (Koss-Harnes et al., 1997; Koss-Harnes et al., 2002). Intriguingly, for some EBS–MD patients signs of neurodegenerative disorders (cerebral and cerebellar atrophy) have been reported (Smith et al., 1996; Schröder et al., 2002). A patient suffering from EBS–MD showed degenerative signs, which were found in intramuscular myelinated nerves (Bauer et al., 2001). More recently, plectin was shown to be implicated in Alexander disease, a rare pathological disorder, which is caused by mutations in glial fibrillary acidic protein (GFAP) (Tian et al., 2006). In addition upregulation of plectin expression during astrocyte activation parallels the increase of GFAP expression and could thus be a general feature of reactive gliosis (Lie et al., 1998; Kalman and Szabo, 2000). Lately, cases of patients with mutations in the sequence encoding the plectin isoforms 1f were reported (Gundesli et al., 2010). These patients

suffered from limb-girdle muscular dystrophy. Probably due to the loss of plectin 1f scaffolding at the sarcolemma of skeletal muscle (Rezniczek et al., 2007).

Plectin mouse models

To study the molecular mechanisms behind these diseases and plectin's other functions, plectin-null mice were generated by targeted gene deletion (Andrä et al., 1997). Plectin-deficient mice died a few days after birth due to severe skin blisterings. They also developed muscular dystrophies in skeletal and heart muscle (Andrä et al., 1997). Impaired food uptake because of blistering on the palates proved to be the reason for their mortality (Ackerl et al., 2007). Striated muscle-specific conditional plectin knock-out mice subsequently generated showed progressive degenerative alterations in striated muscle, including aggregation and partial loss of IF networks, detachment of the contractile apparatus from the sarcolemma, profound changes in myofiber costameric cytoarchitecture, and decreased mitochondrial number and function (Konieczny et al., 2008). To study the function of individual plectin isoforms, specific knockout mice were engineered for plectin 1 – where primary fibroblasts and leukocytes showed reduced migratory potential (Abrahamsberg et al., 2005), plectin 1b – where primary fibroblasts and myoblasts showed altered mitochondrial morphology (Winter et al., 2008) and plectin 1d, which links the IF network to Z-disks and where its loss leads to muscular dystrophy (Konieczny et al., 2008). Plectin 1c-specific KO mice revealed a role of this isoform in motor nerve conduction (Fuchs et al., 2009).

The peripheral nervous system

The peripheral nervous system (PNS) comprises nerves and ganglia outside the central nervous system (CNS). It can be divided further into the somatic and the autonomic nervous system. The main role of the PNS is to relay information in the form of electric currents from the CNS to organs and muscles. For this purpose, there are two types of neurons in the PNS. The motor neurons (or efferent neurons) relay signals away from the CNS towards the periphery, and the sensory neurons (or afferent neurons) relay signals, received in the periphery, to the CNS. Unlike the CNS, the PNS is not protected by a cage of bone (e.g. the skull and the vertebra) and thus is susceptible to mechanical stress and injury. However, similar to CNS the nerves' axons are surrounded by glia cells that fulfill three main functions: i) electrically isolating the axon to enable the saltatory move conduction; ii) connecting the axons to the surrounding basal membrane, thus stabilizing

the nerves and ensuring their protection from mechanical stress; iii) transducing signals from the ECM to influence morphology and differentiation of the nerves. In the CNS, the glia cells consist of astrocytes, oligodendrocytes and microglia. In the PNS there is only a single cell type called the Schwann Cells (SCs).

Myelinating SCs

Myelinated axons are a fundamental adaptation of vertebrates to guarantee a faster and more efficient signal transduction. Upon differentiation SCs wrap around the axons and electrically isolate them by the synthesis of myelin, a biomembrane which is especially rich in lipids. Specific regions of the axons are left uncovered which are called nodes of Ranvier (for review see Salzer et al., 2008). There the action potential, originally generated at the axon initial segment (AIS), is regenerated, resulting in a more rapid and energy efficient propagation of signals than observed in unmyelinated fibers (Salzer, 1997). Named after the german physiologist Theodor Schwann, the SC is the glial cell type that accounts for the myelination of axons in the PNS (Figure 6). The myelinating SCs are highly specialized cells which are radially and longitudinally polarized in their differentiated state (for reviews see Poliak and Peles, 2003; Salzer, 2003). The radial polarization is reflected by the fact that myelinating SCs possess two distinct plasma membrane surfaces: one that faces the axon (axonal membrane) and the other facing the surrounding basal membrane (abaxonal membrane). The two membrane surfaces differ in their protein composition and their domain organization. The inner, adaxonal, membrane and the underlying axolemma form strictly organized domains including the nodes of Ranvier, paranodes, juxtaparanodes and the internodes.

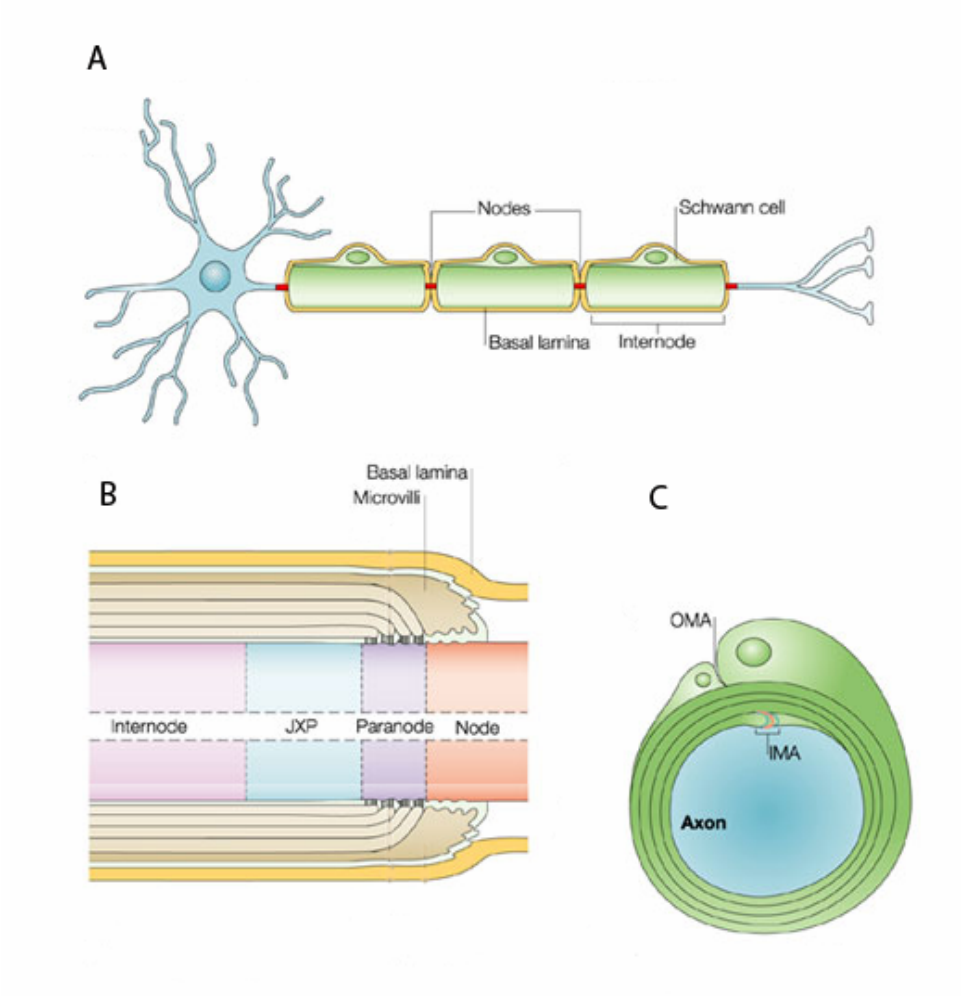

Figure 6. Schematic depiction of myelinating axons. (A) SCs enwrap axons in the PNS, thus forming the myelin sheath and electrically isolating the nerve along the internodes, leaving only the nodes of Ranvier exposed to the basal lamina. The action potential is only regenerated at the nodes (depicted in red). In contrast to oligodendrocytes of the CNS, SCs wrap around one single axon. (B) A longitudinal section through a SC-axon unit illustrating the domain organization of myelinated SCs. Through crosstalk with the SC, the axon becomes structured into nodes, paranodes, juxtaparanodes (JXP) and internodes. Microvilli, formed by the abaxonal SC membrane are in close contact with the nodes of Ranvier. At the paranode, paranodal loops form membrane appositions with the axon called septate like junctions, which are believed to create a physical barrier between the node and the paranode. The node of Ranvier is directly covered by the basal lamina. (C) A schematic cross section of a myelinated nerve fiber showing the two different membrane surfaces. The abaxonal membrane (outer mesaxon – OMA) and the adaxonal membrane (inner mesaxon – IMA). (modified from Poliak and Peles, 2003)

Hence it is not surprising that the concentration of sodium channels (~1500/μ^2) is 25-fold higher at the nodes of Ranvier than at the internode (Hille, 2001). The nodes are flanked by domains called paranodes. Here the SC membranes form loops (septate like junctions), which create a close apposition between SCs and the axonal membranes. These structures are thought to create physical barriers between the node and the

internode. The juxtaparanodes, a domain, that is not well studied and understood to date, separates the paranodes and the internodes. At the internodes, by far the biggest domain in the myelinated nerve fiber, the axolemma and the adaxonal SC membrane are separated by a periaxonal space of 15 nm.

In addition to the domain organization on the axon-facing side of the SC, the abaxonal side of the cell is also compartmentalized. Almost 80 years ago Ramón y Cajal (1933) described channel like structures at the outermost cytoplasm in SCs. He argued that these cytoplasmic tunnels, which where called after him Cajal bands, had nutritive functions. The Cajal bands represent the cytoplasm between the abaxonal SC membrane and the underlying myelin. These cytoplasmic channels are interspersed by regions where the plasma membrane forms tight appositions with the myelin. Thus the cytoplasm forms longitudinal Cajal bands and radial trabeculae.

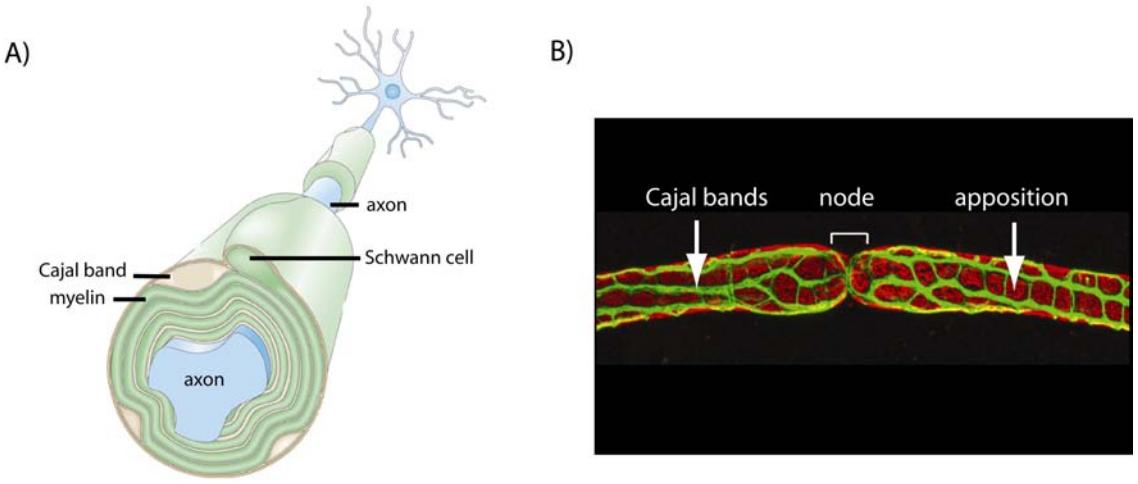

Figure 7. Cajal bands and appositions. (A) A schematic depiction of a myelinated axon. The SC wraps around the axon, forming regions of compact myelin where the myelin is in close apposition to the abaxonal membrane. Other regions, called Cajal bands represent cytosolic longitudinal tunnels which are linked by transverse trabeculae (modified from Nature publishing group). (B) Immunofluorescent staining of teased nerve fibers, featuring a node of Ranvier. A staining of vimentin shows its localization in Cajal bands (green). Appositions are shown with a staining for DRP2 (red).

Schmidt-Lanterman incisures present funnel-shaped interruptions in the compact myelin, creating connections between the cytosol of the SC domain that is apposing the axon and the region that is apposing the basal lamina. Compartmentalization of the SCs is crucially dependent on interactions and crosstalk with the ECM, which is mediated by transmembrane ECM-receptor proteins.

Abaxonal SC receptor complexes

Big advancements have been made in the recent years in understanding on the molecular level what Ramón y Cajal had observed 100 years ago. Myelinating SCs differentiate from immature SCs upon signals derived from axons. In response the SCs organize the compartmentalization of the axons, as already described above. To fulfill their various functions the myelinating SCs need to hold close contact to the surrounding basal membrane through abaxonal SC ECM-receptor complexes. The basal lamina surrounding the myelinated nerves is composed of collagen IV, fibronectin, heparin sulfate proteoglycan, and laminins. Experiments designed to find out which of the major basal lamina components promotes myelination by SCs demonstrated that laminins are necessary and sufficient for the differentiation of SCs to become myelinating SCs (Eldridge et al., 1989). An intact ECM was shown to be necessary for providing mechanical stability during myelination (Podratz et al., 2001). Four laminin 211 receptors in the abaxonal SC membrane have been described: integrin α7β1, integrin α6β4, integrin α6β1 and the dystrophin-glycoprotein complex (DGC). Integrin α6β1 is crucial for the development of the PNS and axonal sorting during development (Previtali et al., 2003b). The other three laminin 211 receptors are expressed postnatally. Integrin α6β4 and the DGC are expressed right before myelination, whereas integrin α7β1, which is dispensable for development and myelination of the peripheral nerve, is expressed during myelination (Previtali et al., 2003a; Previtali et al., 2003b).

Integrin α6β4 is expressed during myelination after axonal contact has been established and subsequently localizes at the abaxonal SC membrane apposing the basal lamina (Feltri et al., 1994). The complex was shown to be dispensable for development, myelination, maturation or regeneration of peripheral nerves. However in older mice lacking integrin α6β4 an increased number of axonal myelin infoldings was observed (Nodari et al., 2008). In line with the observation that the expression of integrin α6β4 increases during adulthood this indicated a similar role for SC-specific integrin α6β4 as in skin: mechanical stabilization of the cells via stable anchorage to the basal lamina (Nodari et al., 2008). Integrin β4 has a uniquely long cytoplasmic tail which facilitates multiple interactions. In SCs integrin α6β4 is associated with another transmembrane protein called peripheral myelin protein 22, whose alterations account for the most common demyelinating hereditary neuropathy, the Charcot-Marie-Tooth disease (Roa et al., 1993).

The DGC (also termed dystroglycan complex) is a well described receptor complex. At its heart there is a heterodimeric adhesion receptor that consists of two glycoproteins which are transcribed from one gene and are then posttranslationally cleaved. The extracellular protein that mediates linkage with the basal lamina is called α-dystroglycan. It is subject to extensive O- and N-linked modifications. α-dystroglycan is bound, noncovalently to the transmembrane protein of the receptor complex called β-dystroglycan. (for reviews see Bozzi et al., 2009b; Moore and Winder, 2010). The DGC is an incredibly versatile receptor with functions ranging from a sarcolemmal stabilizer in skeletal muscle to roles in embryogenesis, cancer progression and cell signaling (Spence et al., 2004; Anderson et al., 2007; Cross et al., 2008). Like integrin α6β4, dystroglycan is expressed after birth but before the onset of myelination and becomes polarized to the abaxonal membrane upon start of myelination. (Previtali et al., 2003b). Specific ablation of dystroglycan in SCs leads to reduced nerve conduction velocity and nodal changes including disorganized microvilli and reduced sodium channel clustering. Additionally, similar to SC-specific integrin α6β4 knockout mice, more myelin infoldings were detected in DG-KO mice (Saito et al., 2003).

In skeletal muscle, β-dystroglycan is intracellularly bound to dystrophin and utrophin. These two proteins link the laminin receptor to filamentous actin (Rybakova et al., 2000). In addition β-dystroglycan was shown to bind plectin, thus being connected to actin and/or intermediate filaments (Rezniczek et al., 2007). In myelinating SCs no full length dystrophin is present, but an alternatively spliced N-terminal isoform (DP116) is expressed (Byers et al., 1993). DP116 contains the dystroglycan binding domain but is lacking the actin binding part. On the other hand, utrophin is expressed in SCs in its original form, thus being likely able to mediate binding to filamentous actin. This laminin-211-dystroglycan-utrophin axis is only present in cytoplasmic compartments (Cajal bands) of the myelinating SCs (Court et al., 2009). It is necessary for compartmentalization and elongation of myelin segments (Court et al., 2009). Another dystroglycan complex was shown to be localized to the appositions, which are segmenting the Cajal band. In this complex α- and β-dystroglycan interact with the dystrophin-related protein 2 (DRP2) to bind to L-periaxin. DRP 2 is the only protein known to date that is solely expressed in appositions (Sherman et al., 2001). Figure 8 gives an overview of the abaxonal SC laminin 211 receptors.

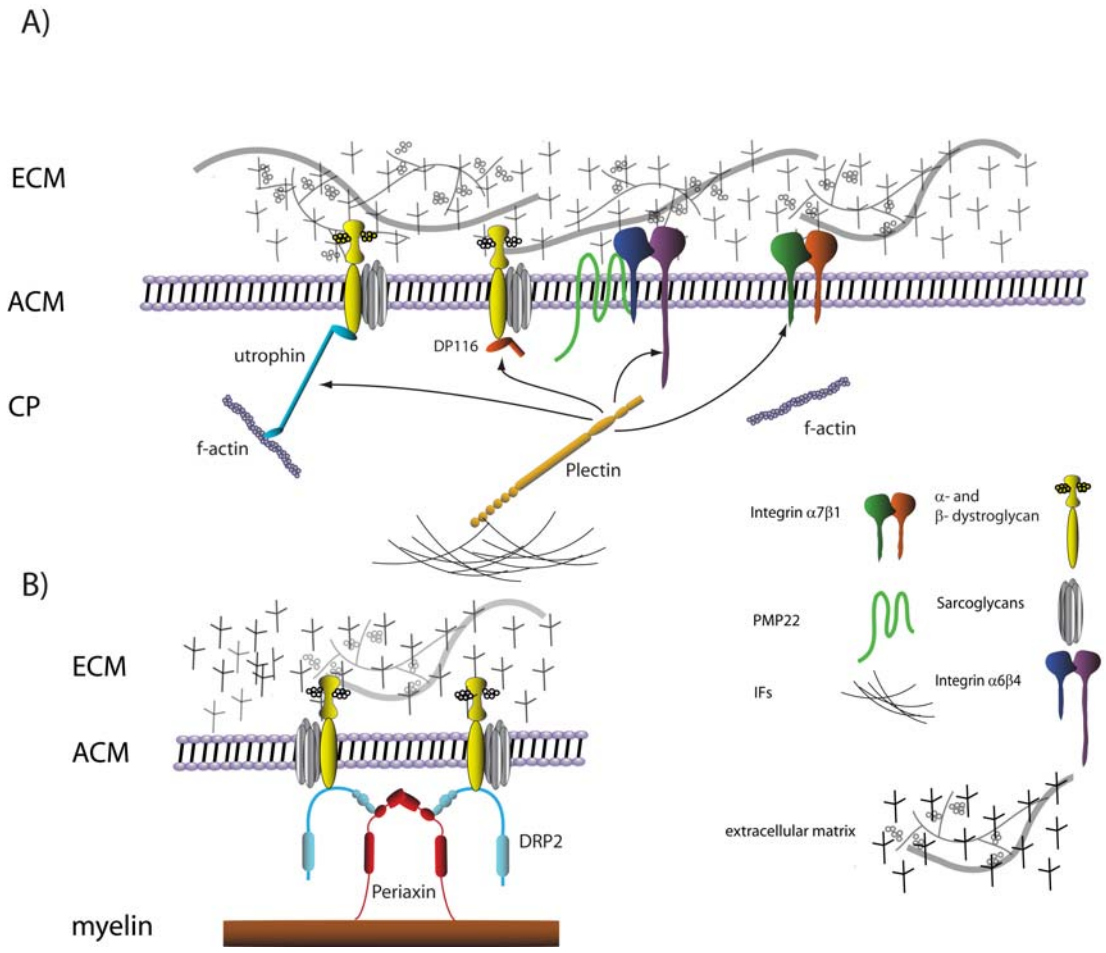

Figure 8. Abaxonal SC membrane laminin receptor complexes. (A) A simplified illustration of laminin 211 receptors found in the abaxonal SC membrane (ACM) of Cajal bands (cytoplasmic regions). Depicted are the dystrophin-glycoprotein complex (DGC), integrin α7β1 and integrin α6β4. In the DGC, dystroglycan can be associated with utrophin and DP116. Utrophin can bind to filamentous actin (f-actin) thus interlinking the ECM via the dystroglycans with the actin cytoskeleton. In contrast to utrophin, DP116 lacks the actin-binding domain. The sarcoglycans, a protein complex consisting of four sarcoglycan subunits that is associated with ß-dystroglycan, is also shown. Integrin α6β4 is associated with PMP22. Plectin could form interactions with all the transmembrane ECM-receptors shown here, as well as with utrophin, DP116 and the intermediate filament system. (B) The DGC is also found in appositions where the abaxonal SC membrane is directly apposing the compact myelin, leaving no space for the cytoplasm. There, β-dystroglycan is binding to the dystrophin-related protein 2 (DRP2) which binds to periaxin. Periaxin forms dimers via its PDZ domain.
(CP – cytoplasm of Cajal bands)

Intriguingly, plectin was shown to directly bind to integrin β4, β-dystroglycan and integrin α7 (unpublished data) in other tissues (Rezniczek et al., 1998; Rezniczek et al., 2007), thus making it a likely candidate for important roles in the SC.

Aims of the thesis

The goal of this thesis was to investigate if plectin forms ECM-IF axes by binding to laminin-receptor complexes of the abaxonal SC membrane. To investigate this possibility I first wanted to identify which plectin isoforms are expressed in SCs of sciatic nerve, by using immunofluorescence microscopy and immunoblotting analyses. The next goal was to find possible interactions of plectin with the laminin 211 receptors by using immunofluorescence microscopy, co-immunoprecipitation and overlay assays. To further investigate plectin's role in association with the laminin-receptors and to assess consequences of a loss of plectin in SCs, I made use of the recently established P0-Cre/ plectin cKO mouse line. Possible alterations in the expression levels of cytoskeletal proteins as well as possible alterations in the stability of the laminin receptor complexes were to be tested. Furthermore the effect of plectin's absence on the compartmentalization of myelinating SCs and the differentiation into distinct domains of myelinated axons should be investigated. Ultimately primary SCs were to be isolated from wild-type and P0-Cre/cKO mice and analyzed for phenotypic changes including adhesion, proliferation, migration and their capability to react to signaling molecules.

Results

1. Identification of the major plectin isoforms expressed in sciatic nerves and SCs

Detection of plectin isoforms 1 and 1c on frozen sciatic nerve cross sections

Plectin, in particular isoform 1c, has been previously shown to be expressed in SCs in situ as well as in cultured SCs ex vivo (Fuchs et al., 2009). However, it remained unclear if other isoforms were expressed in SCs as well. Cryo-fixed sciatic nerve cross sections, were immunofluorescence labeled, using antibodies specific for plectin isoforms 1 (Abrahamsberg et al., 2005), 1a (Rezniczek et al., 1998), 1c (Fuchs et al., 2009) and 1f (Rezniczek et al., 2007) (Figure 9). In addition, the sections were stained with antibodies to the neurofilament medium chain to visualize the axons. Antibodies to plectin isoform 1 as well as those to plectin 1c produced signals and were found to label the cytoplasm of SCs in sciatic nerve cross sections (arrows in Figure 9B,D), whereas antibodies to the isoforms 1a and 1f produced only stainings in other cell types (arrowheads in Figure 9C,E). However, when we stained teased myelinated nerve fibers with antibodies to plectin isoform 1f, we observed its expression in nodes of Ranvier and Schmidt-Lanterman incisures (SLIs) (Figure 9F). The low abundance of the nodes of Ranvier explains why no SC-specific plectin 1f staining could be detected in sciatic nerve cross-sections.

Analysis of plectin isoforms in total cell lysates from sciatic nerve and primary SCs

Subsequently, isoform specific antibodies were used to analyze plectin isoform expression in total cell lysates derived from sciatic nerve of wild-type mice. In peripheral nerves, SCs are present in a differentiated, myelinating state. However, peripheral nerves contain also fibroblasts and blood vessels in addition to SCs, making the interpretation of immunoblots of sciatic nerve total cell lysates difficult to interpret.

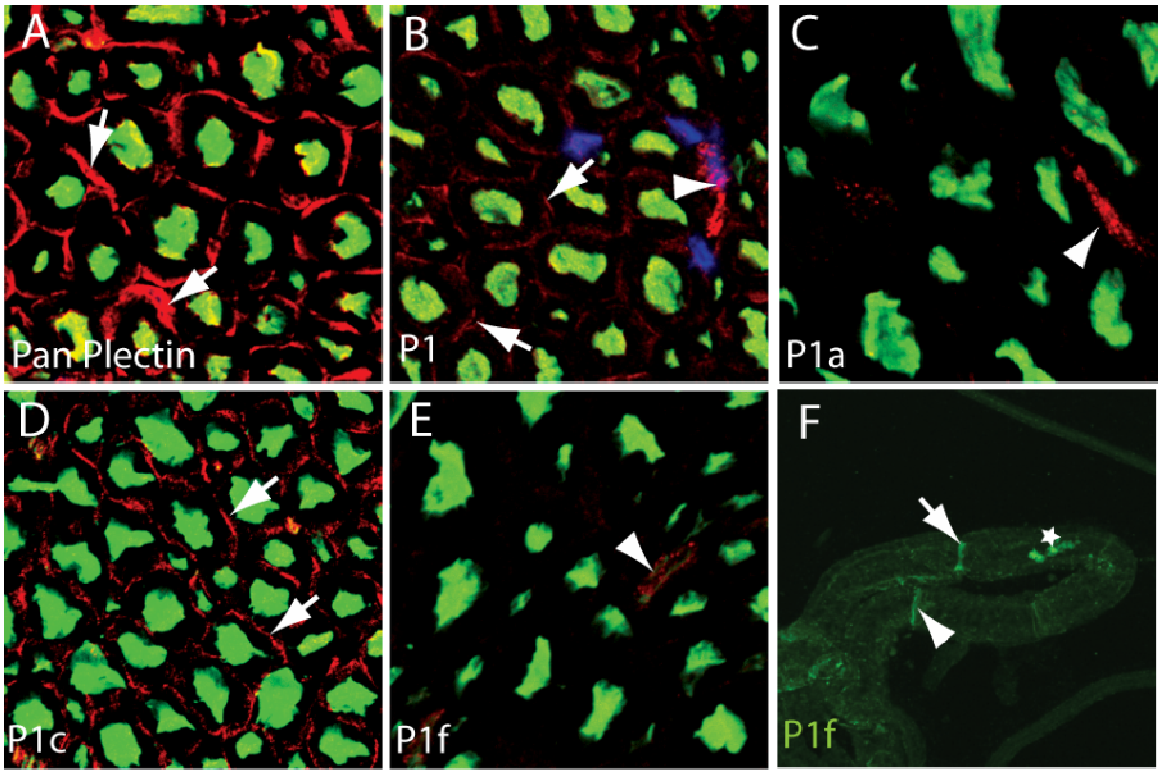

Figure 9. Analysis of plectin isoform expression on frozen sciatic nerve cross sections by immunofluorescence microscopy. (A-E) Cryo-fixed sciatic nerve cross sections were immunostained using plectin isoform-specific antibodies as indicated. Antibodies to the neurofilament medium chain were used to visualize axons. Plectin-specific immunostaining appears in red, neurofilament medium chain-specific immunostaining is shown in green. Expression of plectin 1 and 1c was detected in both SCs and axons (B,D), whereas plectin 1a and 1f expression could be detected only in other cell types, presumably endoneurial fibroblasts and blood vessels (arrowheads in C,E). Arrows depict plectin-specific staining in the cytoplasm of myelinating SCs. Arrowheads show plectin staining in cell types other than SCs, such as endoneurial fibroblasts and blood vessels. (F) Teased sciatic nerve fibers were immunostained using antibodies to plectin 1f. Note specific labeling of nodes of Ranvier and of Schmidt-Lanterman incisures.

To obtain a plectin isoform expression profile specific for SCs, without background signals stemming from endo- and perineuronal fibroblasts, blood vessels, and axons, primary SCs were isolated from sciatic nerves derived from wild-type mice. These cells were grown in culture for three days and total cell lysates were subsequently prepared. Based on assessments using morphologic criteria, such cultures were found to still contain some (<5%) endoneurinal fibroblasts. Therefore we also prepared cultures of the contaminating endoneurinal fibroblasts (eFs), free of SCs. Total cell lysates from sciatic nerve, primary SCs and eFs were subjected to SDS-PAGE and subsequently analyzed by immunoblotting. The results of these analyses are shown in Figure 10.

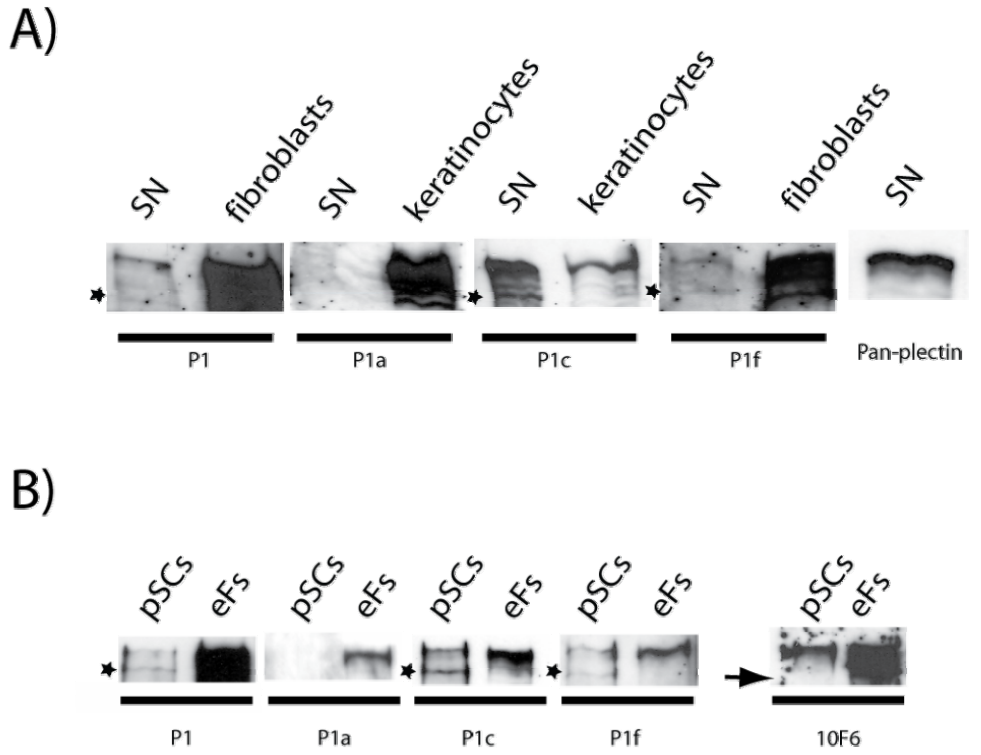

Figure 10. Immunoblotting of plectin isoforms 1, 1c and 1f in total cell lysates from sciatic nerve and primary SCs. (A) Analysis of sciatic nerve cell lysates using an antiserum not discriminating between isoforms (pan-plectin) as well as antibodies to plectin isoforms 1, 1a, 1c and 1f. Note that antibodies to plectin isoforms 1, 1c and 1f all produced a second band of lower molecular mass, likely representing plectin rodless isoforms. Total cell lysates obtained from fibroblasts and keratinocytes (MK +/+ p53 -/- Andrä et al., 2003) were used as positive controls. (B) Primary SCs were isolated from sciatic nerves of wild-type mice, and kept in culture for three days before preparation of total cell lysates for immunoblotting. Antibodies to plectin isoforms 1, 1a, 1c and 1f were used. Endoneurial fibroblasts, isolated from the same sciatic nerves were analyzed in parallel. Note the presence of a second immunoreactive band of lower molecular mass (indicated by asterisks) which was not detected using mAb 10F6.

In both, the sciatic nerve and the primary SC total cell lysates, the antibodies to plectin isoform 1c generated the most prominent signal, indicating that plectin 1c might be the dominant, or at least the strongest expressed isoform in myelinating as well as in undifferentiated SCs. However, since nothing is known about the antigen affinities of the antibodies used, and also the background signals from cell types other than SCs have to be considered, no precise conclusions about relative expression levels of plectin isoforms could be made. Antibodies to plectin isoform 1 produced robust signals in both lysates albeit they were not as strong as the signals obtained with antibodies to plectin isoform 1c. Plectin 1f could be detected as well in both lysates, although the intensity of the signal

in sciatic nerve total cell lysates was at the lower limit of detection. In neither of the lysates, could expression of plectin isoform 1a be detected by immunoblotting. Endoneurial fibroblasts were found to express all four plectin isoforms analyzed.

Strikingly, antibodies to plectin isoforms 1, 1c and 1f all produced a second band of lower molecular mass in sciatic nerve and primary SC total cell lysates (Figure 10). These bands most likely represented the rodless plectin isoforms (Fuchs et al., 1999). To verify this, immunoblotting of primary SC total cell lysates was performed using a monoclonal antibody (mAb) 10F6 which binds to plectin's rod domain, and thus can detect the full length but not the rodless plectin variant. In fact only the upper, full length plectin band was detected on immunoblots using mAb 10F6 (Figure 10B). We also observed, that the rodless isoforms seemed to be more prominent in total cell lysates derived from primary SCs than in those from sciatic nerve (compare asterisks in Figure 10A,B).

Immunolocalization of plectin isoforms in primary SCs

To assess the cellular localization of plectin isoforms primary SCs were subjected to immunofluorescence microscopy using isoform-specific antibodies to plectin 1, 1a, 1c, and 1f. For comparison, anti pan-plectin antiserum was used and cell nuclei were stained with Hoechst dye. The anti pan-plectin staining was used to set the laser intensities and detection thresholds with which all other images shown in Figure 11 were acquired. Using the pan-plectin antiserum, plectin was found to be distributed evenly through the cytoplasm of primary SCs (Figure 11A). In contrast, antibodies to plectin 1 produced a strong signal which was concentrated around the nucleus (Figure 11B). Like on the immunoblots, antibodies to plectin isoform 1c strongly stained primary SCs, but unlike plectin 1, plectin 1c was also found in the SCs' processes (Figure 11C). Again in accordance with the immunoblots, the plectin 1f antibody gave a very faint signal on SCs (Figure 11E). This could indicate that the plectin 1f-specific signals detected in primary SC total cell lysates originated from contaminating fibroblasts. Surprisingly, also antibodies to plectin 1a produced immunofluorescence signals (Figure 11D). On immunoblots plectin 1a antibodies produced a very strong background staining (data not shown). The immunofluorescence signal, likely is unspecific.

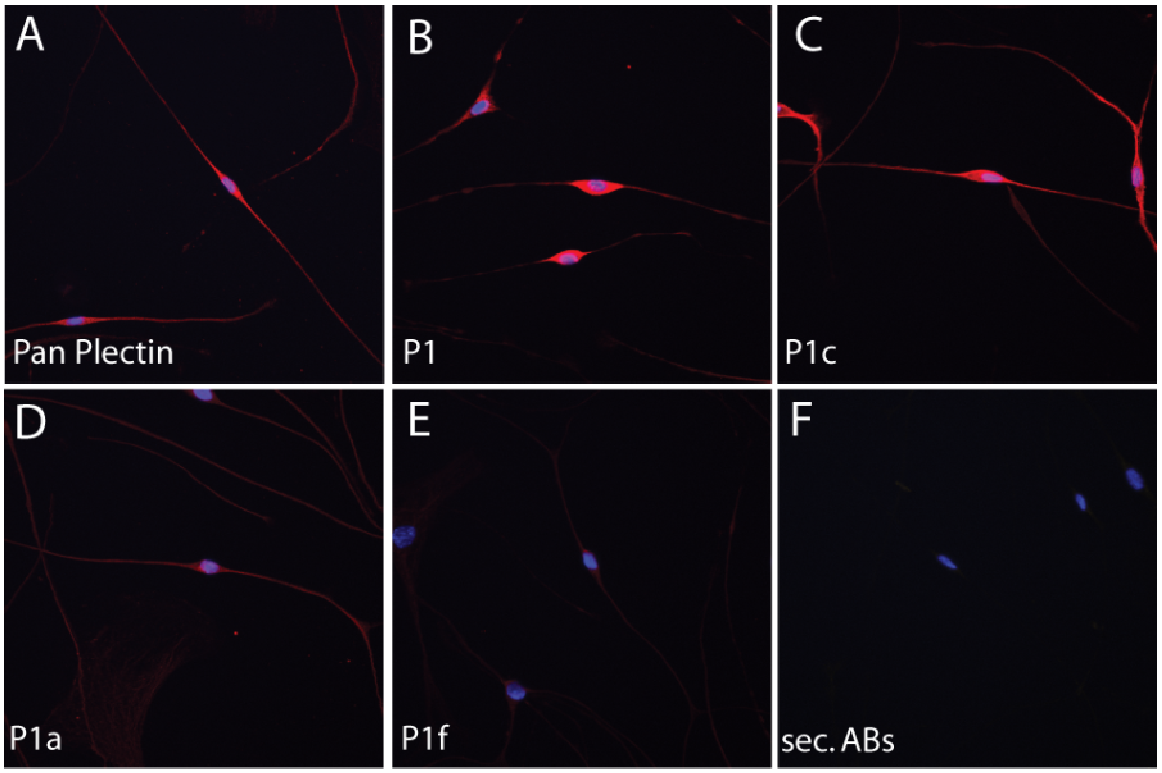

Figure 11. Immunolocalization of the major isoforms of plectin in primary SCs. Primary SC cultures were methanol-fixed and subjected to immunofluorescence microscopy using the same set of antibodies as in Figure 10. The plectin signal is shown in red, nuclear Hoechst staining is shown in blue. Note the presumably unspecific staining of SCs with antibodies to plectin 1a (D).

2. Identification of SC-specific plectin interaction partners

As explained in the introduction, three out of four known laminin 211 receptors located in the abaxonal SC membrane, are found in the same compartment as plectin in mature myelinating SCs, namley integrin α7β1, integrin α6β4 and the DGC. The DRP2 complex is exclusively found in SC membrane appositions, a SC compartment where plectin is not expressed (Figure 12). Therefore, this complex was excluded from our interaction analysis. Due to technical limitations we also did not investigate a potential interaction between plectin and integrin α7. Hence, for the analysis of plectin binding partners in SCs we focused on integrin α6β4 and the DGC, both of which have been previously shown to interact with plectin in other tissues.

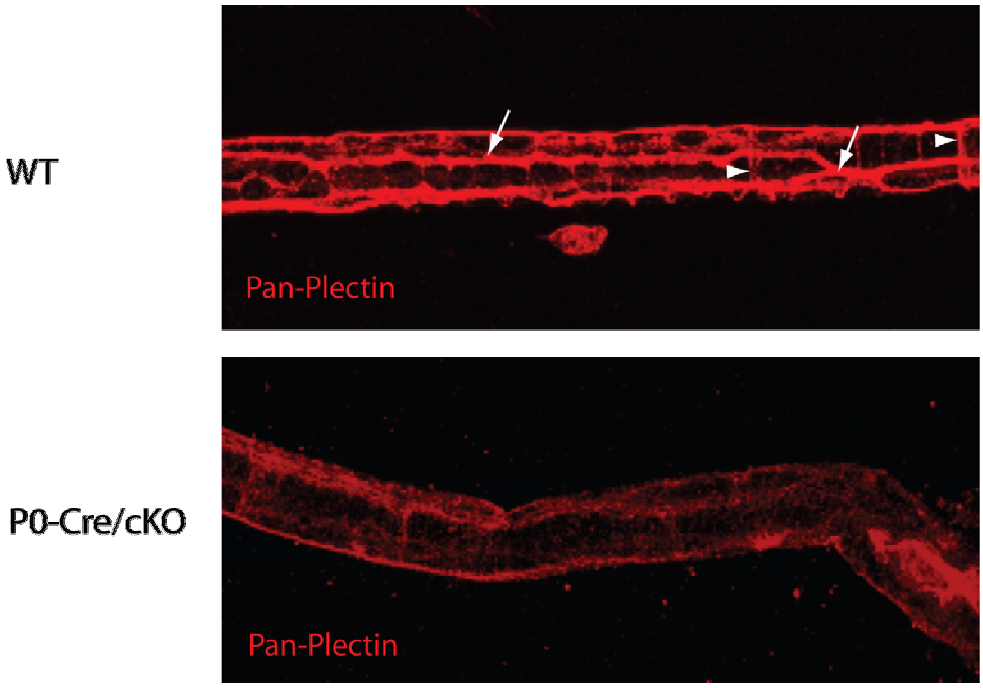

Figure 12. Immunofluorescence microscopy of teased nerve fibers using anti pan-plectin antibodies (#21). Note staining of Cajal bands (arrows) and their interlinking trabeculae (arrowheads). The background staining of sciatic nerve fibers from P0-Cre/cKO mice was considered unspecific, as previous data had shown that plectin is lacking from SCs of P0-Cre/cKO mice (data not shown).

Co-IP of plectin with β-dystroglycan from sciatic nerve homogenates

Rat sciatic nerve homogenates were used to test for the interaction of plectin with the SC-specific DGC. The homogenates were precleared with protein-G agarose beads to avoid

false positive results stemming from proteins unspecifically binding to the beads. The pre-cleared supernatant was then incubated overnight with a mixture of two antisera recognizing β-dystroglycan (Ilsley et al., 2001). A co-immunoprecipitation (Co-IP) using antibodies to GFP was carried out in parallel, using a precleared aliquot of the same sciatic nerve homogenate. The precipitated immunocomplex was separated by SDS-PAGE and tested for the presence of β-dystroglycan and co-precipitated plectin by immunoblotting analysis. Figure 13 shows that plectin as well as full length β-dystroglycan (β-DG 43) and a 30 kDa fragment (β-DG 30) generated by proteolytic cleavage of β-dystroglycan, were co-immunoprecipitated with the antisera directed against β-dystroglycan. Neither plectin, nor β-dystroglycan could be detected in control IPs using an antiserum to GFP. These findings indicated that β-dystroglycan was an interaction partner of plectin in SCs.

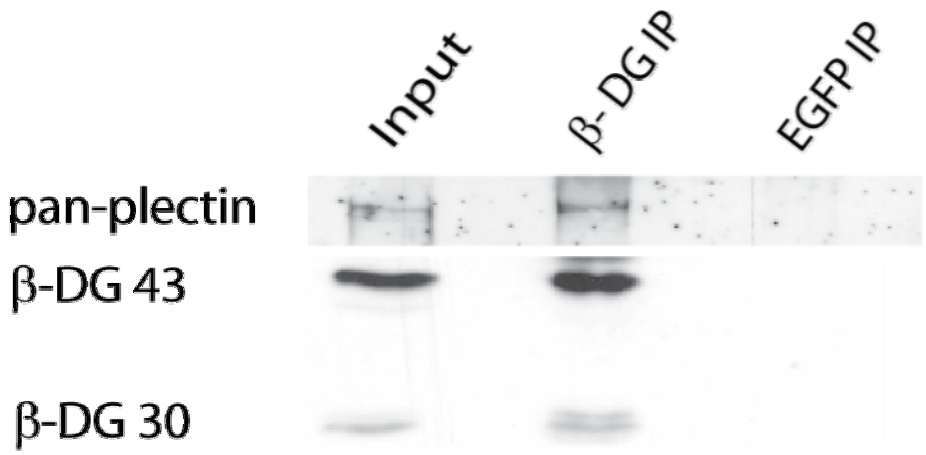

Figure 13. Immunoblots demonstrating co-precipitation of plectin with β-dystroglycan. Rat sciatic nerve homogenates were subjected to immunoprecipitation experiments using a mixture of two anti-β-dystroglycan antisera as bait antibodies and an anti-GFP antiserum as control. Immunoprecipitates were separated on SDS-PAGE and subjected to immunoblotting using antibodies to plectin and β-dystroglycan. Note that full length β-dystroglycan (β-DG 43), as well as a 30 kDa β-dystroglycan fragment (β-DG 30) were found in the precipitate.

Co-precipitation of vimentin and integrin β4 with plectin in sciatic nerve homogenates

To validate the plectin-β-dystroglycan interaction, a second Co-IP experiment was performed, this time using an antiserum to plectin (serum #9 Andrä et al., 2003) as bait antibodies. Again, rat sciatic nerve homogenates were used as input. Like for the dystroglycan IP, a parallel IP with antibodies to GFP as bait antibodies served as negative control and should guarantee the specificity of the signal. However, we were unable to detect β-dystroglycan in the precipitate (Figure 14A).

When the plectin immunoprecipitate was probed on an immunoblot with antibodies to the intermediate filament protein vimentin, a signal could be detected. No vimentin was immunoprecipitated with control antibodies (Figure 14A). To validate this interaction and possibly map plectin's binding domain, a blot-overlay experiment was performed. Cytoskeletal protein fractions derived from rat sciatic nerves were separated on SDS-PAGE and subsequently blotted onto a nitrocellulose membrane. The membrane was overlaid with his-tagged plectin fragments. Cytoskeletal proteins binding to his-tagged plectin fragments were detected by immunoblotting using antibodies to the histidine tags. A ~60 kDa protein binding to the C-terminal plectin fragment was detected, which might likely be vimentin (Figure 14C).

To test if integrin α6β4, another abaxonal SC membrane laminin 211 receptor complex, interacted with plectin, rat sciatic nerve homogenates were used for immunoprecipitation experiments using an antiserum to plectin (serum #9) as bait. The resulting immuno-precipitates and the input were separated on SDS-PAGE and immunoblots for integrin β4 and plectin were performed using an antiserum to plectin (#9) and antibodies to integrin β4. Plectin and integrin β4 could be detected, in the input and the plectin IP but not the control GFP-IP (Figure 14B). This finding indicated that in SCs, plectin is in a complex with integrin β4, like in hemidesmosomes of keratinocytes.

Plectins' interaction with vimentin suggests that in SCs plectin links integrin β4 to the vimentin IF network. Likewise, plectin also interlinks the DGC to the vimentin network.

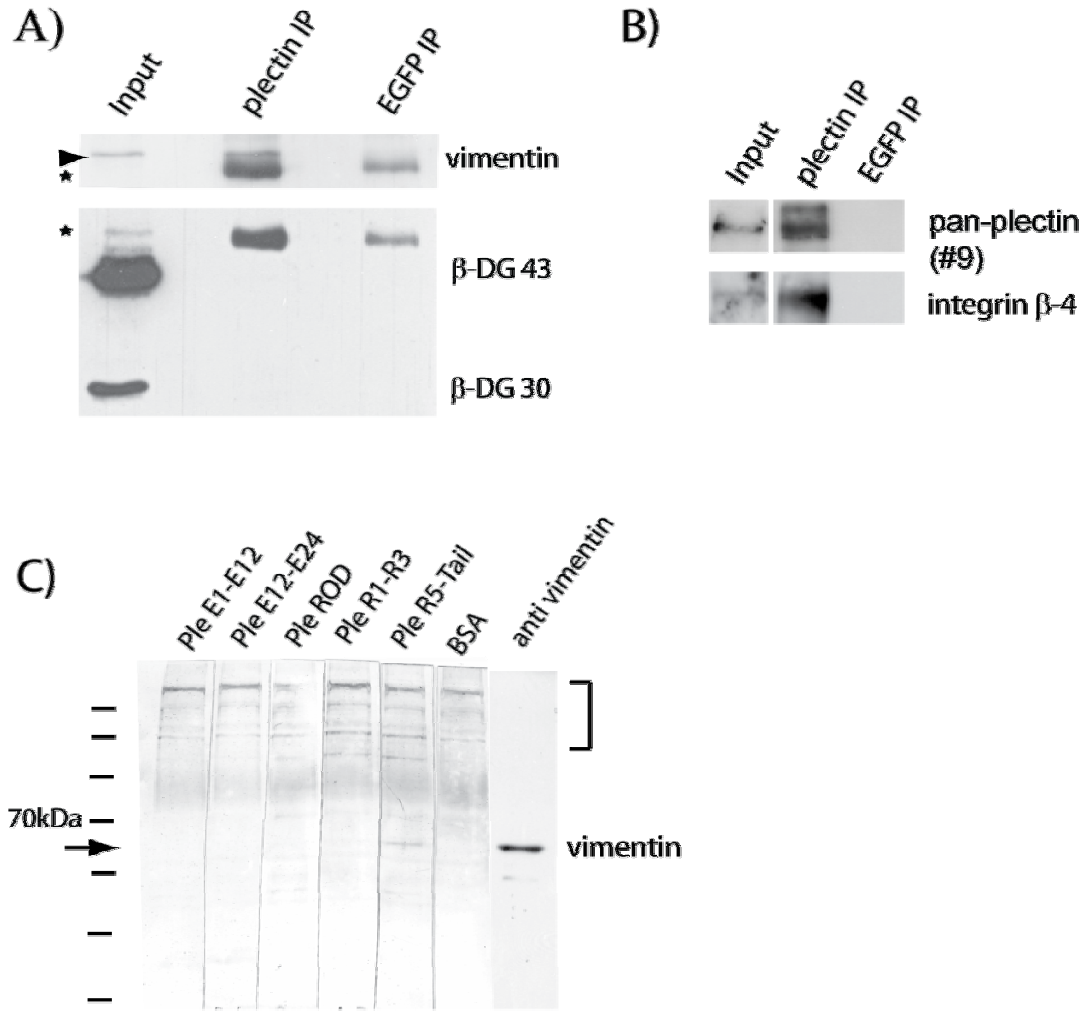

Figure 14. Immunoblots demonstrating co-precipitation of integrin β4 and vimentin, with plectin. (A) Immunoprecipitation was performed as in Figure 13, but using an antiserum to plectin (serum #9) as bait. Samples from the IP were subjected to SDS-PAGE followed by immunoblotting using antibodies to vimentin. Note that the vimentin band (~60 kDa, indicated by an arrowhead), migrates just above the primary antibodies' heavy chain (~55 kDa, indicated by an asterisk). (B) Immunoblot of immuno-precipitations similar to (A) but using a slightly altered protocol (see method section). Antiserum to plectin (#9) was used as bait. The input and the two immuno-precipitates were subjected to immunoblotting using antibodies to plectin and integrin β4. Note, co-precipitation of integrin β4 and plectin. (C) Interaction of a C-terminal plectin fragment with a 60 kDa protein expected to be vimentin. A cytoskeleton-associated protein fraction from sciatic nerve homogenates was separated on SDS-PAGE and blotted on a membrane and probed with his-tagged plectin fragments. A plectin C-terminal fragment was found to bind to a 60 kDa protein (arrow). An immunoblot for vimentin confirmed the same migration of vimentin. The bracket depicts unspecific bands.

3. Changed expression levels of cytoskeletal proteins in P0-Cre/conditional plectin KO sciatic nerves

To test if the loss of plectin in P0-Cre/cKO mice (a mouse line with a conditional plectin specific knock-out in SCs) leads to abnormal expression of its specific binding partners, a series of semi-quantitative immunoblottings was performed using sciatic nerve total cell lysates. Special emphasis was put on the laminin 211 receptors integrin β4 and members of the DGC.

DGC complex: To evaluate the amounts of expressed proteins, total cell lysates from WT and mutant sciatic nerves were prepared. Samples were then separated on SDS-PAGE and stained with Coomassie. The most prominent bands were densiometrically analyzed using the Quantiscan software and samples were normalized to contain equal amounts of total proteins. The lysates were then tested for the expression of proteins of interest by immunoblotting and the relevant protein bands were semi-quantitatively analyzed using the Quantiscan software. The signals derived from P0-Cre/cKO lysates were normalized to the signals from the WT lysates, which were set to the arbitrary unit 1. We observed that full length β-dystroglycan turned out to be slightly reduced in mutant sciatic nerves. The decrease of full length β-dystroglycan might be explained by the dramatic increase in expression levels of the truncated 30 kDa β-dystroglycan fragment (Figure 15). This 30 kDa β-DG fragment is believed to be a result of proteolytic cleavage of the extracellular domain β-DG, resulting in a still membrane bound, version of β-DG lacking the extracellular domain that is still membrane-bound.

The SC specific dystrophin isoform DP116 was highly upregulated in mutant sciatic nerve (Figure 15). This dystrophin isoform with a premature stop codon in its exon (Byers et al., 1993), resulting in a 116 kDa large C-terminal isoform of dystrophin, is the only expressed isoform of dystrophin in the peripheral nerve. DP116 is able to bind to β-dystroglycan, but lacks actin-binding (Byers et al., 1993). Although the precise function of DP116 in SCs is not known, loss of function in humans was found to cause myelin instabilities (Comi et al., 1995). Therefore, its compensatory upregulation, coinciding with the loss of plectin, might indicate a role of plectin in stabilizing the DGC.

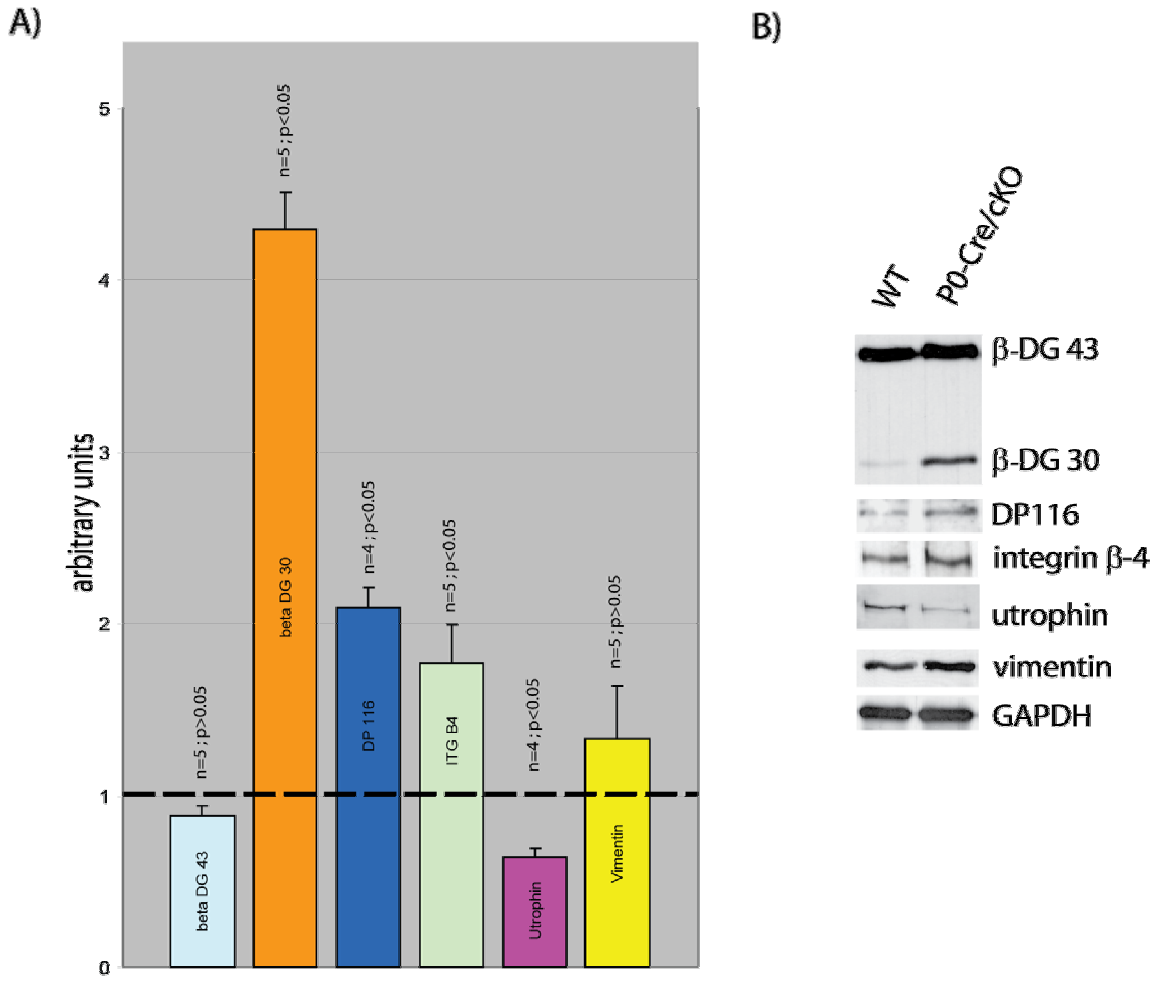

Figure 15. Semiquantitative analysis of expression levels of selected protein members of SC laminin 211 receptor complexes. (A) Column diagrams showing expression levels of proteins in total cell lysates derived from P0-Cre/cKO sciatic nerves, relative to the wild-type samples. Wild-type expression levels were set to an arbitrary unit of 1 and are marked by the dashed black line. The numbers of individual experiments used for quantification are indicated above the columns. Error bars indicate the standard error of the mean. Statistical significance of the observed differences in expression levels was analyzed by unpaired two-tailed student t tests. (B) Representative immunoblots of the proteins shown in panel (A).

Utrophin, another member of the dystrophin family, showed reduced expression levels in total cell lysates derived from P0-Cre/cKO sciatic nerves (Figure 15). Utrophin was shown to link the DGC to actin in SCs (Imamura et al., 2000), and to be responsible for maintaining the compartmentalization of myelinating SCs into Cajal bands and appositions (Court et al., 2009). Expression levels of other protein members of the DGC complex, like α-dystrogylcan and δ-sarcoglycan, were not altered (data not shown).

Integrin β4: We also analyzed the expression levels of integrin β4 in sciatic nerve total cell lysates from wild-type and P0-Cre/cKO mice. We found that the expression levels of integrin β4 in P0-Cre/cKO sciatic nerves were almost two-fold increased relative to

nerves from their wild-type littermates. This finding would be consistent with the idea that due to compromised stability of the DGC other laminin receptors are upregulated to still guarantee sufficient adhesion.

Since vimentin is believed to be the major binding partner of plectin in SCs we also analyzed the expression levels of vimentin. In six separate experiments, most of the sciatic nerve total cell lysates showed increased expression of vimentin, yet there were some samples, where this trend was reversed, overall resulting in an only insignificant increase (Figure 15)

4. Loss of plectin affects the stability of the SC dystrophin-glycoprotein complex

The data obtained from the co-immunoprecipitation experiments demonstrated that in the peripheral nerve the SC-specific DGC is linked to the vimentin filament system via plectin. Moreover, our semiquantitative immunoblotting analysis revealed increased proteolysis of β-dystroglycan, indicating decreased stability of the DGC. To investigate this in more detail, subcellular protein fractions of lysates were prepared from wild-type and P0-Cre/cKO sciatic nerves. These were then tested for the expression of α-, β-dystroglycan, and vimentin.

Reduced β-dystroglycan expression levels in both, the cytoskeletal, and membrane-associated protein fractions of P0-Cre/cKO sciatic nerves

Wild-type and P0-Cre/cKO sciatic nerves were isolated and used to prepare crude homogenates. Subsequently three subcellular fractions were prepared (for details refer to the methods section): a cytosolic protein fraction, a membrane-associated protein fraction, and a cytoskeleton-associated protein fraction. These fractions were separated on an SDS-PAGE and stained with Coomassie. Densitometric analysis was used to normalize wild-type and P0-Cre/cKO protein fractions to contain equal amounts of total proteins (Figure 16A). Subsequently immunoblots were performed with the normalized fractions using antibodies to α-, β-dystroglycan, and vimentin. As shown in Figure 16B, we found that vimentin was faithfully located in the cytoskeleton-associated protein fraction of wild-type and P0-Cre/cKO nerves.

β-dystroglycan was found mainly in the membrane-associated protein fraction and to a lesser extent in the cytoskeletal fraction (Figure 16B). Consistent with the idea that the loss of the plectin-mediated linkage of β-dystroglycan to the vimentin cytoskeletal network could affect the stability of β-dystroglycan, the β-dystroglycan levels in the cyoskeletal fraction of P0-Cre/cKO nerves were found to be severely reduced (Figure 16B). Additionally, the levels of β-dystroglycan in membrane-associated protein fraction were also found to be decreased. This was however contradictory to the observation that in P0-Cre/cKO sciatic nerve total cell lysates the overall expression levels of β-dystroglycan were not reduced (Figure 15A). Similar to β-dystroglycan, the α-

dystroglycan levels in sciatic nerve total cell lysates were not altered in P0-Cre/cKO mice. However, we found the protein levels of α-dystroglycan in the cytoskeleton-associated fractions of P0-Cre/cKO mice to be greatly, and those in the membrane associated fraction moderately reduced. Moreover, we found that concomitant with the reduction of α-dystroglycan in cytoskeletal and membrane fractions, α-dystroglycan was increased in the cytosolic fraction. Since α-dystroglycan is non-covalently bound to β-dystroglycan, loss of plectin apparently also compromised α-dystroglycan's linkage to the vimentin cytoskeleton. Given the results obtained with total cell lysates the reduction in α-dystroglycan levels in the membrane and cytoskeleton-associated protein fractions, cannot be explained by a generally lower protein expression. The relocalization of α-dystroglycan from the cytoskeleton- and membrane-associated protein fractions to the cytosolic fractions could be explained by the increased cleavage of β-dystroglycan in the plectin-deficient sciatic nerve (see models in Figure 17)

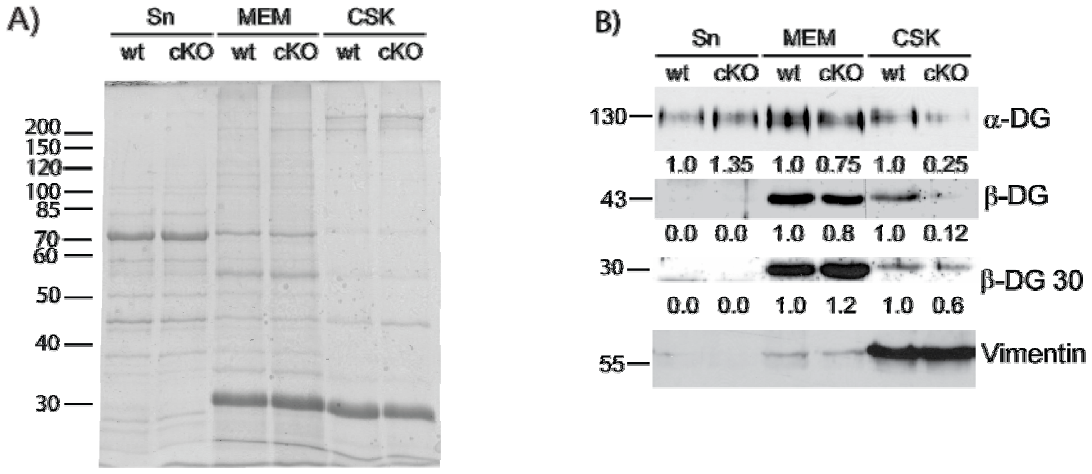

Figure 16. Expression levels of DGC proteins in sciatic nerve subcellular fractions. Crude homogenates from wild-type and P0-Cre/cKO sciatic nerves were prepared and these were used to obtain the following subcellular protein fractions: a cytosolic protein fraction (Sn), a membrane-associated protein fraction (MEM) and a cytoskeleton-associated protein fraction (CSK). These fractions were normalized to contain equal amounts of total proteins. (A) Coomassie stained SDS-polyacrylamid gel with normalized fractions loaded. (B) Representative immunoblots from four individually performed experiments using antibodies to α- and β-dystroglycan and to vimentin on normalized subcellular fractions. The numbers underneath the lanes indicate the relative expression levels of proteins in mutant fractions after densitometric analysis.

Increased proteolytic cleaveage of β-dystroglycan in P0-Cre/conditional plectin KO sciatic nerve

A matrix-metalloprotease, identified as MMP9 (Michaluk et al., 2007), was shown to cleave β-dystroglycan in peripheral nerve, kidney, lung and smooth muscle, but not skeletal muscle, cardiac muscle or brain (Yamada et al., 2001). Interestingly, this processing was shown to be much stronger in a cardiomyopathic hamster lacking sarcoglycan (Matsumura et al., 2003). The main cleavage site is located in the extracellular domain of β-dystroglycan, leaving a membrane-bound intracellular 30 kDa large fragment and thus shedding the extracellular part from the cell (Bozzi et al., 2009a). The extracellular part of β-dystroglycan, and all other bound proteins, like α-dystroglycan, become released from the cell, thus becoming part of the soluble, cytosolic protein fraction (Figure 17).

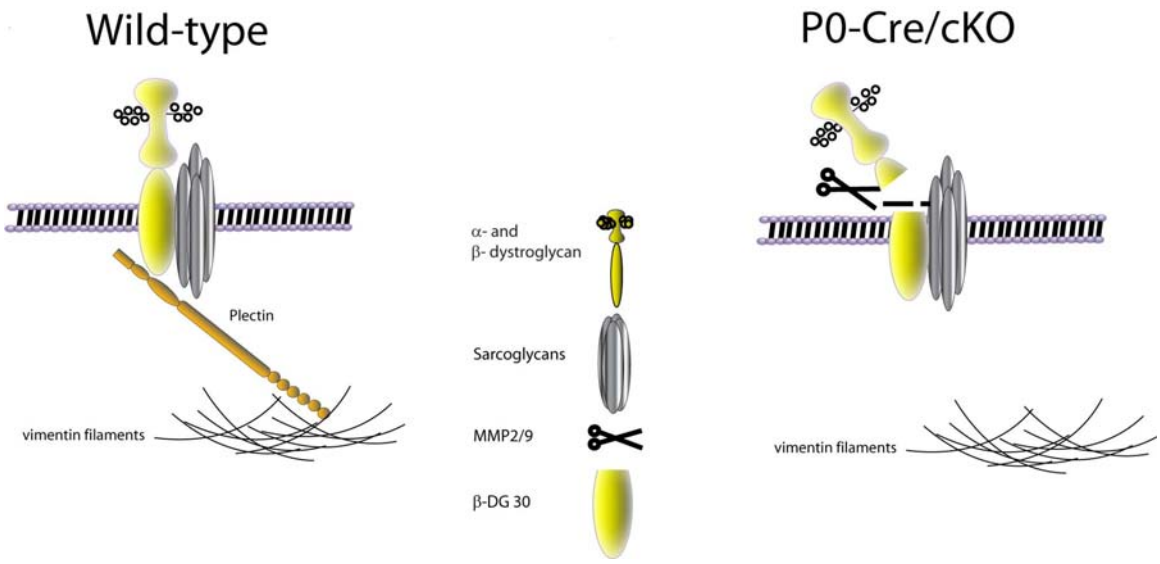

Figure 17. Hypothetical models explaining increased solubility of α-DG in P0-Cre/cKO sciatic nerve. In the wild-type situation, plectin is believed to interlink β-dystroglycan and vimentin, thus stabilizing the receptor complex through its anchorage with the cytoskeleton. In P0-Cre/cKO SCs, increased proteolytic cleavage of β-dystroglycan trough MMPs in the absence of plectin provides an explanation for the loss of α-dystroglycan in the cytoskeletal- and membrane-associated fractions and its accumulation in the cytosolic protein fraction.

To investigate if MMP 2 or MMP 9 expression levels or their activities were upregulated and/or more active in P0-Cre/cKO sciatic nerve, homogenates from sciatic nerves from wild-type and P0-Cre/cKO mice were prepared and subjected to gelatin zymography.

All matrix metalloproteases contain a propeptide, preceding the catalytic domain. The propeptide is covering the catalytic domain to keep the protease in a latent, inactive form. For activation, the propeptide needs to be cleaved (for review see Kerkelä and Saarialho-Kere, 2003). Consequently, during separation by SDS-PAGE, the active enzyme would migrate further and can be distinguished from the latent form. In a gelatin zymography, samples are separated by SDS-PAGE with gelatin being incorporated into the separation gel. The gelatinases in the samples, activated by unfolding through SDS in the gel, cleave the gelatin which becomes visible as negative stainings after incubation and destaining with Coomassie (for details refer to the materials and methods section). Figure 18 shows that we were able to detect MMP2 expression in homogenates prepared from wild-type and P0-Cre/cKO sciatic nerves, and that no alterations in the expression or activity of MMP2 could be observed between wild-type and P0-Cre/cKO samples. The biochemical nature of MMP2 was tested by pre-incubating the samples with EDTA and or serine protease inhibitors before performing the zymography. EDTA slightly reduced the MMP2 signal, whereas the serine protease inhibitors PMSF and AEBSF had no effect, indicating that the signal is really stemming from a matrix metalloprotease (Figure 18). We were unable to detect a signal for MMP9 activity using zymography. Maybe the expression of MMP 9 in sciatic nerve was below the detection limit of our zymography protocol.

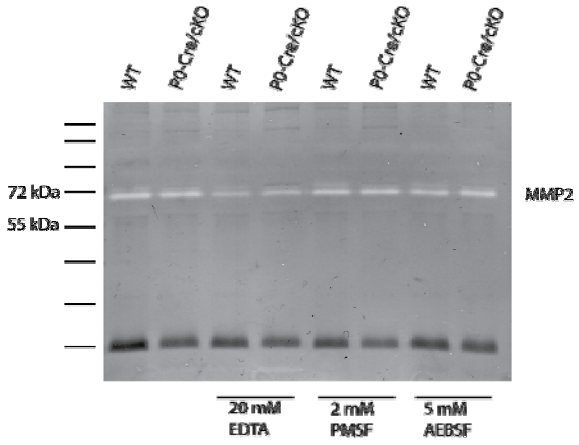

Figure 18. Gelatin zymography using sciatic nerve homogenates as samples. Sciatic nerves from wild-type and P0-Cre/cKO mice were used to prepare homogenates. These samples were then subjected to a gelatin zymography. Proteases in the samples migrate in the SDS acrylamide gel, according to their molecular mass and cleave the gelatin, which then diffuses out of the gel. This can be visualized by staining the gelatin with Coomassie and subsequent destaining. Individual metalloproteases are identified by their specific molecular masses. Incubating the samples with 20 mM EDTA prior to zymography resulted in reduced signal intensity, hardening the assumption that the band visible at ~66 kDa is the matrix metalloprotease MMP2. No variations in the expression levels of MMP2 could be detected between samples from wild-type and P0-Cre/cKO mice. No expression of MMP9 could be detected.

5. Compartmentalization of differentiated SCs is not altered in nerve fibers from P0-Cre/conditional plectin KO mice

The basal lamina, the myelinating SC and the axon were shown to mutually influence each other (Chernousov and Carey, 2000). Contact with an axon triggers a SC to differentiate and form compact myelin (Wood et al., 1990). SCs on the other hand dictate the axonal differentiation into distinct domains (Court et al., 2009). To manage this function, the SCs are dependent on stable anchoring and signals from the basal lamina. Alterations of receptors in the abaxonal and adaxonal SC membrane have been shown to lead to changes in the organization of the myelinating SC, resulting in misorganized axons and neuropathies (Roa et al., 1993; Previtali et al., 2003b; Saito et al., 2003; Nodari et al., 2008) . To test for possible alterations in the compartmentalization of myelinating SCs in sciatic nerves of P0-Cre/cKO mice, immunofluorescence stainings of teased sciatic nerve fibers were performed. We analyzed the compartmentalization of the myelinating SC into Cajal bands and appositions. The appositions are compartments of the SCs where the abaxonal membrane is in close proximity to the compact myelin. Appositions are regions where the dystroglycan-drp2-periaxin complex can be found (see Figure 7B). DRP2 is localized exclusively in appositions and therefore provides a perfect marker for appositions. The intermediate filament protein vimentin was used to label the cytoplasmic region of the SCs, namely Cajal bands and their interlinking trabeculae. As can be seen in Figure 19A,B, the cytoplasm of SCs of wild-type and P0-Cre/cKO sciatic nerves was similarly organized into Cajal bands and appositions. Another important structure in myelinating SCs are the Schmidt-Lanterman incisures (SLIs). They can be viewed as radial cytoplasmic channels which connect the abaxonal and adaxonal cytoplasm. They represent regions where the myelin is not compacted. E-Cadherin was used as a marker for the SLIs. No alterations in the frequency or the architecture of SLIs in fibers from P0-Cre/cKO mice could be detected (Figure 19C,D). A conditional knockout of β-dystroglycan in SCs was recently shown to display problems with the formation of nodes of Ranvier (Saito et al., 2003). Hence, nodes and paranodes in teased nerve fibers of wild-type and mutant mice were stained with antibodies to ezrin and an antiserum to paranodin, respectively. Again no changes in the architecture of the paranodes and the nodes could be detected between wild-type and P0-Cre/cKO mice (Figure 19G-J).

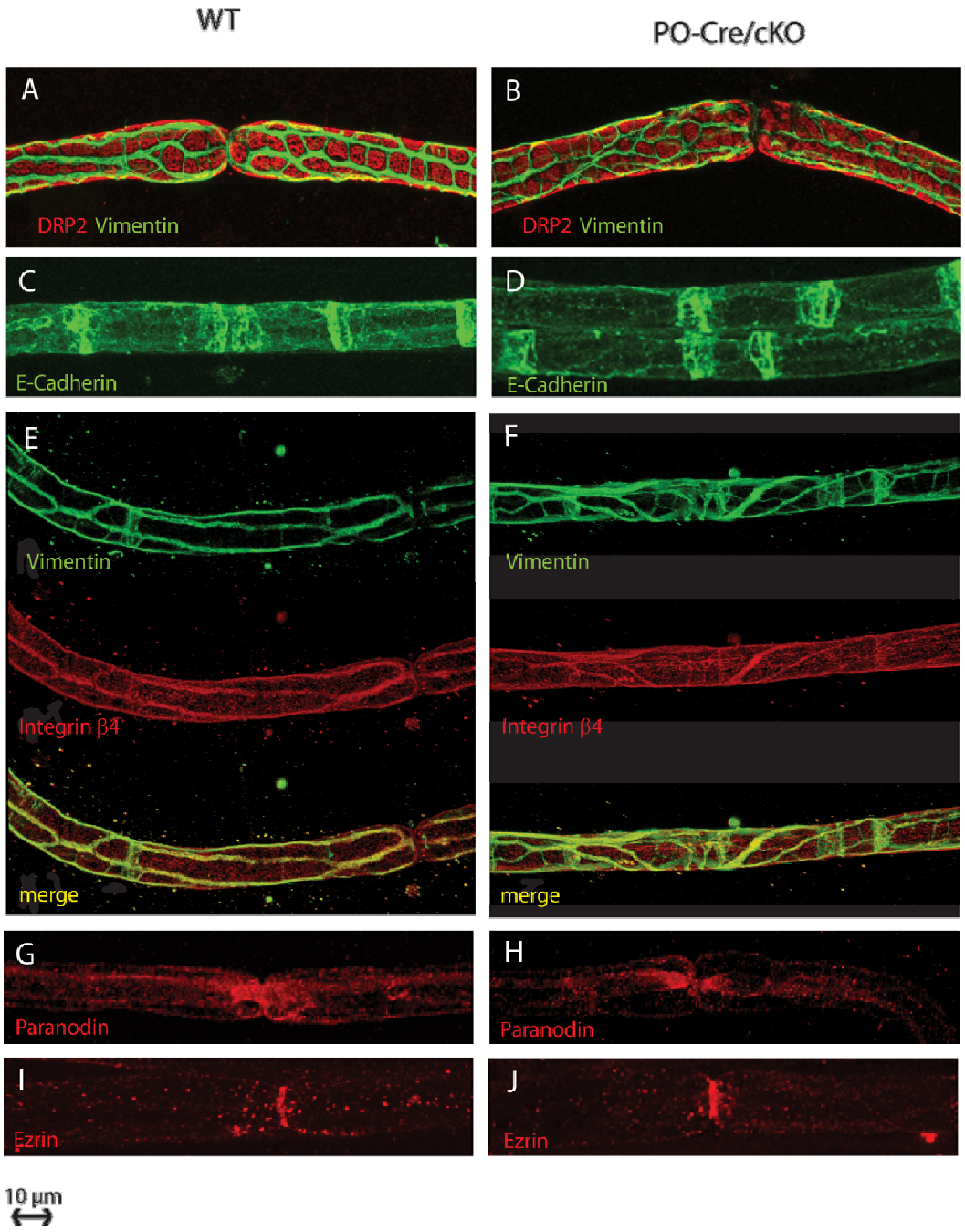

Figure 19. Immunofluorescence stainings of teased nerve fibers. Wild-type and P0-Cre/cKO nerves were fixed with PFA and individual nerve fibers were teased apart and immobilized on object carriers. They were subjected to immunofluorescence microscopy to test for alterations in their compartmentalization. Fibers were immunostained using antibodies to DRP2 (A,B), vimentin (A,B,E,F), E-cadherin (C,D), integrin β4 (E,F), paranodin (G,H) and ezrin (I,J). Note, normal compartmentalization of the SC cytoplasm into Cajal bands and trabeculae (A,B) and Schmidt-Lantermann incisures (C,D). Also note that contrary to previous reports integrin β4 was found to be concentrated in Cajal bands (E,F). SCs also showed no abnormalities in the formation of paranodes (G,H) and nodes (I,J) in teased fibers from P0-Cre/cKO mice.

Having identified integrin β4 as binding partner of plectin in SCs, we also analyzed its localization in the myelinating SC. Although integrin β4 has been described before to be evenly distributed in the abaxonal membrane of myelinating SCs we found it to be concentrated in Cajal bands (Figure 19E,F). However no changes in the localization of integrin β4 were found between wild-type and P0-Cre/cKO SCs.

6. Phenotypic analyses of primary wild-type and P0-Cre/conditional plectin KO SCs

Primary SCs represent SCs in their undifferentiated state. These non-myelinating SCs provide a good model for the behavior of SCs in the regenerating nerve when the SCs are actively migrating and proliferating. Primary SCs derived from wild-type and P0-Cre/cKO sciatic nerves were isolated and tested for basic cell parameters, including morphology, adhesion, migration, proliferation and their capacity to react to extracellular signals.

P0-Cre/cKO primary SCs display unaltered morphology

To analyze the morphology of wild-type and P0-Cre/cKO primary SCs, they were isolated and seeded on cell culture dishes coated with laminin 111. They were fixed by treatment with methanol and, after blocking, immunostained with antibodies to actin and P75, a SC-specific protein. Ten individual images of randomly chosen fields were recorded with a 10 x objective using an LSM 510 microscope (Carl Zeiss). The SCs were counted and classified according to the numbers of their extensions. This experiment has only be performed once and therefore the results have to be considered as preliminary. However, from the 500 SCs counted per genotype it appeared that there were no alterations in the numbers of extensions. Most SCs did exhibit a bipolar shape, and about 10 percent of the SCs counted showed a tripolar shape. SCs posessing only one or more than three extensions were rarely observed (Figure 20).

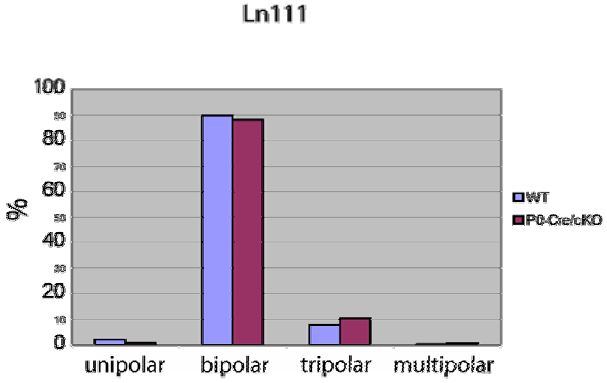

Figure 20. Comparison of wild-type and P0-Cre/cKO SC morphology. Wild-type and P0-Cre/cKO primary SCs were isolated and seeded on laminin 111- or 211-coated dishes. Three days later, the cells were fixed with methanol and immunostained using antibodies for actin and P75. In this experiment, 500 cells of each genotype were scored for their number of processes. Most cells exhibited a bipolar phenotype. No alterations between wild-type and P0-Cre/cKO SCs could be observed.

Reduced migratory potential of primary P0-Cre/conditional plectin KO SCs on laminin 211 but not on laminin 111

Several different cell types including fibroblasts, T cells and keratinocytes have been shown to display altered migratory behavior in the absence of functional plectin (Abrahamsberg et al., 2005; Osmanagic-Myers et al., 2006). To assess their migration potential, SCs were isolated from wild-type and P0-Cre/cKO sciatic nerves and seeded onto laminin 111 or 211. Phase-contrast images were taken every 30 minutes for a total of 24 hours from 10 randomly chosen positions. The migration of individual cells was analyzed by tracking the position of SC nuclei using the ImageJ software (NIH). On laminin 111, three individual experiments were performed, monitoring the migration of a total of 90 cells. The results presented in Figure 21 show that the migration of plectin-negative primary SCs on laminin 111 was not altered. Despite large variations between migration velocities of individual cells, the bulk of cells migrated with velocities in the range of 0.02-0.05 µm/min. Two individual experiments, monitoring the migration of a total of 90 cells were performed with SCs seeded onto laminin 2. The results, albeit being preliminary, showed a reduction in the migration velocities of P0-Cre/cKO primary SCs. The migration velocities of wild-type SCs on laminin 211 were comparable to that of SCs on laminin 111. These results indicate a role for plectin in regulating laminin 211 dependent cell migration.

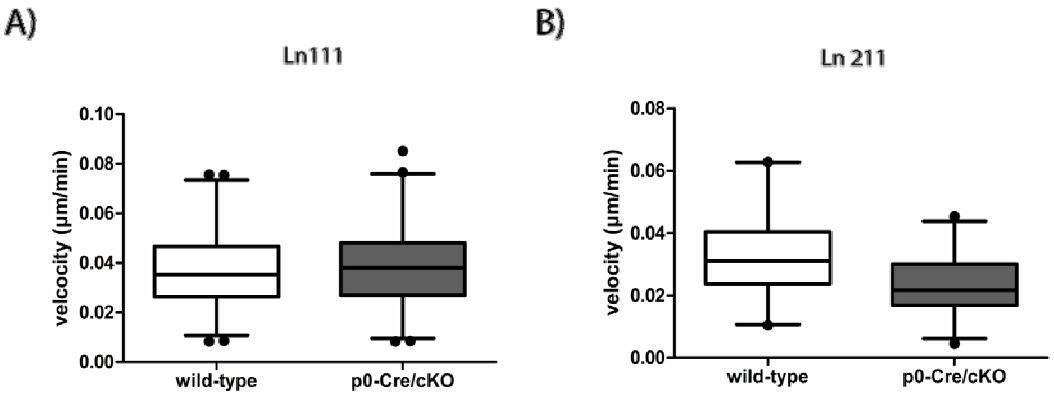

Figure 21. Analyses of the migratory potential of wild-type and P0-Cre/cKO SCs. Wild-type and P0-Cre/cKO primary SCs were seeded onto laminin 111 (A) or laminin 211 (B) and tested for their migration potential. Phase-contrast images were taken in 30 minutes intervals for a total timeframe of 24 hours. The manual tracking plugin from the ImageJ software (NIH) was used to track nuclei of single, bipolar SCs. Box and whiskers indicate the median (middle line in the box) 25th percentile (bottom line of the box), 75th percentile (top line of the box) and 2,5th and 97,5th percentiles (whiskers). n=3 for cells (total number 90) growing on ln 111, n=2 for cells (total numbers 60) growing on ln 211.

Altered adhesion and proliferation of primary P0-Cre/conditional plectin KO SCs on laminin 111 and 211

One of the functions of laminin receptors is to mechanically attach the cell to the basal lamina. Given that plectin is a cytoskeletal component of the laminin receptor complexes found in SCs, an experiment was performed to test for the ability of wild-type and P0-Cre/cKO primary SCs to attach to laminin 111- or 211-coated surfaces. Equal cell numbers of wild-type and mutant primary SCs were seeded on dishes coated with either laminin 111 or 211. 24 hours after seeding, phase-contrast images were recorded and the cells were counted. Attached cells were also counted after 72 and 96 hours after seeding to detect changes in survival and proliferation rates. This experiment has only been repeated once and therefore the results have to be considered preliminary. However, the results indicated not only differences in the attachment of SCs to laminin 111- and 211-coated surfaces, but also between the adhesion potentials of wild-type and P0-Cre/cKO SCs. Figure 22 shows the percent increase in the number of SCs growing on laminin 211, compared to the number of SCs growing on laminin 111. Twenty four hours after seeding, 81% more wild-type SCs were counted, attached to the laminin 211 surface compared to laminin 111. Intringuingly, P0-Cre/cKO SCs when seeded on laminin 211 were increased in number by only 16%, compared to laminin 111. This trend also persisted 72 and 96 hours after seeding. These data indicated an advantage for SCs to attach to laminin 211 compared to laminin 111. However, SCs lacking plectin seemed to be unable to benefit from this advantage. These results, albeit preliminary, further stress plectin's role as part of a laminin 211 receptor complex in SCs.

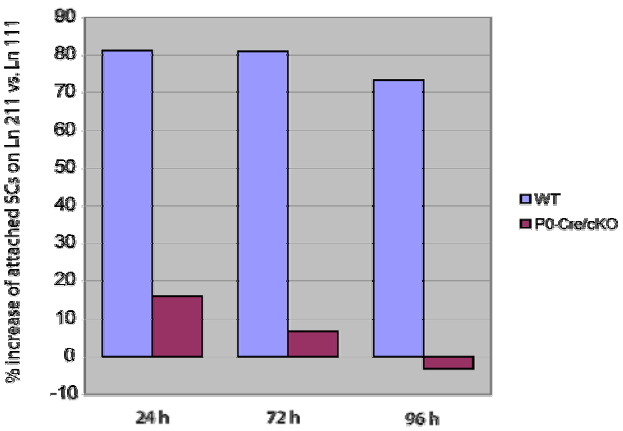

Figure 22. Altered adhesion of wild-type and P0-Cre/cKO SCs. Primary wild-type and P0-Cre/cKO SCs were seeded onto laminin 111- or 211-coated dishes. After 24, 72 and 96 hours, phase-contrast images were taken with a 10x objective from randomly chosen optical fields and attached SCs were counted. More than 400 cells of each genotype were counted for each timepoint in this experiment.

Increased extension retraction of primary P0-Cre/conditional plectin KO SCs upon treatment with LPA

Lysophosphatidylic acid (LPA) is a small serum phospholipid which is also active in the nervous system. Its many biological roles are mediated by G-protein-coupled receptors (Noguchi et al., 2009). SCs were shown to express receptors for LPA (Weiner and Chun, 1999) and LPA-mediated responses include changes in SC morphology (Weiner et al., 2001; Bouquet et al., 2007), promotion of SC survival and differentiation (Weiner and Chun, 1999) and demyelination in ex vivo culture of dorsal root ganglia (Fujita et al., 2007) as well as in dorsal roots in vivo leading to initiation of neuropathic pain (Inoue et al., 2004). To monitor possible alterations of P0-Cre/cKO SCs in response to LPA treatment, wild-type and primary P0-Cre/cKO SCs were isolated and grown on laminin 111-coated dishes. Phase-contrast images were taken and LPA was added to the medium in a final concentration of 10 µM. Images were taken in 30 second intervals for a total of 30 minutes. The ImageJ software (NIH) was used to measure the length of cell-processes from single bipolar SCs. Three individual experiments were performed and in each experiment 30 cell processes were measured. In P0-Cre/cKO SCs, the processes started to retract within 10 minutes after addition of LPA and became reduced to 50% of their original length. In contrast, in wild-type SCs no abrupt reduction in cell process length could be observed. Thirty minutes after addition of LPA, wild-type SC cell process length was still at 60% of T0 (Figure 23).

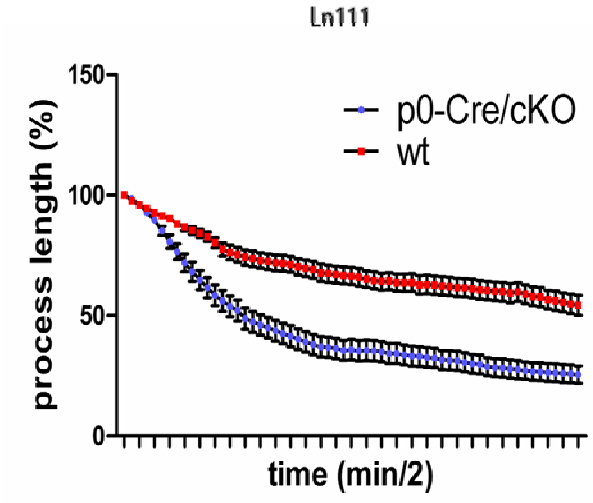

Figure 23. Altered reaction of wild-type and P0-Cre/cKO SCs to LPA treatment. SCs were cultivated for 48 hours. Lysophosphatidic acid (end-concentration: 10 µM) was added and images were taken each 30 seconds for a total timeframe of 30 minutes. Cell process lengths of SCs with a bipolar shape, not attached to other SCs, were measured for each timepoint using the ImageJ software (NIH). The graph shows the mean results ± SEM, from 3 individual experiments with 90 SCs per genotype analyzed in total.

Discussion

In this diploma thesis, I provide evidence for the existence of stable ECM-receptor-plectin-IF network connections in SCs. With biochemical methods I could show direct interaction of plectin with two membrane-bound receptor complexes, integrin α6ß4 and the DGC. Making use of a recently established mouse line (P0-Cre/cKO) with a SC-specific conditional plectin knock-out, the destabilization of these receptor complexes upon plectin deficiency could be shown. The finding that a reduced linkage of the DGC to the IF network coincided with an increased cleavage of ß-dystroglycan in plectin-deficient mice was particularly interesting, as this cleavage leads to the loss of the extracellular, laminin-binding part of the DGC. This loss of laminin-binding capacity could offer an explanation for the phenotypes observed in plectin-deficient primary SCs, which included reduced migratory potential, reduced attachment to laminin 211, and increased process retraction upon treatment with LPA. Important questions arising from these data were if the above phenotypes were caused by changes in receptor stability or by other mechanisms such as compromised signaling.

The ECM-plectin-IF axes

In this diploma thesis I could demonstrate interaction of plectin with two laminin 211 receptors of sciatic nerve, integrin β4 and β-dystroglycan. In keratinocytes, integrin β4 and plectin isoform 1a constitute (among other proteins) the hemidesmosome, a junctional complex that links the keratinocytes cytoskeleton to the basal lamina (Rezniczek et al., 1998). No hemidesmosome-like structure can be found in SCs and expression of plectin isoform 1a could not be detected. However, integrin β4 was found to be expressed in SCs and could be co-precipitated with plectin from sciatic nerve homogenates. In keratinocytes, plectin was shown to interact with integrin β4 via multiple domains including the ABD, the plakin domain and the C-terminal repeats, with the intermediate filament binding domain (IFBD) in particular (Rezniczek et al., 1998). Although there was evidence that plectin's first (isoform-specific) exon influences the binding efficiency to integrin β4 (Litjens et al., 2003), theoretically all plectin isoforms, including 1 and 1c, should be able to bind to integrin β4. In hemidesmosomes, plectin interlinks integrin β4 to the IF network by binding to keratins via its C terminus. In this thesis, plectin was shown by Co-IP and blot-overlay assays to bind to vimentin expressed

in sciatic nerve. Furthermore plectin, integrin β4, and vimentin were shown by immunofluorescence microscopy of teased nerve fibers to be localized in the same compartment in myelinating SCs, namely the Cajal bands and interlinking trabeculae. These results suggest the existence of an integrin β4-plectin-vimentin IF network axis in SCs.

Plectin was shown to bind to β-dystroglycan directly (Rezniczek et al., 2007) and to associate indirectly with the DGC, via α-dystrobrevin (Hijikata et al., 2008). In this thesis, the binding of plectin to β-dystroglycan in SCs was demonstrated using Co-IP. With β-dystroglycan binding sites residing at the N terminus (plakin domain) as well as the C terminus, theoretically all plectin isoforms are able to interact with β-dystroglycan. Two isoforms, plectin 1 and 1f, were found to be expressed in SCs at low levels, consistent with previously reported protein and mRNA levels in brain (Fuchs et al., 1999). However lower expression levels would not exclude them from playing critical roles in the peripheral nerve. When concentrated at specific subcellular locations, the local concentration of plectin isoforms 1 or 1f might be higher than that of plectin 1c, which probably is the most prominently expressed isoform of plectin in SCs. Intringuingly, both isoforms were shown to be associated with the sarcolemma in skeletal muscle (Rezniczek et al., 2007; Hijikata et al., 2008). Plectin isoform 1 was shown to bind to α-dystrobrevin via the sequence encoded by its exon 1 (Hijikata et al., 2008). α-dystrobrevin as component of the DGC would thus link plectin to the costamers. The authors proposed a model where plectin isoform 1 would help to build a basal lamina-dystroglycan-dystrobrevin-plectin-actin/IF axis (Hijikata et al., 2008). Plectin isoform 1f is even more prominently expressed at the sarcolemma of skeletal muscle (Rezniczek et al., 2007). Plectin was shown to directly bind β-dystroglycan via its plakin domain (Rezniczek et al., 2007). All plectin isoforms could theoretically bind to β-dystroglycan in this manner but only plectin isoforms 1 and 1f were shown to be membrane associated by immunfluorescence microscopy (Rezniczek et al., 2007). These findings make plectin isoforms 1 and 1f the most likely candidates to mediate interactions with laminin 211 receptors in SCs.

To assess the functional consequences of plectin's association with the DGC, subcellular protein fractions were prepared from wild-type and P0-Cre/cKO sciatic nerves and tested for the expression of DGC constituent proteins. The observed decrease of β-dystroglycan

in the cytoskeleton-associated fraction in P0-Cre/cKO could be explained by the loss of plectin-mediated linkage to the IF network. The same experiment revealed that the expression of α-dystroglycan was reduced in the cytoskeleton and membrane-associated protein fraction, but was increased in the cytosolic fraction. This shift in α-dystroglycan's distribution could be the consequence of increased cleavage of β-dystroglycan in P0-Cre/cKO sciatic nerve, resulting in generation of a 30 kDa β-dystroglycan fragment. There is evidence that this fragment is the product of proteolytic cleavage of β-dystroglycan, mediated by the matrix metalloprotease 9 (MMP9) (Michaluk et al., 2007). This phenomenon was termed β-dystroglycan processing. Increased β-dystroglycan cleavage is frequently observed in tumor cells (Kerkelä and Saarialho-Kere, 2003; Singh et al., 2004), in pathologies like autoimmune neuritis (Zhao et al., 2010) and, intriguingly, also whenever an important component of the DGC is missing. In basal keratinocytes β-dystroglycan processing was shown to be increased when perlecan, a major ligand of α-dystroglycan was missing. This led to the assumption that a destabilization of the DGC makes it more accessible to processing (Herzog et al., 2004). In another report it was shown that also the loss of the sarcoglycan complex led to a destabilization of the DGC complex, resulting in increased cleavage of β-dystroglycan in skeletal, cardiac, and smooth muscle (Matsumura et al., 2003). The authors hypothesized that the sarcoglycan complex would mask the cleavage site. In sarcoglycan-deficient mice the site would be accessible, leading to increased cleavage. Increased processing of β-dystroglycan in SCs was also reported in *mdx* mice (mice lacking dystrophin) (Hnia et al., 2006). The authors could show increased expression of MMP9 in these mice. In this thesis I was able to show, using zymographic analyses, that the MMP2 expression level in P0-Cre/cKO sciatic nerve was comparable to that of wild-type. However, I was unable to detect MMP9, neither in wild-type nor P0-Cre/cKO nor *mdx* sciatic nerve homogenates. Possible reasons could include the insufficient amount of input material or an inappropriate protocol. Further efforts are needed to clarify this matter. Consequently, the question if the increased cleavage of β-dystroglycan was caused by an increased activity/expression of MMP9 or an increased accessibility of the cleavage site can not be answered to date. Nevertheless, a hypothetical model of MMP9-mediated processing of β-dystroglycan in the wild-type and the P0-Cre/cKO situation in SCs is depicted in Figure 13C,D. In this model, the loss of plectin destabilizes the DGC, leading to increased MMP9-mediated cleavage of β-dystroglycan. Consequently the extracellular

part of β-dystroglycan, and all bound proteins (like α-dystroglycan) are shed from the cell.

Phenotypic consequences of plectin deficiency

To study the phenotypic consequences of plectin deficiency in SCs I isolated wild-type and P0-Cre/cKO primary SCs and assessed some of their basic properties such as attachment and migration. My results showed a reduction of migration velocity of P0-Cre/cKO SCs grown on laminin 211. Previous studies had created an ambivalent picture regarding the consequences of plectin ablation for cell migration. Plectin-null fibroblasts were shown to exhibit reduced motility (Andrä et al., 1998) compared to wild-type cells, while in contrast, plectin-null keratinocytes showed increased motility in wound closure assays compared to their wild-type counterparts (Osmanagic-Myers et al., 2006). These differences in the migratory potential of different cell types could be explained by the fact that migration represents a highly complicated and well regulated task for cells. Migration is dependent on the combined and precisely orchestrated actions of the actin-myosin-based cytoskeleton and junctional complexes that attach the cell to its substratum. It has been demonstrated that plectin-null fibroblasts show delayed reaction to stimuli of the Rho/Rac/Cdc42 pathways, which are known to be major regulators of actin dynamics (Andrä et al., 1998). Furthermore plectin might sequester actin or act as a capping protein to alter actin dynamics. Additionally, plectin was suggested to act as a scaffold for signaling molecules or receptors like RACK1 (Osmanagic-Myers and Wiche, 2004) or members of the MAP kinase pathway (Osmanagic-Myers et al., 2006). In this role, plectin could control the intracellular localization of these molecules, thus regulating their activity. Furthermore, one could think of a situation where signals transduced from an ECM-receptor need linkage to the cytoskeleton to work properly. In fact, this scenario has been described in a study of Zhu and Assoian, 1995, where it was shown that activation of ERK1/2 and MAP kinase by binding to fibronectin was dependent on an intact microfilament system. The fact, that migration was reduced in P0-Cre/cKO SCs growing on laminin 211, but not growing on laminin 111 points to a role for a laminin 211 receptor. The model, that loss of plectin blocks signaling mediated by a laminin 211 receptor, thereby reducing the migratory potential, is appealing but highly speculative at this timepoint. A recent publication where ß-dystroglycan was knocked-down using siRNA in myoblasts showed that reduced ß-dystroglycan levels led to reduced migration velocity accompanied by increased numbers of fibrillar contacts (Thompson et al., 2010).

These data correspond with the observations of reduced migration velocities of plectin-deficient SCs.

To assess the capacity of plectin-deficient primary SCs to react to extracellular signals, they were treated with LPA. My studies indicated that process retraction after the addition of LPA was increased in P0-Cre/cKO SCs. Like migration, the event of process retraction is highly regulated and influenced by many parameters. In a study highlighting the importance of MAP1b for this process, evidence was provided that process retraction in SCs after the addition of LPA requires the combined action of actin and tubulin rearrangement (Bouquet et al., 2007). Actin remodelling in response to LPA treatment in SCs and neurons was shown to be dependent on an increase in myosin activity (Bouquet et al., 2007). This is in accordance with reports, demonstrating that LPA treatment increases Rho signaling (Amano et al., 1998; Hirose et al., 1998). Since it was shown that fibroblasts lacking plectin display delayed reactions to stimuli of the Rho/Rac/Cdc42 pathway (Andrä et al., 1998) one might assume that the retraction in P0-Cre/cKO SCs would be slowed down. However, the delayed reaction to stimuli of the Rho pathway was shown in fibroblasts and the situation in SCs might be different. Furthermore, there is evidence, that also the microtubules in SCs undergo rearrangement after treatment with LPA (Bouquet et al., 2007). Plectin's mechanical stabilizing might hinder the collapse of SC extensions. Of course, attachment to the substratum is another parameter that has to be considered in the event of process retraction. The experiments with LPA were performed with SCs grown on laminin 111. A preliminary experiment suggested that there were no variations in the attachment of wild-type and P0-Cre/cKO SCs on laminin 111 (data not shown). However, altered signaling via laminin 111 receptors can not be ruled out. It will need further experiments to find out if the reduced retraction is due to changes in signaling, altered mechanical features, or a combination of the two.

No role for plectin in compartmenatlization of myelinating SCs?

Immunofluorescence microscopy of teased nerve fibers from wild-type and P0-Cre/cKO sciatic nerves indicated that plectin is dispensable for the correct compartmentalization of myelinating SCs and differentiation of axonal domains. Using antibodies to proteins that are specifically located in certain subcellular domains of myelinating SCs, these domains were visualized to monitor possible alterations. No variations of P0-Cre/cKO nerve fibers could be observed regarding the organization of nodes, paranodes and Schmid-

Lantermann incisures. Furthermore, mutant nerve fibers did not display any alterations in the organization of Cajal bands and membrane-myelin appositions. These observations suggest that SCs do neither need plectin to receive and transduce myelination and differentiation signals, nor to orchestrate the necessary intracellular changes.

Most undifferentiated primary SCs exhibit a bipolar phenotype with a central cell body and two long, slim extensions. Primary SCs isolated from P0-Cre/cKO mice showed no altered morphology, with respect to their extension numbers. However further morphological analyses of P0-Cre/cKO SCs have to be performed, including cell size and process cytoarchitecture. Compensatory mechanisms could explain the lack of alterations in SC compartmentalization, SC morphology, and axonal organization of P0-Cre/cKO mice. To adress this question, I analyzed the expression levels of the key protein constituents forming the ECM-IF network axes in SCs. A similar analysis in wild-type and P0-Cre/cKO sciatic nerve revealed a statistical significant increase of DP116 and integrin β4 as well as a decrease in the expression of utrophin in plectin-null nerves. DP116 is a SC-specific isoform of dystrophin (Byers et al., 1993), which possesses a premature stop codon, resulting in the expression of a 116 kDa large C-terminal isoform of dystrophin. This isoform is able to bind to β-dystroglycan, but lacks an actin-binding domain, and hence is unable to link β-dystroglycan to actin, such as dystrophin does in skeletal muscle. Although the precise function of DP116 in SCs is not known, loss of function in humans was found to cause myelin instabilities (Comi et al., 1995). Therefore, its upregulation appears to compensate for the destabilization of the α/β-dystroglycan-cytoskeleton axis in the absence of plectin.

The upregulation of integrin β4 in P0-Cre/cKO sciatic nerve is likely a result of the SCs' efforts to compensate for the loss of plectin's mechanical linkage. Thus, the decrease in the expression levels of utrophin in P0-Cre/cKO sciatic nerve compared to wild-type came as a surprise, as one might have expected that this protein, too, would show upregulation. In fact in skeletal muscle utrophin is upregulated in plectin-null mice. It will be highly interesting to investigate these differences in regulation in various cell types.

This diploma thesis delivered insights into the roles, plectin plays in SCs of the peripheral nervous system. The acquired data suggests a stabilizing role for plectin in interaction

with the DGC and the integrin α6ß4 laminin receptor complex. Absence of plectin was shown to lead to compensatory upregulation of key constituents of these complexes as well as a destabilization of the DGC, ultimately resulting in the loss of the laminin binding part of the receptor complex – α-dystroglycan. It will be interesting to adress the question how the increased proteolytic cleavage of ß-dystroglycan in plectin deficient sciatic nerve is mediated. One could assume that either the destabilization of the complex leads to increased accessibility of the cleavage site, or an increased expression or activity of the metalloproteinase cleaving ß-dystroglycan leads to the observed changes. Further it will be of great interest to investigate what caused the observed reduction in motility and the increased process retraction upon stimulation with LPA of primary plectin-null SCs. Assessing the capability of plectin-null SCs to react to stimuli of the Rho/Rac/Cdc42 pathways might help solve this puzzle. Generally, we are far from a comprehensive understanding of plectins functions in Schwann cells but this thesis helped guide the directions for further research.

Materials and Methods:

Preparation of subcellular fractions from mouse and rat sciatic nerve

Mice were anesthetized with 200 µl of isofluoran (Abbott) and subsequently killed by cervical dislocation. Rats were euthanized with CO_2. The sciatic nerves were removed, snap frozen in liquid nitrogen and pulverized thoroughly using a mortar and pistil under permanent coverage with LN_2. 75 µl of phosphate extraction buffer were added per 1 cm, of original nerve length and the pulverized nerves were homogenized with 20 strokes using a dounce homogenizer. The resulting crude homogenate was transferred to Eppendorf tubes and centrifuged at 4° C for 10 minutes at 82 x g to sediment cell debris. The resulting supernatant was transferred to a fresh Eppendorf tube and the pellet discarded. 50 µl of the supernatant were mixed with 50 µl 6 x SDS sample buffer, incubated for 5 minutes at 95° C and stored at -20° C as crude homogenate (CH).

The rest of the supernatant was centrifuged at 53,000 rpm in a Beckman TLX Ultracentrifuge (TLA-120.2) for 1 hour at 4° C to pellet crude vesicles. The supernatant after ultra-centrifugation was carefully taken off using a needle attached to a small syringe and mixed with an equal volume of 6 x SDS sample buffer and treated as described above. This fraction was supposed to contain the cytosolic proteins and it was marked as cytosolic fraction (CS).

The pellet of the ultra centrifugation was rinsed with 200 µl of Phosphate Buffer and re-homogenized in 1/8 volume of phosphate detergent extraction buffer (of that of phosphate buffer used in the first homogenization step) with a yellow pipette tip by pipetting up and down 50 times. The resulting suspension was incubated for 1 h at 4° C on a rocking platform to extract membrane proteins. The suspension was then centrifuged at 20,000 rpm in a Beckman TLX Ultracentrifuge (TLA-45) for 10 min at 4° C. The supernatant containing membrane proteins was carefully removed with a needle attached to a syringe and transferred to a fresh Eppendorf tube. The supernatant was mixed with an equal volume of 6 x SDS sample buffer and trated as described above. This fraction was marked as crude membrane extract, ME.

The pellet was rinsed carefully with 200 µl phosphate buffer and rehomogenized in 1/8 volume of 8 M Urea (of that of phosphate buffer used in the first homogenization step). The resulting suspension was incubated on a rocking platform at RT for 30 min. 50 µl of this suspension was mixed with an equal volume of 6 x SDS sample buffer, treated as described above and marked as cytoskeletal fraction (CSK).

Phosphate Extraction Buffer:

- 20 mM Na-Pyrophosphate
- 20 mM Na-Phosphate
- 1 mM $MgCl_2$
- 0.303 M sucrose
- 2 mM PMSF
- pH 7.4
- 1 x Protease Inhibitor Cocktail (Roche)

Phosphate Detergent Extraction Buffer:

- 20 mM Na-Pyrophosphate
- 20 mM Na-Phosphate
- 1 mM $MgCl_2$
- 0.303 M sucrose
- 1 % (v/v) Triton X-100
- 0.1 % (v/v) SDS
- 2 mM PMSF
- pH 7.4
- 1 x Protease Inhibitor Cocktail (Roche)
- 1 x Phosphatase Inhibitor Cocktail 1 (Sigma)
- 1 x Phosphatase Inhibitor Cocktail 2 (Sigma)

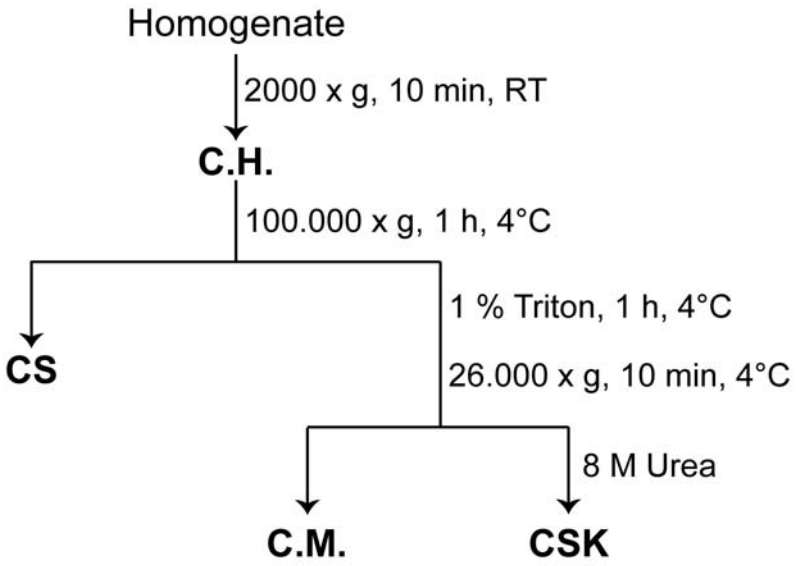

Figure 24. schematic presentation of the steps involved in the membrane fractionation

Co-Immunoprecipitation of β-dystroglycan-binding proteins from rat sciatic nerve

Only cut-off pipette tips were used during the co-IPs in order to not disrupt fragile protein complexes by shear forces. If not otherwise stated, all steps were carried out on at 4° C.

One adult rat was euthanized with CO_2. The sciatic nerves were removed, snap frozen in liquid nitrogen and pulverized thoroughly under LN_2 coverage using a mortar and pistil. The grinded nerve powder was transferred into a 2ml glass-in-glass dounce homogenizer and homogenized in 500 µl Hepes-Extraction Buffer with 30 strokes. The suspension was transferred into Eppendorf tubes, incubated at RT for 10 min and subsequently centrifuged at 4° C for 10 minutes at 1,306 x g to sediment cell debris. The supernatant was transferred to a new Eppendorf tube and the pellet was discarded. A 50 µl aliquot was removed, mixed with 50 µl of 6 x SDS sample buffer, incubated for 5 minutes at 95° C, marked as crude homogenate and stored at -20° C. To the rest of the crude homogenate, 100 µl Protein G-sepharose were added and incubated on a rotator for 3 hours at 4° C to pre-clear the homogenate of proteins that bind unspecific to the beads. The sepharose beads were pelleted by centrifugation at 2,040 x g for 5 minutes at 4° C. The supernatant was transferred to a fresh 2 ml Eppendorf tube and split into two aliquots.

To the first aliquot a mix of the anti-β-dystroglycan antisera was added (sera #1709 and #1710 kindly provided by S. Winder, diluted 1:20 in PBS). To the second aliquot 10 µg anti-EGFP-antibodies (mAb; mouse anti GFP, Roche diagnostics), serving as a control were added. The mixtures were incubated over night on a rotator at 4° C.

The next day, 50 µl protein G-sepharose were added and incubated for 6 h at 4° C on a rotator. The sepharose beads were pelleted by centrifugation at 326 x g for 3 minutes. The supernatant was removed with a needle/syringe, shock frozen in liquid nitrogen and stored at -80° C. The sepharose-beads were washed 3 times by addition of 500 µl hepes-extraction buffer, resuspending the beads by turning the Eppendorf tube bottom up and centrifugation at 326 x g for 2 minutes at room temperature. Each time the supernatant was removed with a needle/syringe and discarded. Ultimately 50 µl 6 x SDS buffer were added to the pelleted sepharose beads, briefly vortexed and boiled at 95° C for 5 minutes. After 5 min of centrifugation at 326 x g at RT the supernatant was carefully removed with a needle attached to a syringe and stored as immunprecipitate at -80° C.

Hepes extraction buffer:

- 50 mM Hepes/HCl
- 0.5 mM EGTA
- 5 mM $MgCl_2$
- 1% (v/v) Triton X-100
- 0.5 mg/ml DNAse I
- 0.2 mg/ml RNAse A
- 2mM PMSF
- pH 7.4
- 1 x Protease Inhibitor Cocktail (Roche)
- 1 x Phosphatase Inhibitor Cocktail 1 (Sigma)
- 1 x Phosphatase Inhibitor Cocktail 2 (Sigma)

Co-immunoprecipitation of plectin-binding proteins from mouse sciatic nerve

Only cut-off pipette tips were used during the co-IPs in order to not disrupt fragile protein complexes by shear forces. If not otherwise stated, all steps were carried out on ice.

Adult wild-type mice were anesthetized with 150 µl of isofluran (Abbott) and killed by cervical dislocation. The sciatic nerves were removed, immediately transferred into a 2 ml glass-in-glass dounce homogenizer and homogenized in 70 µl of phosphate-triton buffer per cm nerve with 20 strokes. The resulting suspension was transferred into Eppendorf tubes and centrifuged at 4° C for 10 minutes at 1,306 x g to sediment cell debris. The supernatant was removed and filled up to 1,900 µl with phosphate-triton buffer. 100 µl of phosphate-SDS buffer were added to the remaining pellet, followed by pipetting to solubilize the otherwise insoluble cytoskeletal proteins. The resuspended pellet was incubated for 10 minutes at room temperature and centrifuged at room temperature for 10 minutes at 1,306 x g to sediment the still insoluble proteins. The 100 µl of supernatant were removed and portion-wise added to the 1,900 µl of the initial supernatant. This solution was then carefully mixed by pipetting. A 50 µl aliquot was removed, mixed with 50 µl of 6 x SDS-sample buffer, incubated for 5 minutes at 95° C, marked as crude homogenate and stored at - 20° C. To the rest of the crude homogenate, 100 µl protein G-sepharose were added and incubated on a rotator for 3 hours at 4° C for the purpose of pre-clearing the crude homogenate. The sepharose beads were pelleted by centrifugation at 735 x g for 5 minutes at 4° C. The supernatant was transferred to a fresh 2 ml Eppendorf tube and split into 2 aliquots.

To the first aliquot anti plectin antibodies were added (a mix of 150µl 10F6 and 4µl #46). To the second aliquot anti-EGFP antibodies were added to serve as a negative sample (a mix of 5 µl of rabbit-anti-EGFP antibodies and 5 µl of mouse-anti-EGFP antibodies + 140 µl PBS). The mixtures were incubated on a rotator over night at 4° C.

The next day, 50 µl protein G-sepharose were added and incubated for 6 h at 4° C on a rotator. The sepharose-beads were pelleted by centrifugation at 326 x g for 2 minutes. The supernatant was removed with a needle/syringe and shock frozen in liquid nitrogen and stored at - 80° C. The sepharose-beads were washed 3 times by adding 500 µl washing-PBS, resuspending the beads by turning the Eppi tube bottom up and

centrifugation at 326 x g for 2 minutes at room temperature. Each time the supernatant was removed with a needle attached to a syringe and discarded. 50 µl 6 x SDS buffer were added to the pelleted sepharose beads, briefly vortexed and boiled at 95° C for 5 minutes. After 5 min of centrifugation at 326 x g at RT the supernatant was carefully removed with a needle/syringe and stored as immunprecipitate at - 80° C.

Phosphate-triton extraction buffer:

- 20 mM $Na_2P_2O_7$
- 20 mM Na-$P0_4$
- 0.5 mM EDTA
- 1 mM $MgCl_2$
- 0.303 M Sucrose
- 1 % (v/v) Triton X-100
- 2 mM PMSF
- pH 7.4
- 1 x Protease Inhibitor Cocktail (Roche)
- 1 x Phosphatase Inhibitor Cocktail 1 (Sigma)
- 1 x Phosphatase Inhibitor Cocktail 2 (Sigma)

Phosphate-SDS extraction buffer:

- 20 mM $Na_2P_2O_7$
- 20 mM Na-$P0_4$
- 0.5 mM EDTA
- 1 mM $MgCl_2$
- 0.303 M Sucrose
- 0.2 % BSA
- 1 % (v/v) Triton X-100
- 2 % SDS
- 2 mM PMSF
- pH 7.5
- 1 x Protease Inhibitor Cocktail (Roche)
- 1 x Phosphatase Inhibitor Cocktail 1 (Sigma)
- 1 x Phosphatase Inhibitor Cocktail 2 (Sigma)

washing-PBS:

- 1 x PBS
- 0.5 % (v/v) Triton X-100
- 1 x Protease Inhibitor Cocktail (Roche)
- 1 x Phosphatase Inhibitor Cocktail 1 (Sigma)
- 1 x Phosphatase Inhibitor Cocktail 2 (Sigma)

Preparation of mouse sciatic nerve total cell lysates

Mice were anesthetized with 150 µl isofluran (Abbott) and killed by cervical dislocation. The sciatic nerves were removed, shock frozen in liquid nitrogen and subsequently pulverized under permanent LN_2-cover using a mortar and pilsit. The pulverized nerves were further homogenized in a 2 ml glass-in-glass dounce homogenizer using 100 µl detergent extraction buffer per 1 cm nerve.

The resulting suspension was transferred to Eppendorf tubes and centrifuged at 4° C for 5 minutes at 2,040 x g to remove cell debris. The supernatant was transferred to a fresh tube and mixed with an equal volume of 5 x SDS - sample buffer. The mixture was incubated for 5 minutes at 95° C and centrifuged for 10 minutes at 13,793 x g. The supernatant, which was termed sciatic nerve total cell lysate, was transferred to a new tube and stored at - 80° C.

Detergent Extraction buffer:

- 20 mM Tris/HCl
- 150 mM NaCl
- 1 mM EDTA
- 1 % (v/v) Triton X-100
- 0.5 % (v/v) NP-40
- 1 mM PMSF
- pH 7.5
- 1 x Protease Inhibitor Cocktail (Roche)
- 1 x Phosphatase Inhibitor Cocktail 1 (Sigma)
- 1 x Phosphatase Inhibitor Cocktail 2 (Sigma)

Preparation and immunostaining of teased nerve fibers from sciatic nerves

Mice were anesthetized with 150 µl isofluran (Abbott) and killed by cervical dislocation. The sciatic nerves were removed and subsequently fixed for 20 minutes in 4 or 2 % PFA at RT. The fixed nerves were washed three times with PBS and mounted on an object slide. The individual nerve fibers were teased aparat using micro-forceps under a stereomicroscope. The slides were stored at -80° C.

All subsequent immunostaining steps were carried out at room temperature.
For immunostaining, the teased nerve fibers were thawed at room temperature and allowed to dry for 15 minutes. After encircling the fibers with a hydrophobic marker they were permabilized with 0.1 % Triton X-100 in PBS for 30 minutes. The primary antibodies were diluted in PBS and incubated on the slides for 1 h. The slides were then washed with PBS and incubated with 0.1 % Triton X-100 in PBS for 5 minutes. The secondary antibody coupled to a fluorophor was diluted in PBS and incubated with the teased fibers for 1 h. The slides were washed with PBS and incubated with 0.1 % Triton X-100 as described above and subsequently incubated with Hoechst dye for 5 minutes (Sigma, diluted 1:3,000). The slides were washed one last time with PBS and incubated with 0.1 % Triton X-100 for 5 minutes. The slides were washed shortly in ddH_2O and allowed to dry completely. Finally the slides were mounted with mowiol and air-dried for at least 24 hours. Storage was performed at 4° C.

Expression of recombinant proteins in E. Coli

Preparation of bacterial glycerol stocks:

E. Coli (strain BL21, DE3), carrying plasmids expressing recombinant HIS-fusion proteins were plated on agar plates containing 100 µg/ml ampicilin and grown overnight at 37° C. After colonies were then used to inoculate 100 ml TB medium containing 1 % glucose and 100 µg/ml ampicilin. The cultures were incubated over night at 37° C. The bacteria were harvested by centrifugation at 3,000 x g for 10 minutes at 4° C and subsequently resuspended in sterile TB medium supplemented with 10 % glycerol and 200 µg/ml ampicilin. The bacteria were aliquoted into 200 µl aliquots, frozen in liquid nitrogen and stored at -80° C.

Expression and purification of recombinant proteins in E. coli:

Bacterial stocks were used to inoculate 200 ml TB medium supplemented with 1 % glucose and 100 µg/ml ampicilin. The cultures were incubated at 37° C until an OD_{600} of 0,6 was reached. Expression was started by addition of 1 mM IPTG and the bacteria were incubated for 4 h at 30° C. The cells were harvested by centrifugation at 10,000 x g for 15 min at 4° C. The supernatant was discarded and the pellet resuspended in 10 ml buffer A and frozen at - 20° C o/n.

Next day the bacteria were thawn on ice and subsequently incubated with lysozyme (200 µg/ml) for 15 minutes at 30° C. The suspension was transferred to SS 34 rotor tubes (Sorvall) and sonicated on ice for 10 cycles, 30 sec continuous pulse with 90 % power (Bandolin Sonopuls HD70) and cooling with liquid nitrogen in between the cycles. Cell debris was pelleted by centrifugation at 10,000 x g for 15 min at 4° C. The supernatant was subsequently subjected to affinity purification.

The supernatant was filtered through a 40 µm filter. Purification was performed using a fast protein liquid chromatography system (Amersham Biosciences ÄKTA FPLC).
HIS tagged proteins were purified using a 5 ml HIS tag chelating column (Amersham Biosciences). The columns were equilibrated with 5 column volumes (cv) buffer A. The filtered protein lysate was applied to the column, which was subsequently washed with 4 cv buffer A containing 25 mM imidazol. The proteins were eluted with 4 cv buffer B.

The collected fractions were analyzed by separation on SDS polyacrylamid gels and staining with Coomassie.

Buffer A:

- 50 mM Tris/HCl pH 9,0
- 0,5 M Triton X-100
- 0,1 mM PMSF

Buffer B:

- 50 mM Tris/HCl pH 9,0
- 0,5 M Triton X-100
- 500 mM Imidazol

all buffers were filtered through a 22 µm filter and degassed for 2 h.

Dialysis:

The protein lysates to be dialyzed were pipetted into tubes discriminating particles below 12 kDa. The tubes were incubated o/n at 4° C in the desired destination buffer (1000 x the volume of the sample).

Measurements of protein concentrations

Protein concentrations were determined using the BCA Protein Assay Kit (Pierce).
Alternatively absorption at λ280 nm was measured using the Nanodrop 2000c according to the instructions of the manufacturer (Thermo Scientific).
To normalize total cell lysates derived from wild-type and P0-Cre/cKO sciatic nerve to equal protein content, the lysates were separated on SDS polyacrylamid gels and stained with Coomassie. The gels were scanned (HP ScanJet 8250C, 300 dpi, 8 bit) and the pixel intensities of the most prominent bands were analyzed by densitometry using Quantiscan software (Biosoft). Thus the lysates could be normalized to each other.

SDS-Polyacrylamid gels / Gel electrophoresis

The SDS-polyacrylamid gels were casted containing the desired acrylamid concentration according to table 1.

Separation gels were overlaid with isopropanol during polymerization. The gel was given approximately 20 minutes to polymerize, the isopropanol was removed, the stacking gel was added and the comb (10 or 15 slots) was installed. After another 20 minutes SDS-polyacrylamid gel electrophoresis was performed using the BioRAD Protean Mini II apparatures.

	6%	8%	10%	12%	15%	stacking gel 4%
ddH_2O	2,6 ml	2,3 ml	1,9 ml	1,6 ml	1,1 ml	0,68 ml
30 % acrylamide	1,0 ml	1,3 ml	1,7 ml	2,0 ml	2,5 ml	170 µl
1,5 M Tris/HCl (pH 8,8)	1,3 ml	1,3 ml	1,3 ml	1,3 ml	1,3 ml	130 µl
10 % SDS	50 µl	50 µl	50 µl	50 µl	50 µl	10 µl
10 % ammonium persulfate	50 µl	50 µl	50 µl	50 µl	50 µl	10 µl
TEMED	10 µl	8 µl	6 µl	6 µl	4 µl	2 µl

Table 1. Solutions for preparing gels for SDS-PAGE. Quantities for 5 ml separation and 1 ml stacking gel respectively

In cases were samples had not yet been mixed with SDS-sample buffer, they were mixed 1:1 with 5 x SDS sample buffer and incubated at 95° C for 5 minutes. Samples already pre-mixed with SDS-sample buffer were incubated at 95° C for 3 minutes. Immediately after heating, the samples were pipetted into the slots of the SDS polyacrylamid gels. The gels were covered with electrophoresis buffer and run with the current limited to 20 mA for about 2 h at RT.

Electrophoresis buffer:

25 mM Tris

250 mM Glycine

0.1 % SDS

Coomassie staining

The polyacrylamid gels were incubated in Coomassie staining solution for 30 minutes at RT. They were subsequently destained in destaining solution until the desired contrast was achieved.

Coomassie staining solution:

- 0.5 g Coomassie blue R250
- 400 ml methanol
- 70 ml acetic acid

ddH_2O ad 1l.

Coomassie destaining solution:

- 10 % (v/v) acetic acid
- 30 % (v/v) methanol
- 60 % (v/v) ddH_2O

Gelatin Zymography

A 12 % SDS-Polyacrylamid gel was casted as described above, except that gelatin (1mg/ml) was added to the separation gel. Mouse sciatic nerve extracts were prepared as follows:

Mice were anesthetized with 150 µl isofluran (Abbott) and killed by cervical dislocation. The sciatic nerves were removed, snap frozen in liquid nitrogen and subsequently pulverized using a mortar and a pistil. The pulverized nerves were further homogenized in a 2 ml glass-in-glass dounce homogenizer with 100 µl phosphate extraction buffer per 1 cm nerve.

The suspension was transferred to Eppendorf tubes and centrifuged at 4° C for 5 minutes at 209 x g to remove cell debris. The resulting supernatant was transferred to a fresh tube and mixed with an equal volume of 1 x non-reducing SDS - sample buffer.

The sciatic nerve-extracts were loaded into the gel and electrophoresis was performed as described in the SDS-PAGE section. All incubation steps were carried out on a shaker. After protein separation the gel was placed in 2.5 % Triton X-100 in PBS for 1 h at RT to wash away the SDS. The gel was then washed twice with substrate buffer and incubated in substrate buffer over night at 37° C. Next day the gel was stained for 30 min with Coomassie solution and destained by boiling in ddH_2O using a microwave oven, until optimal contrast was achieved.

Phosphate extraction buffer:

20 mM	NaH_2P0_4
20 mM	Na_2HP0_4
1 mM	$MgCl_2$
0,303 M	Sucrose
pH 7,4	

5 x non-reducing sample buffer:

400 mM	Tris/HCl
50 % (v/v)	Glycerol
0.1 % (w/v)	Bromphenol blue
2.5 % (w/v)	SDS
pH 6.8	

Substrate buffer:

50 mM	Tris/HCl
5 mM	$CaCl_2$
0,02 % (w/v)	NaN_3

Electrotransfer of proteins onto nitrocellular membranes

The blot-sandwich for electric transfer was prepared as depicted in Figure 25:

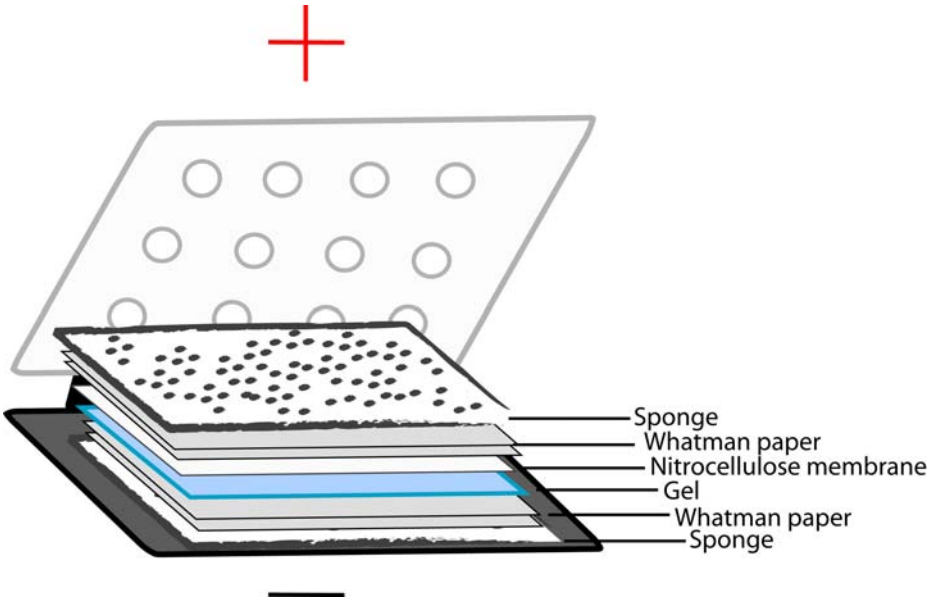

Figure 25. Immunoblot sandwich assembly

All components were soaked in transfer buffer prior to the sandwich assembly. The sponges were additionally rinsed with ddH_2O before being soaked in transfer buffer to remove remaining salts. Electrotransfer was performed in a wet-blotting tank filled with transfer buffer at 4° C o/n at 25 V.

The successful protein transfer was verified by staining with 1 x Ponceau solution for 3 minutes and subsequent counterstaining with ddH_2O. If necessary molecular weight standard bands were marked and the membrane was cropped. The membrane was then destained with PBS-T.

Transfer buffer:

25 mM	Tris
250 mM	Glycine

10 x Ponceau Solution:

2 % (w/v)	Ponceau S
30 % (v/v)	trichloracetic acid
30 % (v/v)	sulfonsalicylic acid
40 % (v/v)	ddH_2O

Immunoblotting

All steps were carried out on a shaker.

To block unspecific binding sites on the nitrocellulose membrane, it was incubated in either 5 % skimmed milk in PBS - T or 5 % BSA/PBS-T for one hour at RT. The primary antibodies directed against the proteins of interest were diluted in 5 % BSA/PBS-T – 0.02 % NaN_3 was added as preservative. The membrane was incubated overnight at 4° C with the primary antibodies. On the next day, the membrane was washed 3 x 10 min with PBS-T and incubated with the secondary antibody (diluted in PBS-T) for one hour at RT. The secondary antibodies were coupled to either HRP0 (horseradish peroxidase) or AP (alkaline phosphatase) to allow for visual/chemi-luminescent detection. The membrane was washed 3 times 10 minutes in PBS-T before progressing to detection.

Chemiluminescent detection of HRP0-coupled antibodies was performed using the SuperSignal West Pico Chemiluminescence substrate (Thermo Scientific) and X-Ray films.

For detection of AP-coupled antibodies the membrane was washed once with AP buffer and subsequently incubated in AP substrate until optimal intensities of stained bands had been achieved. The staining was stopped with PBS.

AP buffer:

100 mM	Tris pH 9.5
100 mM	NaCl
5 mM	$MgCl_2$

AP substrate:

66 µl	BCIP stock solution
66 µl	NBT stock solution

in 10 ml AP buffer

BCIP stock solution:

50 mg/ml	BCIP in 100 % (v/v) DMF

NBT stock solution:

50 mg/ml NBT in 70 % (v/v) DMF

Protein overlay assay

Subcellular fractions prepared from sciatic nerves (membranous/cytoskeletal) were separated by SDS-Page as described above. The proteins were transferred onto a nitrocellulose membrane by electrotransfer as described above.

All incubation steps were carried out on a shaker.

On the next day the membranes were blocked with 5 % skimmed milk in PBS-T for 3 h. The membranes were then incubated with recombinant his-tagged plectin fragments (10 µg/ml diluted in overlay buffer) over night at 4° C. On the next day the membrane was washed 3 x 10 min with PBS-T and subsequently incubated with monoclonal mouse anti-penta-His antibodies for one hour at RT. The membrane was then washed 3 x 10 min with PBS-T and subsequently incubated with goat anti-mouse antibodies coupled to HRP0 for one hour at RT. Finally, the membrane was washed 3 x 10 min with PBS-T and subjected to chemiluminescent detection as described above.

Cell culture:

All cell cultur techniques were carried out under aseptic conditions in a laminar flow hood. Unless otherwise stated all media and solutions used, were pre-heated to 37° C in a waterbath.

.Thawing of frozen cells

Cells stored in liquid nitrogen were rapidly thawed in a water bath at 37° C. The thawed cell suspension was immediately pipetted into 10 ml medium and this mixture was centrifuged for 3 minutes at 184 x g. The supernatant was discarded and the pellet was resuspended in 5 ml of appropriate medium. The suspension was pipetted into a 10 cm dish already containing 5 ml medium. The dish was incubated at 37° C, 5 % CO_2.

.Passaging of cells

The medium was aspirated and the dish was washed with PBS. The cells were incubated with trypsin-EDTA until they detached from the dish. The reaction was stopped by addition of medium containing serum. The cells were resuspended using a 5 ml pipette and transferred to a centrifuge tube. The cell suspension was centrifuged for 3 minutes at 1.000 rpm. The supernatant was discarded and the pellet was resuspended in appropriate medium. Aliquots of the cells were pipetted on new dishes and incubated at 37°C, 5 % CO_2.

.Freezing of cells

The pellet containing trypsinized cells was resuspended in 500 µl medium B. 500 µl medium A were added dropwise and the mixture was transferred to a cryotube that was placed in a specialized freezing device (Nalgene, "Mr. Frosty") filled with isopropanol to guarantee slow freezing in a -80° C freezer overnight. On the next day the cells were transferred to storage in liquid nitrogen.

medium A:

20 %	DMSO
80 %	medium
4° C	

medium B:

40 %	medium
60 %	FCS
37° C	

Isolation of primary SCs from adult mice

The protocol used was modified from Manent et al. 2002, Mauritz et al. 2004, Niapour et al. 2010.

Mice were anesthetized with 150 µl isofluran (Abbott) and killed by cervical dislocation. The sciatic nerves were removed and immediately put in 4° C cold DMEM-F12 containing penicillin and streptomycin. The dishes were transferred to a sterile laminar flow hood and the nerves were rinsed 3 times with sterile DMEM-F12. Then the nerves were placed in a plastic cell culture dish filled with degeneration medium and incubated for 10 days at 37° C, 5 % CO_2. The degeneration medium was changed twice a week. For dissociation, the nerves were rinsed three times in PBS -/- and placed in a 75 cm^2 flask containing 10 ml dissociation medium. The nerves were incubated for 6 h at 37° C, 5 % CO_2 with regular agitation. The dissociation was stopped by addition of 20 ml DMEM + 10 % FCS and the cells were dissociated by pipetting up and down with a fire polished 5 ml pipet. The suspension was transferred to a falcon tube and centrifuged for 5 min at 300 x g. The supernatant was aspirated and the pellet resuspended in primary plating medium. The SCs were counted in a counting chamber and seeded at the appropriate density (usually 1 x 10^6 cells per 35 mm dish) on laminin 111 coated dishes/coverslips. After 24 h the primary plating medium was removed and replaced with growth medium. The growth medium was changed twice a week.

Degeneration medium:

DMEM supplemented with

10 % (v/v)	FCS
50 µg/ml	Gentamycin
2.5 µg/ml	Fungizone
2 µM	Forskolin
10 ng/ml	Heregulin-β1 (HRG)

Dissociation medium:

Leibovitz Medium L-15 supplemented with

130 U/ml	Collagenase Typ I
1.25 U/ml	Dispase II
50 µg/ml	Gentamycin
2.5 µg/ml	Fungizone

Penicillin/Streptomycin.

Primary plating medium:

DMEM supplemented with

10 % (v/v)	FCS
50 µg/ml	Gentamycin
2.5 µg/ml	Fungizone
2 µM	Forskolin
1 % (w/v)	BSA

Growth medium:

Melanocyte growth medium supplemented with:

50 µg/ml	Gentamycin
2,5 µg/ml	Fungizone
2 µM	Forskolin
5 µg/ml	bovine pituitary extract
10 ng/ml	FGF-2 (basic fibroblast factor)

Coverslip preparation:

Coverslips were washed several times with 70 % EtOH, dried and left under the UV light in the hood for sterilization. Then they were coated appropriately

Coating of coverslips / cell culture dishes with laminin 111 or 211:

Dishes were washed once with ddH_2O. Laminin 111 or 211 (10 µg/ml in ddH_2O) was added and incubated for at least 3 h at 37° C. The unbound laminin 111 or 211 was removed and medium was added for 15 minutes. The medium was aspirated and the cells seeded.

Induction of process retraction of primary SCs upon treatment with lysophosphatidic acid (LPA)

Wild-type and mutant (P0) primary SCs were isolated as described above and plated on either laminin 111 or 211.

Next day, they were split in six well plates suitable for time lapse video-microscopy. The following day the growth medium was replaced by growth medium containing 10 µM LPA (lysophosphatidylic acid). On two individual wells, five different areas were monitored with a 10 x objective. Phase contrast images were taken every 30 seconds for a total of 30 minutes. The retraction of processes from free-growing SCs that showed a bipolar shape was measured using the ImageJ software.

Measuring the migration of primary SCs growing on laminin

Wild-type and P0-Cre/cKO primary SCs were isolated as described above and plated on either laminin 111 or 211. Next day the cells were split in six well plates suitable for time lapse video-microscopy. Six hours later, after making sure the cells had attached, the time lapse analysis was started. Phase contrast images were taken every 30 minutes for 24 h in total. The migration of free growing bi-polar shaped SCs was measured by tracking their nuclei using the multitracker plugin for ImageJ.

Image acquisition / microscopes

A Zeiss laser scanning microscope (LSM) 510 microscope was used for taking immunfluorescent images from cells and teased nerve fibers. Digital images were processed using Adobe Photoshop, Adobe Illustrator and ImageJ software.

Time-lapse video microscopy was performed using a motorized AxioObserver Z1 microscope coupled to AxioCam MRm (Carl Zeiss MicroImaging, Inc.) and equipped with phase contrast optics. During the analysis the cells were cultivated in a PM S1 incubator (Carl Zeiss MicroImaging, Inc.) at 37°C and 5% CO_2, pictures were acquired using the “mark and find” module of AxioVision 4.8.1 image analysis software. Images were processed with Zeiss AxioVision 4.8.1 image analysis software (Carl Zeiss MicroImaging, Inc.) and further analyzed using open source software ImageJ (Rasband, W.S., ImageJ, NIH) for manual tracking of migrating cells.

Digital images were processed using Adobe Photoshop, Adobe Illustrator and ImageJ (Rasband, W.S., ImageJ, NIH) software.

Animal husbandry

To reveal functions of plectin essential for myelinating SCs, a new mouse line was generated, by mating mice carrying *floxed* plectin alleles (Ackerl et al., 2007) with myelin protein zero (P0)–Cre mice (from L. Feltri & L. Wrabetz, San Raffaele Scientific Institute, DIBIT, Milano, Italy), to selectively ablate the whole set of plectin isoforms expressed in myelinating SCs (Feltri et al., 1999). Preliminary analyses showed that the resulting P0–Cre/cKO mice selectively lack plectin in myelinating SCs (data not shown), live to adulthood, and are fertile. Thus, they could be considered as an ideal tool to study the role of plectin in peripheral nerve cell function and regeneration. The P0–Cre/cKO mouse line has been back–crossed to the C57BL/6 background to congenicity.

Mice were kept under standard housing conditions at the animal facility of the Department of Molecular Cell Biology at the Vienna Biocenter. All experiments involving animals were performed in accordance with Austrian Federal Government laws and regulations.

Rats were purchased from *Institut für biomedizinische Forschung, Abteilung für Labortierkunde und Genetik Himberg.*.

Common buffers and solutions

5 x SDS-sample buffer:

- 400 mM Tris/HCl
- 10 % (v/v) SDS
- 50 % (v/v) Glycerol
- 500 mM DTT
- 0.1 % Bromphenolblue
- pH 6.8

10 x PBS:

- 81.8 g NaCl
- 2.01 g KCl
- 2.04 g KH_2P0_4
- 11.3 g K_2HP0_4

pH 7.4; ddH_2O to 1000 ml

PBS - T:

PBS containing 0.05 % Tween-20

TB Medium:

- 1.2 % Tryptone or Peptone
- 2.4 % Yeast extract
- 0.4 % Glycerol

autoclaved and mixed with a sterile phosphate buffer

- 17 mM KH_2P0_4
- 72 mM K_2HP0_4

Antibodies

Antibody name Clone name	Antibody type	Antigen/ Epitope	Dilution WB	Dilution IF	Dilution IP	Vendor/ Reference
Plectin 1	polyclonal rabbit	Exon 1 encoded amino acids	1:500			(Abrahamsberg et al., 2005)
P1a	polyclonal rabbit	Exon 1a encoded amino acids	1:400			(Rezniczek et al., 1998)
P1c	polyclonal rabbit	Exon 1c encoded amino acids	1:400			(Fuchs et al., 2009)
P1f	polyclonal rabbit	Exon 1f encoded amino acids	1:1.000			(Rezniczek et al., 2007)
#9	polyclonal rabbit	Exon 9-12 amino acids	1:3.333			(Andrä et al., 2003)
10F6	monoclonal mouse	plectin rod	1:5		undiluted	(Wiche et al., 1984)
beta-DG 43DAG1/8D5	monoclonal mouse	synthetic peptide c-terminus of human β-DG	1:100	1:20		Novocastra
beta-DG #1709 #1710	rabbit sera	β-dystroglycan phosphopeptide			1:20 1:20	(Ilsley et al., 2001)
DP116 NCL-DYS 2	monoclonal mouse		1:100	1:20		Novocastra
Integrin beta4 (C-20) sc-6628	polyclonal goat	human integrin β4C terminus	1:200	1:50	1 µg per 100 µg protein	Santa Cruz
Vimentin	goat		1:10.000	1:400		Taub
Actin ac40	monoclonal mouse	synthetic peptide c-terminal	1:500	1:100		sigma-aldrich
Caveolin	rabbit		1:10.000			
Utrophin	rabbit	aa 3204-3433 of human utrophin	1:5.000			(Winder and Kendrick-Jones, 1995)
GFAP (GA5)	monoclonal mouse	purified pig GFAP	1:1.000	1:300	1:50	cell signaling
GAPDH g9545	rabbit	synthetic peptide aa 314-333 mouse GAPDH	1:5.000	1:200		sigma-aldrich
beta III tubulin	polyclonal rabbit	Aa 441-450	1:1.000	1:100		sigma-aldrich
GST (GST-2)	monoclonal mouse	Purified recombinant GST	1:1.000			Sigma-Aldrich
α–tubulin B-5-1-2	monoclonal mouse	c-terminus	1:6.666			Sigma-Aldrich
α – dystroglycan	monoclonal	rabbit skeletal muscle membrane	1:2.000			Millipore

IIH6C4	mouse	preparation Clone IIH6C4				
δ–Sarcoglycan	rabbit		1:4.000			G. Piluso
penta HIS	monoclonal mouse		1:1.000			Qiagen
p75 NGFR Cat. #AB1554	polyclonal rabbit	GST-tagged NGF receptor p75	1:1.000	1:100		Millipore
DRP2 (2164)	rabbit	synthetic peptide aa 947–957		1:300		(Sherman et al., 2001)
CASPR 2	rabbit			1:500		(Denisenko-Nehrbass et al., 2003)
EZRIN	rabbit	human ezrin aa 479-498		1:100		Upstate Biotech
SL-51	rabbit			1:1.000		J. A. Girault
E-Cadherin 36/E-Cadherin	monoclonal mouse	Human E-Cadherin aa. 735-883		1:100		BD Transduct. Laboratories
#21	rabbit sera	Plectin rod		1:200		G. Wiche
#46	rabbit sera	Plectin rod		1:400	1:40	G. Wiche
GFP clones 7.1 and 13.1	monoclonal mouse	partially purified recombinant Aequorea victoria GFP			1:40	Roche diagnostics

Secondary ABs:						
AP anti-rabbit IgG	goat		1:5.000			Jackson Lab.
AP anti-mouse IgG	goat		1:5.000			Jackson Lab.
HRP0 anti-mouse IgG	goat		1:10.000			Jackson Lab.
HRP0 anti-mouse IgM	donkey		1:50.000			Jackson Lab.
HRP0 anti-rabbit IgG	goat		1:20.000			Vector Labs
HRP0 anti-goat IgG	donkey		1:50.000			Jackson Lab.
Secondary ABs: IF						
RRX anti-rabbit IgG	donkey			1:200		Jackson Lab.
Cy2 anti-rat	donkey			1:200		Jackson Lab.
Cy5 anti rabbit	donkey			1:500		Jackson Lab.
Cy5 anti-rat	donkey			1:500		Jackson Lab.
Cy5 anti-mouse	donkey			1:500		Jackson Lab.
RRX anti-mouse	donkey			1:200		Jackson Lab.
RRX anti-rat	donkey			1:200		Jackson Lab.
Alexa 488 anti goat	donkey			1:800		Molecular Probes
Alexa 488 anti-rabbit	donkey			1:1.000		Molecular Probes

List of chemicals:

Reagent	Vendor	Article number
30 % Acrylamide mix (29:1)	Gerbu	1108
Acetic acid	Merck	100063
Agar	Gerbu	1340
$AgNO_3$	Fluka	85228
Ammoniumpersulfate (APS)	Serva	13375
Ampicilin	Gerbu	1046
BCIP (X-Phos)	Gerbu	71290
bovine pituitary extract	PromoCell	C-24110
bovine serum albumin (BSA)	Gerbu	1063
Bromphenolblue-Solution	Sigma-Aldrich	B7021
Collagenase Typ I	Gibco	17100-017
Coomassie blue R250	Gerbu	1097
Deoxycholat	Sigma-Aldrich	06750
Dispase Typ II	Gibco	17105-041
Dithiothreitol (DTT)	Gerbu	1008
DMEM-F12	Gibco	11320-074
Dimethylformamid (DMF)	Loba	402480
Dimethylsulfoxid (DMSO)	Fluka	41640
DNAse I	Roche	104159
DMEM	Gibco	52100-039
EGTA	Sigma-Aldrich	E-4378
Ethanol	Merck	100983 RdH 32221
Ethylenediaminetetraacetic acid (EDTA)	Gerbu	1034
Fetal calf serum (FCS)	Sigma-Aldrich	F-7524
FGF 2 (basic fibroblast growth factor)	PromoCell	C-24110
Forskolin	Calbiochem	344270
Fungizon	Gibco	15290-026
Gentamycin	Gibco	15710-049
Glucose	Merck	8346
Glutathion-reduced	Sigma-Aldrich	G4251-504
Glutathion sepharose beads	GE-Healthcare	17-0756-01

Glycerol	Gerbu	2006
Glycine	Gerbu	1023
Formaldehyde	Merck	C3914003
Hepes	Gerbu	1009
Heregulin-beta-1	R&D Systems	396-HB-050
Hoechst dye (#33258)	Hoechst	382061
Hydrochloric acid (HCl)	Merck	100317
Imidazol	Fluka	56750
IPTG	Gerbu	1010
Isofluran (Isoflo)	Abbott	34480VA
Isopropanol	Merck	109634
K_2HP0_4	Fluka	60356
KCl	Loba	58648
KH_2P0_4	Fluka	60230
Laminin-1	Sigma-Aldrich	L2020
L-glutamine	Gibco	25030-024
Lysophosphatidylic acid (LPA)	Cayman	62215
Lysozyme	Gerbu	1603
Merosin	Chemicon	CC085
Methanol	Merck	106009-RdH 32213
MgCl2	Fluka	63072
Na_2CO_3	Loba	70598
$Na_2S_2O_3*5H_2O$	Merck	6512
Na_2HP0_4 Disodiumhydrogenphosphate	Fluka	71645
NaH_2P0_4 Sodiumdihydrogenphosphate	Fluka	71506
NaCl	Gerbu	1112
Natriumazid (NaN_3)	Fluka	71290
NBT	Sigma-Aldrich	N-6876
NP-40 (nonident P-40)	Sigma-Aldrich	I-3021
Paraformaldehyde (PFA)	Fluka	47629
Phosphate buffered saline (PBS)	Gibco	21300-074
Penicilin/Streptomycin	Gibco	15070-22
Peptone	Gibco	30392
Phenylmethanesulfonylfluoride-(PMSF)	Sigma-Aldrich	P-7626

Phosphatase Inhibitor Cocktail 3	Sigma-Aldrich	P0044
Phosphatase Inhibitor Cocktail 2	Sigma-Aldrich	P5726
Ponceau S	Sigma-Aldrich	P3504
Protease inhibitor cocktail complete mini	Roche	11836153001
Protein-G Agarose	Pierce	20398
RNAse A	Roche	10109142001
Skim milk powder	Gerbu	1602
Sodium bicarbonate	Gibco	043-5080
Sodiumdodecylsulfate (SDS)	Sigma-Aldrich	L-4509
Sodium hydroxide solution (NaOH)	Gerbu	2020
Sodium pyrovate	Sigma	P-5280
Sucrose	Gerbu	1366
Sulfonsalicylic acid	Fluka	86195
TEMED	Serva	35925
Trichloracetic acid (TCA)	Sigma-Aldrich	T-4885
Tris-X	Gerbu	1018
Triton-X-100	Gerbu	9002-93-1
Trypsin	Gibco	15090-046
Tween-20	Gerbu	2001
Urea	Gerbu	1044
Yeast-extract	Gerbu	1133

Dishes/flasks (cell culture) were purchased from NUNC

References

„Ich habe mich bemüht, sämtliche Inhaber der Bildrechte ausfindig zu machen und ihre Zustimmung zur Verwendung der Bilder in dieser Arbeit eingeholt. Sollte dennoch eine Urheberrechtsverletzung bekannt werden, ersuche ich um Meldung bei mir.“

Abrahamsberg, C., P. Fuchs, S. Osmanagic-Myers, I. Fischer, F. Propst, A. Elbe-Burger, and G. Wiche. 2005. Targeted ablation of plectin isoform 1 uncovers role of cytolinker proteins in leukocyte recruitment. *Proc Natl Acad Sci U S A*. 102:18449-18454.

Ackerl, R., G. Walko, P. Fuchs, I. Fischer, M. Schmuth, and G. Wiche. 2007. Conditional targeting of plectin in prenatal and adult mouse stratified epithelia causes keratinocyte fragility and lesional epidermal barrier defects. *J Cell Sci*. 120:2435-2443.

Alberts, B. 2008. Molecular biology of the cell. Garland Science, New York. 1 v. (various pagings) pp.

Amano, M., K. Chihara, N. Nakamura, Y. Fukata, T. Yano, M. Shibata, M. Ikebe, and K. Kaibuchi. 1998. Myosin II activation promotes neurite retraction during the action of Rho and Rho-kinase. *Genes Cells*. 3:177-188.

Anderson, C., S.J. Winder, and A.G. Borycki. 2007. Dystroglycan protein distribution coincides with basement membranes and muscle differentiation during mouse embryogenesis. *Dev Dyn*. 236:2627-2635.

Andrä, K., I. Kornacker, A. Jorgl, M. Zörer, D. Spazierer, P. Fuchs, I. Fischer, and G. Wiche. 2003. Plectin-isoform-specific rescue of hemidesmosomal defects in plectin (-/-) keratinocytes. *J Invest Dermatol*. 120:189-197.

Andrä, K., I. Kornacker, A. Jorgl, M. Zörer, D. Spazierer, P. Fuchs, I. Fischer, and G. Wiche. 2003. Plectin-isoform-specific rescue of hemidesmosomal defects in plectin (-/-) keratinocytes. *J Invest Dermatol*. 120:189-197.

Andrä, K., H. Lassmann, R. Bittner, S. Shorny, R. Fassler, F. Propst, and G. Wiche. 1997. Targeted inactivation of plectin reveals essential function in maintaining the integrity of skin, muscle, and heart cytoarchitecture. *Genes Dev*. 11:3143-3156.

Andrä, K., B. Nikolic, M. Stocher, D. Drenckhahn, and G. Wiche. 1998. Not just scaffolding: plectin regulates actin dynamics in cultured cells. *Genes Dev*. 12:3442-3451.

Andrä, K., B. Nikolic, M. Stocher, D. Drenckhahn, and G. Wiche. 1998. Not just scaffolding: plectin regulates actin dynamics in cultured cells. *Genes Dev*. 12:3442-3451.

Bauer, J.W., F. Rouan, B. Kofler, G.A. Rezniczek, I. Kornacker, W. Muss, R. Hametner, A. Klausegger, A. Huber, G. Pohla-Gubo, G. Wiche, J. Uitto, and H. Hintner. 2001. A compound heterozygous one amino-acid insertion/nonsense mutation in the plectin gene causes epidermolysis bullosa simplex with plectin deficiency. *Am J Pathol*. 158:617-625.

Bonifas, J.M., A.L. Rothman, and E.H. Epstein, Jr. 1991. Epidermolysis bullosa simplex: evidence in two families for keratin gene abnormalities. *Science*. 254:1202-1205.

Bonne, G., M.R. Di Barletta, S. Varnous, H.M. Becane, E.H. Hammouda, L. Merlini, F. Muntoni, C.R. Greenberg, F. Gary, J.A. Urtizberea, D. Duboc, M. Fardeau, D. Toniolo, and K. Schwartz. 1999. Mutations in the gene encoding lamin A/C cause autosomal dominant Emery-Dreifuss muscular dystrophy. *Nat Genet*. 21:285-288.

Bouquet, C., M. Ravaille-Veron, F. Propst, and F. Nothias. 2007. MAP1B coordinates microtubule and actin filament remodeling in adult mouse SC tips and DRG neuron growth cones. *Mol Cell Neurosci*. 36:235-247.

Bozzi, M., R. Inzitari, D. Sbardell, S. Monaco, E. Pavoni, M. Gioia, S. Marini, S. Morlacchi, F. Sciandra, M. Castagnola, B. Giardina, A. Brancaccio, and M. Coletta. 2009a. Enzymatic processing of beta-dystroglycan recombinant ectodomain by MMP-9: identification of the main cleavage site. *IUBMB Life*. 61:1143-1152.

Bozzi, M., S. Morlacchi, M.G. Bigotti, F. Sciandra, and A. Brancaccio. 2009b. Functional diversity of dystroglycan. *Matrix Biol*. 28:179-187.

Bugyi, B., and M.F. Carlier. 2010. Control of actin filament treadmilling in cell motility. *Annu Rev Biophys*. 39:449-470.

Byers, T.J., H.G. Lidov, and L.M. Kunkel. 1993. An alternative dystrophin transcript specific to peripheral nerve. *Nat Genet*. 4:77-81.

Chavanas, S., L. Pulkkinen, Y. Gache, F.J. Smith, W.H. McLean, J. Uitto, J.P. Ortonne, and G. Meneguzzi. 1996. A homozygous nonsense mutation in the PLEC1 gene in patients with epidermolysis bullosa simplex with muscular dystrophy. *J Clin Invest*. 98:2196-2200.

Chernousov, M.A., and D.J. Carey. 2000. SC extracellular matrix molecules and their receptors. *Histol Histopathol*. 15:593-601.

Comi, G.P., E. Ciafaloni, H.A. de Silva, A. Prelle, A. Bardoni, C. Rigoletto, M. Robotti, N. Bresolin, M. Moggio, and F. Fortunato. 1995. A G+1-->A transversion at the 5' splice site of intron 69 of the dystrophin gene causing the absence of peripheral nerve Dp116 and severe clinical involvement in a DMD patient. *Hum Mol Genet*. 4:2171-2174.

Coulombe, P.A., M.E. Hutton, A. Letai, A. Hebert, A.S. Paller, and E. Fuchs. 1991. Point mutations in human keratin 14 genes of epidermolysis bullosa simplex patients: genetic and functional analyses. *Cell*. 66:1301-1311.

Court, F.A., J.E. Hewitt, K. Davies, B.L. Patton, A. Uncini, L. Wrabetz, and M.L. Feltri. 2009. A laminin-2, dystroglycan, utrophin axis is required for compartmentalization and elongation of myelin segments. *J Neurosci*. 29:3908-3919.

Cross, S.S., J. Lippitt, A. Mitchell, F. Hollingsbury, S.P. Balasubramanian, M.W. Reed, C. Eaton, J.W. Catto, F. Hamdy, and S.J. Winder. 2008. Expression of beta-dystroglycan is reduced or absent in many human carcinomas. *Histopathology*. 53:561-566.

Denisenko-Nehrbass, N., K. Oguievetskaia, L. Goutebroze, T. Galvez, H. Yamakawa, O. Ohara, M. Carnaud, and J.A. Girault. 2003. Protein 4.1B associates with both Caspr/paranodin and Caspr2 at paranodes and juxtaparanodes of myelinated fibres. *Eur J Neurosci*. 17:411-416.

Desai, A., and T.J. Mitchison. 1997. Microtubule polymerization dynamics. *Annu Rev Cell Dev Biol*. 13:83-117.

Eldridge, C.F., M.B. Bunge, and R.P. Bunge. 1989. Differentiation of axon-related SCs in vitro: II. Control of myelin formation by basal lamina. *J Neurosci*. 9:625-638.

Elliott, C.E., B. Becker, S. Oehler, M.J. Castãnón, R. Hauptmann, and G. Wiche. 1997. Plectin transcript diversity: identification and tissue distribution of variants with distinct first coding exons and rodless isoforms. *Genomics*. 42:115-125.

Eriksson, J.E., T. Dechat, B. Grin, B. Helfand, M. Mendez, H.M. Pallari, and R.D. Goldman. 2009. Introducing intermediate filaments: from discovery to disease. *J Clin Invest*. 119:1763-1771.

Feltri, M.L., M. D'Antonio, S. Previtali, M. Fasolini, A. Messing, and L. Wrabetz. 1999. P0-Cre transgenic mice for inactivation of adhesion molecules in SCs. *Ann N Y Acad Sci*. 883:116-123.

Feltri, M.L., S.S. Scherer, R. Nemni, J. Kamholz, H. Vogelbacker, M.O. Scott, N. Canal, V. Quaranta, and L. Wrabetz. 1994. Beta 4 integrin expression in myelinating SCs is polarized, developmentally regulated and axonally dependent. *Development*. 120:1287-1301.

Foisner, R., F.E. Leichtfried, H. Herrmann, J.V. Small, D. Lawson, and G. Wiche. 1988. Cytoskeleton-associated plectin: in situ localization, in vitro reconstitution, and binding to immobilized intermediate filament proteins. *J Cell Biol*. 106:723-733.

Foisner, R., and G. Wiche. 1987. Structure and hydrodynamic properties of plectin molecules. *J Mol Biol*. 198:515-531.

Fuchs, E., and D.W. Cleveland. 1998. A structural scaffolding of intermediate filaments in health and disease. *Science*. 279:514-519.

Fuchs, P., M. Zörer, S. Reipert, G.A. Rezniczek, F. Propst, G. Walko, I. Fischer, J. Bauer, M.W. Leschnik, B. Luscher, J.G. Thalhammer, H. Lassmann, and G. Wiche. 2009. Targeted inactivation of a developmentally regulated neural plectin isoform (plectin 1c) in mice leads to reduced motor nerve conduction velocity. *J Biol Chem*. 284:26502-26509.

Fuchs, P., M. Zörer, G.A. Rezniczek, D. Spazierer, S. Oehler, M.J. Castãnón, R. Hauptmann, and G. Wiche. 1999. Unusual 5' transcript complexity of plectin isoforms: novel tissue-specific exons modulate actin binding activity. *Hum Mol Genet*. 8:2461-2472.

Fujita, R., N. Kiguchi, and H. Ueda. 2007. LPA-mediated demyelination in ex vivo culture of dorsal root. *Neurochem Int*. 50:351-355.

Gache, Y., S. Chavanas, J.P. Lacour, G. Wiche, K. Owaribe, G. Meneguzzi, and J.P. Ortonne. 1996. Defective expression of plectin/HD1 in epidermolysis bullosa simplex with muscular dystrophy. *J Clin Invest*. 97:2289-2298.

Goldfarb, L.G., P. Vicart, H.H. Goebel, and M.C. Dalakas. 2004. Desmin myopathy. *Brain*. 127:723-734.

Goley, E.D., and M.D. Welch. 2006. The ARP2/3 complex: an actin nucleator comes of age. *Nat Rev Mol Cell Biol*. 7:713-726.

Green, K.J., M. Bohringer, T. Gocken, and J.C. Jones. 2005. Intermediate filament associated proteins. *Adv Protein Chem*. 70:143-202.

Gregor, M., A. Zeold, S. Oehler, K.A. Marobela, P. Fuchs, G. Weigel, D.G. Hardie, and G. Wiche. 2006. Plectin scaffolds recruit energy-controlling AMP-activated protein kinase (AMPK) in differentiated myofibres. *J Cell Sci*. 119:1864-1875.

Gundesli, H., B. Talim, P. Korkusuz, B. Balci-Hayta, S. Cirak, N.A. Akarsu, H. Topaloglu, and P. Dincer. 2010. Mutation in Exon 1f of PLEC, Leading to Disruption of Plectin Isoform 1f, Causes Autosomal-Recessive Limb-Girdle Muscular Dystrophy. *Am J Hum Genet*. 87:834-841.

Herrmann, H., H. Bar, L. Kreplak, S.V. Strelkov, and U. Aebi. 2007. Intermediate filaments: from cell architecture to nanomechanics. *Nat Rev Mol Cell Biol*. 8:562-573.

Herzog, C., C. Has, C.W. Franzke, F.G. Echtermeyer, U. Schlotzer-Schrehardt, S. Kroger, E. Gustafsson, R. Fassler, and L. Bruckner-Tuderman. 2004. Dystroglycan in skin and cutaneous cells: beta-subunit is shed from the cell surface. *J Invest Dermatol*. 122:1372-1380.

Hijikata, T., A. Nakamura, K. Isokawa, M. Imamura, K. Yuasa, R. Ishikawa, K. Kohama, S. Takeda, and H. Yorifuji. 2008. Plectin 1 links intermediate filaments to

costameric sarcolemma through beta-synemin, alpha-dystrobrevin and actin. *J Cell Sci*. 121:2062-2074.

Hille, B. 2001. Ion channels of excitable membranes. Sinauer, Sunderland, Mass. xviii, 814 p. pp.

Hirose, M., T. Ishizaki, N. Watanabe, M. Uehata, O. Kranenburg, W.H. Moolenaar, F. Matsumura, M. Maekawa, H. Bito, and S. Narumiya. 1998. Molecular dissection of the Rho-associated protein kinase (p160ROCK)-regulated neurite remodeling in neuroblastoma N1E-115 cells. *J Cell Biol*. 141:1625-1636.

Hnia, K., G. Hugon, A. Masmoudi, J. Mercier, F. Rivier, and D. Mornet. 2006. Effect of beta-dystroglycan processing on utrophin/Dp116 anchorage in normal and mdx mouse SC membrane. *Neuroscience*. 141:607-620.

Ilsley, J.L., M. Sudol, and S.J. Winder. 2001. The interaction of dystrophin with beta-dystroglycan is regulated by tyrosine phosphorylation. *Cell Signal*. 13:625-632.

Imamura, M., K. Araishi, S. Noguchi, and E. Ozawa. 2000. A sarcoglycan-dystroglycan complex anchors Dp116 and utrophin in the peripheral nervous system. *Hum Mol Genet*. 9:3091-3100.

Inoue, A., H. Takenaka, T. Arata, and Y. Tonomura. 1979. Functional implications of the two-headed structure of myosin. *Adv Biophys*. 13:1-194.

Inoue, M., M.H. Rashid, R. Fujita, J.J. Contos, J. Chun, and H. Ueda. 2004. Initiation of neuropathic pain requires lysophosphatidic acid receptor signaling. *Nat Med*. 10:712-718.

Irvine, A.D., and W.H. McLean. 1999. Human keratin diseases: the increasing spectrum of disease and subtlety of the phenotype-genotype correlation. *Br J Dermatol*. 140:815-828.

Janda, L., J. Damborsky, G.A. Rezniczek, and G. Wiche. 2001. Plectin repeats and modules: strategic cysteines and their presumed impact on cytolinker functions. *Bioessays*. 23:1064-1069.

Jefferson, J.J., C.L. Leung, and R.K. Liem. 2004. Plakins: goliaths that link cell junctions and the cytoskeleton. *Nat Rev Mol Cell Biol*. 5:542-553.

Kalman, M., and A. Szabo. 2000. Plectin immunopositivity appears in the astrocytes in the white matter but not in the gray matter after stab wounds. *Brain Res*. 857:291-294.

Kerkelä, E., and U. Saarialho-Kere. 2003. Matrix metalloproteinases in tumor progression: focus on basal and squamous cell skin cancer. *Exp Dermatol*. 12:109-125.

Kim, S., and P.A. Coulombe. 2007. Intermediate filament scaffolds fulfill mechanical, organizational, and signaling functions in the cytoplasm. *Genes Dev*. 21:1581-1597.

Konieczny, P., P. Fuchs, S. Reipert, W.S. Kunz, A. Zeold, I. Fischer, D. Paulin, R. Schröder, and G. Wiche. 2008. Myofiber integrity depends on desmin network targeting to Z-disks and costameres via distinct plectin isoforms. *J Cell Biol*. 181:667-681.

Koss-Harnes, D., B. Hoyheim, I. Anton-Lamprecht, A. Gjesti, R.S. Jorgensen, F.L. Jahnsen, B. Olaisen, G. Wiche, and T. Gedde-Dahl, Jr. 2002. A site-specific plectin mutation causes dominant epidermolysis bullosa simplex Ogna: two identical de novo mutations. *J Invest Dermatol*. 118:87-93.

Koss-Harnes, D., F.L. Jahnsen, G. Wiche, E. Soyland, P. Brandtzaeg, and T. Gedde-Dahl, Jr. 1997. Plectin abnormality in epidermolysis bullosa simplex Ogna: non-responsiveness of basal keratinocytes to some anti-rat plectin antibodies. *Exp Dermatol*. 6:41-48.

Kostan, J., M. Gregor, G. Walko, and G. Wiche. 2009. Plectin isoform-dependent regulation of keratin-integrin alpha6beta4 anchorage via Ca2+/calmodulin. *J Biol Chem*. 284:18525-18536.

Koszka, C., F.E. Leichtfried, and G. Wiche. 1985. Identification and spatial arrangement of high molecular weight proteins (Mr 300 000-330 000) co-assembling with microtubules from a cultured cell line (rat glioma C6). *Eur J Cell Biol*. 38:149-156.

Kueh, H.Y., and T.J. Mitchison. 2009. Structural plasticity in actin and tubulin polymer dynamics. *Science*. 325:960-963.

Lane, E.B., E.L. Rugg, H. Navsaria, I.M. Leigh, A.H. Heagerty, A. Ishida-Yamamoto, and R.A. Eady. 1992. A mutation in the conserved helix termination peptide of keratin 5 in hereditary skin blistering. *Nature*. 356:244-246.

Lee, S.H., and R. Dominguez. 2010. Regulation of actin cytoskeleton dynamics in cells. *Mol Cells*. 29:311-325.

Leung, C.L., K.J. Green, and R.K. Liem. 2002. Plakins: a family of versatile cytolinker proteins. *Trends Cell Biol*. 12:37-45.

Li, R., A. Messing, J.E. Goldman, and M. Brenner. 2002. GFAP mutations in Alexander disease. *Int J Dev Neurosci*. 20:259-268.

Lie, A.A., R. Schröder, I. Blumcke, T.M. Magin, O.D. Wiestler, and C.E. Elger. 1998. Plectin in the human central nervous system: predominant expression at pia/glia and endothelia/glia interfaces. *Acta Neuropathol*. 96:215-221.

Litjens, S.H., J. Koster, I. Kuikman, S. van Wilpe, J.M. de Pereda, and A. Sonnenberg. 2003. Specificity of binding of the plectin actin-binding domain to beta4 integrin. *Mol Biol Cell*. 14:4039-4050.

Liu, B., and Z. Zhou. 2008. Lamin A/C, laminopathies and premature ageing. *Histol Histopathol*. 23:747-763.

Ma, L., R. Rohatgi, and M.W. Kirschner. 1998. The Arp2/3 complex mediates actin polymerization induced by the small GTP-binding protein Cdc42. *Proc Natl Acad Sci U S A*. 95:15362-15367.

Mallik, R., and S.P. Gross. 2004. Molecular motors: strategies to get along. *Curr Biol*. 14:R971-982.

Mandelkow, E., and E.M. Mandelkow. 1995. Microtubules and microtubule-associated proteins. *Curr Opin Cell Biol*. 7:72-81.

Matsumura, K., K. Arai, D. Zhong, F. Saito, H. Fukuta-Ohi, R. Maekawa, H. Yamada, and T. Shimizu. 2003. Disruption of dystroglycan axis by beta-dystroglycan processing in cardiomyopathic hamster muscle. *Neuromuscul Disord*. 13:796-803.

McGough, A.M., C.J. Staiger, J.K. Min, and K.D. Simonetti. 2003. The gelsolin family of actin regulatory proteins: modular structures, versatile functions. *FEBS Lett*. 552:75-81.

McLean, W.H., L. Pulkkinen, F.J. Smith, E.L. Rugg, E.B. Lane, F. Bullrich, R.E. Burgeson, S. Amano, D.L. Hudson, K. Owaribe, J.A. McGrath, J.R. McMillan, R.A. Eady, I.M. Leigh, A.M. Christiano, and J. Uitto. 1996. Loss of plectin causes epidermolysis bullosa with muscular dystrophy: cDNA cloning and genomic organization. *Genes Dev*. 10:1724-1735.

Michaluk, P., L. Kolodziej, B. Mioduszewska, G.M. Wilczynski, J. Dzwonek, J. Jaworski, D.C. Gorecki, O.P. Ottersen, and L. Kaczmarek. 2007. Beta-dystroglycan as a target for MMP-9, in response to enhanced neuronal activity. *J Biol Chem*. 282:16036-16041.

Moore, C.J., and S.J. Winder. 2010. Dystroglycan versatility in cell adhesion: a tale of multiple motifs. *Cell Commun Signal*. 8:3.

Mueller, H., and W.W. Franke. 1983. Biochemical and immunological characterization of desmoplakins I and II, the major polypeptides of the desmosomal plaque. *J Mol Biol*. 163:647-671.

Muhua, L., N.R. Adames, M.D. Murphy, C.R. Shields, and J.A. Cooper. 1998. A cytokinesis checkpoint requiring the yeast homologue of an APC-binding protein. *Nature*. 393:487-491.

Naumanen, P., P. Lappalainen, and P. Hotulainen. 2008. Mechanisms of actin stress fibre assembly. *J Microsc*. 231:446-454.

Nikolic, B., E. Mac Nulty, B. Mir, and G. Wiche. 1996. Basic amino acid residue cluster within nuclear targeting sequence motif is essential for cytoplasmic plectin-vimentin network junctions. *J Cell Biol*. 134:1455-1467.

Nodari, A., S.C. Previtali, G. Dati, S. Occhi, F.A. Court, C. Colombelli, D. Zambroni, G. Dina, U. Del Carro, K.P. Campbell, A. Quattrini, L. Wrabetz, and M.L. Feltri. 2008. Alpha6beta4 integrin and dystroglycan cooperate to stabilize the myelin sheath. *J Neurosci*. 28:6714-6719.

Noguchi, K., D. Herr, T. Mutoh, and J. Chun. 2009. Lysophosphatidic acid (LPA) and its receptors. *Curr Opin Pharmacol*. 9:15-23.

O'Neill, G.M. 2009. The coordination between actin filaments and adhesion in mesenchymal migration. *Cell Adh Migr*. 3:355-357.

Omary, M.B., P.A. Coulombe, and W.H. McLean. 2004. Intermediate filament proteins and their associated diseases. *N Engl J Med*. 351:2087-2100.

Osmanagic-Myers, S., M. Gregor, G. Walko, G. Burgstaller, S. Reipert, and G. Wiche. 2006. Plectin-controlled keratin cytoarchitecture affects MAP kinases involved in cellular stress response and migration. *J Cell Biol*. 174:557-568.

Osmanagic-Myers, S., and G. Wiche. 2004. Plectin-RACK1 (receptor for activated C kinase 1) scaffolding: a novel mechanism to regulate protein kinase C activity. *J Biol Chem*. 279:18701-18710.

Otto, J.J. 1994. Actin-bundling proteins. *Curr Opin Cell Biol*. 6:105-109.

Pfendner, E., and J. Uitto. 2005. Plectin gene mutations can cause epidermolysis bullosa with pyloric atresia. *J Invest Dermatol*. 124:111-115.

Podratz, J.L., E. Rodriguez, and A.J. Windebank. 2001. Role of the extracellular matrix in myelination of peripheral nerve. *Glia*. 35:35-40.

Poliak, S., and E. Peles. 2003. The local differentiation of myelinated axons at nodes of Ranvier. *Nat Rev Neurosci*. 4:968-980.

Previtali, S.C., G. Dina, A. Nodari, M. Fasolini, L. Wrabetz, U. Mayer, M.L. Feltri, and A. Quattrini. 2003a. SCs synthesize alpha7beta1 integrin which is dispensable for peripheral nerve development and myelination. *Mol Cell Neurosci*. 23:210-218.

Previtali, S.C., A. Nodari, C. Taveggia, C. Pardini, G. Dina, A. Villa, L. Wrabetz, A. Quattrini, and M.L. Feltri. 2003b. Expression of laminin receptors in SC differentiation: evidence for distinct roles. *J Neurosci*. 23:5520-5530.

Pulkkinen, L., F.J. Smith, H. Shimizu, S. Murata, H. Yaoita, H. Hachisuka, T. Nishikawa, W.H. McLean, and J. Uitto. 1996. Homozygous deletion mutations in the plectin gene (PLEC1) in patients with epidermolysis bullosa simplex associated with late-onset muscular dystrophy. *Hum Mol Genet*. 5:1539-1546.

Pytela, R., and G. Wiche. 1980. High molecular weight polypeptides (270,000-340,000) from cultured cells are related to hog brain microtubule-associated proteins but copurify with intermediate filaments. *Proc Natl Acad Sci U S A*. 77:4808-4812.

Reipert, S., F. Steinbock, I. Fischer, R.E. Bittner, A. Zeold, and G. Wiche. 1999. Association of mitochondria with plectin and desmin intermediate filaments in striated muscle. *Exp Cell Res*. 252:479-491.

Rezniczek, G.A., C. Abrahamsberg, P. Fuchs, D. Spazierer, and G. Wiche. 2003. Plectin 5'-transcript diversity: short alternative sequences determine stability of gene products, initiation of translation and subcellular localization of isoforms. *Hum Mol Genet*. 12:3181-3194.

Rezniczek, G.A., J.M. de Pereda, S. Reipert, and G. Wiche. 1998. Linking integrin alpha6beta4-based cell adhesion to the intermediate filament cytoskeleton: direct interaction between the beta4 subunit and plectin at multiple molecular sites. *J Cell Biol*. 141:209-225.

Rezniczek, G.A., P. Konieczny, B. Nikolic, S. Reipert, D. Schneller, C. Abrahamsberg, K.E. Davies, S.J. Winder, and G. Wiche. 2007. Plectin 1f scaffolding at the sarcolemma of dystrophic (mdx) muscle fibers through multiple interactions with beta-dystroglycan. *J Cell Biol*. 176:965-977.

Ridley, A.J., W.E. Allen, M. Peppelenbosch, and G.E. Jones. 1999. Rho family proteins and cell migration. *Biochem Soc Symp*. 65:111-123.

Roa, B.B., C.A. Garcia, L. Pentao, J.M. Killian, B.J. Trask, U. Suter, G.J. Snipes, R. Ortiz-Lopez, E.M. Shooter, P.I. Patel, and J.R. Lupski. 1993. Evidence for a recessive PMP22 point mutation in Charcot-Marie-Tooth disease type 1A. *Nat Genet*. 5:189-194.

Ruhrberg, C., and F.M. Watt. 1997. The plakin family: versatile organizers of cytoskeletal architecture. *Curr Opin Genet Dev*. 7:392-397.

Rybakova, I.N., J.R. Patel, and J.M. Ervasti. 2000. The dystrophin complex forms a mechanically strong link between the sarcolemma and costameric actin. *J Cell Biol*. 150:1209-1214.

Saito, F., S.A. Moore, R. Barresi, M.D. Henry, A. Messing, S.E. Ross-Barta, R.D. Cohn, R.A. Williamson, K.A. Sluka, D.L. Sherman, P.J. Brophy, J.D. Schmelzer, P.A. Low, L. Wrabetz, M.L. Feltri, and K.P. Campbell. 2003. Unique role of dystroglycan in peripheral nerve myelination, nodal structure, and sodium channel stabilization. *Neuron*. 38:747-758.

Salzer, J.L. 1997. Clustering sodium channels at the node of Ranvier: close encounters of the axon-glia kind. *Neuron*. 18:843-846.

Salzer, J.L. 2003. Polarized domains of myelinated axons. *Neuron*. 40:297-318.

Salzer, J.L., P.J. Brophy, and E. Peles. 2008. Molecular domains of myelinated axons in the peripheral nervous system. *Glia*. 56:1532-1540.

Schröder, R., W.S. Kunz, F. Rouan, E. Pfendner, K. Tolksdorf, K. Kappes-Horn, M. Altenschmidt-Mehring, R. Knoblich, P.F. van der Ven, J. Reimann, D.O. Furst, I. Blumcke, S. Vielhaber, D. Zillikens, S. Eming, T. Klockgether, J. Uitto, G. Wiche, and A. Rolfs. 2002. Disorganization of the desmin cytoskeleton and mitochondrial dysfunction in plectin-related epidermolysis bullosa simplex with muscular dystrophy. *J Neuropathol Exp Neurol*. 61:520-530.

Seifert, G.J., D. Lawson, and G. Wiche. 1992. Immunolocalization of the intermediate filament-associated protein plectin at focal contacts and actin stress fibers. *Eur J Cell Biol*. 59:138-147.

Sevcik, J., L. Urbanikova, J. Kost'an, L. Janda, and G. Wiche. 2004. Actin-binding domain of mouse plectin. Crystal structure and binding to vimentin. *Eur J Biochem*. 271:1873-1884.

Sherman, D.L., C. Fabrizi, C.S. Gillespie, and P.J. Brophy. 2001. Specific disruption of a SC dystrophin-related protein complex in a demyelinating neuropathy. *Neuron*. 30:677-687.

Singh, J., Y. Itahana, S. Knight-Krajewski, M. Kanagawa, K.P. Campbell, M.J. Bissell, and J. Muschler. 2004. Proteolytic enzymes and altered glycosylation modulate dystroglycan function in carcinoma cells. *Cancer Res*. 64:6152-6159.

Smith, F.J., R.A. Eady, I.M. Leigh, J.R. McMillan, E.L. Rugg, D.P. Kelsell, S.P. Bryant, N.K. Spurr, J.F. Geddes, G. Kirtschig, G. Milana, A.G. de Bono, K. Owaribe, G. Wiche, L. Pulkkinen, J. Uitto, W.H. McLean, and E.B. Lane. 1996. Plectin deficiency results in muscular dystrophy with epidermolysis bullosa. *Nat Genet*. 13:450-457.

Sonnenberg, A., and R.K. Liem. 2007. Plakins in development and disease. *Exp Cell Res*. 313:2189-2203.

Spence, H.J., A.S. Dhillon, M. James, and S.J. Winder. 2004. Dystroglycan, a scaffold for the ERK-MAP kinase cascade. *EMBO Rep*. 5:484-489.

Thompson, O., C.J. Moore, S.A. Hussain, I. Kleino, M. Peckham, E. Hohenester, K.R. Ayscough, K. Saksela, and S.J. Winder. 2010. Modulation of cell spreading and cell-substrate adhesion dynamics by dystroglycan. *J Cell Sci*. 123:118-127.

Tian, R., M. Gregor, G. Wiche, and J.E. Goldman. 2006. Plectin regulates the organization of glial fibrillary acidic protein in Alexander disease. *Am J Pathol*. 168:888-897.

Toivola, D.M., G.Z. Tao, A. Habtezion, J. Liao, and M.B. Omary. 2005. Cellular integrity plus: organelle-related and protein-targeting functions of intermediate filaments. *Trends Cell Biol*. 15:608-617.

Tseng, Y., K.M. An, O. Esue, and D. Wirtz. 2004. The bimodal role of filamin in controlling the architecture and mechanics of F-actin networks. *J Biol Chem*. 279:1819-1826.

Wade, R.H. 2009. On and around microtubules: an overview. *Mol Biotechnol*. 43:177-191.

Waters, J.C., and E.D. Salmon. 1996. Cytoskeleton: a catastrophic kinesin. *Curr Biol*. 6:361-363.

Wegner, A. 1976. Head to tail polymerization of actin. *J Mol Biol*. 108:139-150.

Weiner, J.A., and J. Chun. 1999. SC survival mediated by the signaling phospholipid lysophosphatidic acid. *Proc Natl Acad Sci U S A*. 96:5233-5238.

Weiner, J.A., N. Fukushima, J.J. Contos, S.S. Scherer, and J. Chun. 2001. Regulation of SC morphology and adhesion by receptor-mediated lysophosphatidic acid signaling. *J Neurosci*. 21:7069-7078.

Weisshaar, B., and A. Matus. 1993. Microtubule-associated protein 2 and the organization of cellular microtubules. *J Neurocytol*. 22:727-734.

Wiche, G. 1989. Plectin: general overview and appraisal of its potential role as a subunit protein of the cytomatrix. *Crit Rev Biochem Mol Biol*. 24:41-67.

Wiche, G. 1998. Role of plectin in cytoskeleton organization and dynamics. *J Cell Sci*. 111 (Pt 17):2477-2486.

Wiche, G., B. Becker, K. Luber, G. Weitzer, M.J. Castãnón, R. Hauptmann, C. Stratowa, and M. Stewart. 1991. Cloning and sequencing of rat plectin indicates a 466-kD polypeptide chain with a three-domain structure based on a central alpha-helical coiled coil. *J Cell Biol*. 114:83-99.

Wiche, G., R. Krepler, U. Artlieb, R. Pytela, and W. Aberer. 1984. Identification of plectin in different human cell types and immunolocalization at epithelial basal cell surface membranes. *Exp Cell Res*. 155:43-49.

Wilhelmsen, K., S.H. Litjens, I. Kuikman, N. Tshimbalanga, H. Janssen, I. van den Bout, K. Raymond, and A. Sonnenberg. 2005. Nesprin-3, a novel outer nuclear membrane protein, associates with the cytoskeletal linker protein plectin. *J Cell Biol*. 171:799-810.

Winder, S.J., and J. Kendrick-Jones. 1995. Protein production in three different expression vectors from a single polymerase chain reaction product. *Anal Biochem*. 231:271-273.

Winter, L., C. Abrahamsberg, and G. Wiche. 2008. Plectin isoform 1b mediates mitochondrion-intermediate filament network linkage and controls organelle shape. *J Cell Biol*. 181:903-911.

Wood, P., F. Moya, C. Eldridge, G. Owens, B. Ranscht, M. Schachner, M. Bunge, and R. Bunge. 1990. Studies of the initiation of myelination by SCs. *Ann N Y Acad Sci*. 605:1-14.

Yamada, H., F. Saito, H. Fukuta-Ohi, D. Zhong, A. Hase, K. Arai, A. Okuyama, R. Maekawa, T. Shimizu, and K. Matsumura. 2001. Processing of beta-dystroglycan by matrix metalloproteinase disrupts the link between the extracellular matrix and cell membrane via the dystroglycan complex. *Hum Mol Genet*. 10:1563-1569.

Yarmola, E.G., and M.R. Bubb. 2004. Effects of profilin and thymosin beta4 on the critical concentration of actin demonstrated in vitro and in cell extracts with a novel direct assay. *J Biol Chem*. 279:33519-33527.

Zhao, X.L., G.Z. Li, B. Sun, Z.L. Zhang, Y.H. Yin, Y.S. Tian, H. Li, H.L. Li, S. Wang de, and D. Zhong. 2010. MMP-mediated cleavage of beta-dystroglycan in myelin sheath is involved in autoimmune neuritis. *Biochem Biophys Res Commun*. 392:551-556.

Zhu, X., and R.K. Assoian. 1995. Integrin-dependent activation of MAP kinase: a link to shape-dependent cell proliferation. *Mol Biol Cell*. 6:273-282.

Abstract

Plectin is a large (~ 500 kDa) and versatile cytoskeletal linker protein which belongs to a protein family called plakins or cytolinkers. It is able to bind to all major cytoskeletal filament systems: actin (micro)filaments, intermediate filaments and microtubules. Furthermore, plectin binds to cell-matrix junctional complexes, thus confering mechanical stability not only to single cells but whole tissues. In this diploma thesis, plectin's roles in Schwann cells (SCs) were investigated. SCs are the glia cells of the peripheral nervous system (PNS), where they play essential roles in electrically isolating the axon, connecting the axons to the surrounding basal membrane and transducing signals from the extracellular matrix (ECM) and the axon.

Performing immunoblotting experiments and immunofluorescence microscopy I could demonstrate the expression of plectin isoforms 1, 1c and 1f in SCs in sciatic nerve as well as in primary SCs. Results from co-immunoprecipitation (Co-IP) experiments suggested that in SCs plectin interacts with integrin α6β4 and the dystrophin-glycoprotein complex (DGC), two laminin 211 binding receptor complexes in the abaxonal SC membrane. Furthermore, I have shown that plectin binds to sciatic nerve vimentin via co-IP and overlay experiments. Using a mouse model with a SC-specific conditional plectin knockout (P0-Cre/cKO) I could investigate the effects of plectin ablation on SC functions. I found that protein expression levels of constituents of DGC as well as of the integrin α6β4 complex were altered in P0-Cre/cKO sciatic nerves. Furthermore I could detect changes in the subcellular distribution of α- and β-dystroglycan (members of the DGC) in P0-Cre/cKO sciatic nerve which possibly resulted from increased cleavage of β-dystroglycan by a matrix metalloprotease. No changes in the compartmentalization and molecular differentiation of myelinating SCs could be observed in P0-Cre/cKO nerve fibers by immunofluorescence microscopy. Phenotypic analysis of primary SCs derived from sciatic nerve of wild-type and P0-Cre/cKO mice demonstrated reduced motility of plectin-null SCs growing on laminin 211. Furthermore P0-Cre/cKO SCs showed increased process retraction upon treatment with the signaling molecule lysophosatidic acid (LPA).

Zusammenfassung

Plectin ist ein etwa 500 kDa großes und sehr vielseitiges cytoskelettäres Linkerprotein. Es ist ein Mitglied der Plakine oder Cytolinker. Plectin kann an alle drei cytoskelettären Filament Systeme binden: das Aktin Filamentsystem, das Intermediärfilamentsystem und Mikrotubuli. Des Weiteren verleiht Plectin auch ganzen Geweben Stabilität indem es an Zell-Matrix Kontaktstellen bindet. Im Zuge dieser Diplomarbeit wurden Plectins Rollen in Schwann Zellen (SZ) untersucht. SZ sind die Glia Zellen des peripheren Nervensystems (PNS). Zu ihren Funktionen gehören die elektrische Isolation des Axons, sowie die mechanische Verbindung des Axons mit der umgebenden Basalmembran und die Signaltransduktion zwischen Axon und extrazellulärer Matrix.

Mittels Immunoblotting-Analyse und Immunfluoreszenz-Mikroskopie konnte ich die Expression der Plectin-Isoformen 1, 1c und 1f sowohl in SZ des Ischiasnervs als auch in primären SZ zeigen. Hinweise auf zwei stabilisierende Verbindungen, bei denen Plectin zwei Laminin 211-Rezeptor-Komplexe [Dystrophin-Glycoprotein-Komplex (DGK) und Integrin α6ß4] an das Intermediärfilamentsystem koppelt, ergaben sich durch Co-Immunopräzipitation und Protein-Overlay-Experimente. Mithilfe einer Mauslinie, mit einem konditionellen Plectin-Knockout in SZ (P0-Cre/cKO), konnte ich die Effekte von fehlendem Plectin auf die Funktion von SZ in situ untersuchen. Ich konnte Veränderungen in der subzellulären Verteilung von α- und ß-Dystroglycan (Mitglieder des DGK) in Ischiasnerven aus P0-Cre/cKO Mäusen beobachten. Diese Veränderungen wurden vermutlich durch den Verlust der Verankerung des DGK am Intermediärfilament-System und der daraus resultierenden verstärkten Spaltung von ß-Dystroglycan durch Matrix-Metalloproteinasen verursacht. Immunfluoreszenz-Mikroskopie von gezupften P0-Cre/cKO Nervenfasern zeigte keine Veränderungen in der Kompartmentalisierung von myelinisierenden SZ oder des Axons. Möglicherweise wurde der Verlust von Plectin durch verstärkte Expression wichtiger Proteine des DGK und des Integrin α6ß4 Komplexes kompensiert. Solche verstärkten Expressionen konnte ich durch semiquantitative komparitive Immunoblotting-Analysen zeigen. Die phenotypische Analyse primärer SZ, isoliert aus Ischiasnerven von Wildtyp und P0-Cre/cKO Mäusen, zeigte reduzierte Motilität von Plectin-defizienten SZ. Zusätzlich konnte ich bei Plectin defizienten-SZ eine erhöhte Retraktion von Fortsätzen nach Behandlung mit dem Signalmolekül Lysophosphatidylsäure beobachten.

Curriculum vitae

Personal Data

Name:	Karl-Leopold Wögenstein
Present address:	Strohgasse 26/20, 1030 Vienna, Austria
Date of birth:	12.03.1985
Place of birth:	Seebarn
Marital status:	partnership
Parents:	Elisabeth Wögenstein
	Erwin Wögenstein

Education

1991-1995	Primary school, Harmannsdorf, Niederösterreich
1995-1999	Secondary school, Harmannsdorf, Niederösterreich
1999-2003	Secondary school, BORG3, Vienna
Jun 2003	Graduation (Matura)
2004-present	Diploma thesis under the supervision of Prof. Dr. G. Wiche at the Department of Biochemistry and Cell Biology, Max F. Perutz Laboratories GmbH, Campus Vienna biocenter, University of Vienna, Dr. Bohrgasse 9, A-1030

Teaching activities at the University of Vienna

2010	Assignments as tutor for the cell-biologic courses for biologists and chemists.

Language skills

German (native), English (fluent), French (basic)